SIN-3 transcriptional coregulator maintains mitochondrial hormesis and polyamine flux

[1, 2] Giovannetti M., [1]Fabrizio P., [3]Nicolle O., [1]Bedet C., [4]Rodríguez-Palero, MJ., [3]Michaux G., [4]Artal-Sanz M., [5] Witting M., [1]Palladino F

[1] Laboratory of Biology and Modeling of the Cell, UMR5239 CNRS/Ecole Normale Supérieure de Lyon, INSERM U1210, UMS 3444 Biosciences Lyon Gerland, Université de Lyon, Lyon, France, [2] present address : Université Paris Cité, CNRS, Institut Jacques Monod, 75013 Paris, France ; [3]Univ Rennes, CNRS, IGDR (Institut de Génétique et Développement de Rennes), UMR 6290, F-35000 Rennes, France ; [4]Andalusian Centre for Developmental Biology (CABD), Consejo Superior de Investigaciones Científicas/Junta de Andalucía/Universidad Pablo de Olavide and Department of Molecular Biology and Biochemical Engineering, Universidad Pablo de Olavide, CSIC-Universidad Pablo de Olavide-Junta de Andalucía, Sevilla, Spain. [5] Metabolomics and Proteomics Core, Helmholtz Zentrum München, Ingolstädter Landstraße 1, 85764 Neuherberg, Germany and Chair of Analytical Food Chemistry, TUM School of Life Sciences, Technical University of Munich, Maximus-von-Imhof Forum 2, 85354 Freising-Weihenstephan, Germany

Abstract

Mitochondrial function relies on the coordinated transcription of mitochondrial and nuclear genomes to assemble respiratory chain complexes. Across species, the SIN3 coregulator influences mitochondrial functions, but how its loss impacts mitochondrial homeostasis and metabolism in the context of a whole organism is unknown. Exploring this link is important because *SIN3* haploinsufficiency causes intellectual disability/autism syndromes and SIN3 plays an important role in tumor biology. Here we show that loss of *C. elegans* SIN-3 results in transcriptional deregulation of mitochondrial- and nuclear encoded mitochondrial genes, potentially leading to mito-nuclear imbalance. Consistent with impaired mitochondrial function, *sin-3* mutants show extensive mitochondrial fragmentation by transmission electron microscopy (TEM) and *in vivo* imaging, and altered oxygen consumption. Metabolomic analysis of *sin-3* mutant animals identifies a signature of mitochondria stress, and deregulation of methionine flux resulting in decreased S-adenosyl methionine (SAM), and increased polyamine levels. Our results identify SIN3 as a key regulator of mitochondrial dynamics and metabolic flux, with important implications for human pathologies.

Introduction

Mitochondria, the main energy providers within cells, produce ATP through oxidative phosphorylation (OXPHOS) and control the levels of metabolites essential for various cellular functions. The OXPHOS system consists of four multimeric complexes, coenzyme Q and cytochrome *c* that form the mitochondrial respiratory chain (I–IV) and couple redox reactions, creating an electrochemical gradient leading to the creation of ATP through a fifth complex, the F_1F_0 ATPase (Signes and Fernandez-Vizarra, 2018). Assembly of functional mitochondria relies on coordinated transcription and translation of mitochondrial and nuclear genomes (Richter-Dennerlein et al., 2016), and both mitochondrial and nuclear DNA mutations affecting the accumulation and function of OXPHOS enzymes are the most common cause of mitochondrial diseases and are associated with neurodegeneration and aging (DiMauro and Schon, 2003; Fernandez-Vizarra and Zeviani, 2021; Reeve et al., 2008). The mitochondrial genome, which is highly conserved among species, comprises 37 genes coding for two ribosomal RNAs, 22 transfer RNAs, and 13 protein subunits (12 for *C. elegans*) of the mitochondrial respiratory chain performing OXPHOS (Taanman, 1999). The rest of the mitochondrial proteome, comprising over a thousand proteins, is encoded in the nucleus (Ali et al., 2019; Barshad et al., 2018; Mercer et al., 2011). The bidirectional regulation between mitochondria and the nucleus, referred to as mito-nuclear communication, maintains homeostasis and regulates stress responses (Quirós et al., 2016). Mitochondrial damage or alterations in mitochondrial function trigger specific quality control mechanisms. Of these, the best characterized is the mitochondrial unfolded protein response (UPR^{mt}), a cellular stress response that leads to increased transcription of mitochondrial chaperones and proteases (Anderson and Haynes, 2020). In addition to an imbalance between mitochondrial and nuclear protein quantities (Matilainen et al., 2017), reduced levels of TCA cycle components (Yang et al., 2022), reduction of β-oxidation and lipid biosynthesis (Rolland and Conradt, 2022; Rolland et al., 2019) and defective mitochondrial import (Lionaki et al., 2022), can all trigger UPR^{mt}. Recent data has shown that mitochondrial stress leads to extensive chromatin reorganization (Tian et al., 2016; Zhu et al., 2020), and chromatin regulatory factors contribute to

mitochondrial gene expression (Matilainen et al., 2017). Conversely, metabolites originating from the mitochondria can initiate modifications in the nucleus (Matilainen et al., 2017).

Depletion experiments in various models have shown that the highly conserved SIN3/HDAC coregulator plays a role in mitochondrial functions and metabolism (Chaubal and Pile, 2018). Yeast *sin3* null mutants grow poorly on non-fermentable carbon sources, have lower ATP levels, and reduced respiration rates (Barnes et al., 2010). In Drosophila cultured cells, reduction of SIN3 levels also resulted in altered ATP levels and deregulation of genes encoded by the mitochondrial genome (Barnes et al., 2010; Pile et al., 2003). Lower levels of ATP and increased sensitivity to oxidative stress were also observed in *C. elegans* animals carrying the *sin-3(tm1276)* partial loss of function allele (Sharma et al., 2018). In mice, Sin3a was detected in a transcriptional complex with the MafA pancreatic β-cell-specific activator (Scoville et al., 2015), and its inactivation reduced the fitness of β-cells and altered glucose production in liver (Yang et al., 2020a). Significantly, in mammalian cells, SIN3 and its associated protein SUDS3 were identified in a screen for modifiers of drug-induced mitochondrial dysfunction (To et al., 2019). Altogether, these data from different systems support a conserved role for SIN3 in mitochondrial homeostasis and metabolism, but how SIN3 affects mitochondrial dynamics and metabolic pathways in the context of a whole organism remains largely unknown. This is particularly important given that heterozygous loss-of-function variants, as well as point mutations in *SIN3* were recently identified as the underlying cause of intellectual disability (ID)/autism syndromes (Balasubramanian et al., 2021; Latypova et al., 2021; Witteveen et al., 2016), and SIN3 levels play an important role in tumor biology (Bansal et al., 2015; Bansal et al., 2016; Farias et al., 2010; Lewis et al., 2016).

Previous studies in *C. elegans* have shown that knock-down of *sin-3*, the single SIN3 homolog in this organism, results in a decreased lifespan, altered mitochondrial membrane potential, enhanced autophagy and increased oxidative stress (Pandey et al., 2018; Sharma et al., 2018). How these changes affect mitochondrial morphology and function was not investigated. Here, using a *sin-3* CRISPR-Cas9 knock-out allele, we show that loss of SIN-3 results in the deregulation of both mitochondria- and nuclear-encoded genes. Transmission electron microscopy (TEM) and *in vivo* imaging revealed extensive

fragmentation of mitochondria in all tissues examined, including muscle, intestine, hypodermis, and the germline. Consistent with severe defects in mitochondrial function, both basal and maximal oxygen consumption are increased in the absence of SIN3, while spare respiratory capacity is decreased. Metabolomic analysis identified a signature of mitochondria stress and deregulation of methionine flux, resulting in decreased levels of SAM and a shift towards higher polyamine levels. Together our data identify SIN3 as an important regulator of mitochondrial dynamics in an organismal context, and reveal a SIN-3 dependent connection between expression of OXPHOS subunits, mitochondrial homeostasis, and metabolic fluxes.

Results

Loss of *sin-3* results in altered expression of genes with mitochondrial functions

Previous transcriptomic profiling of animals carrying the *sin-3(tm1276)* partial loss-of-function allele revealed deregulation of the germline transcriptome, including metabolic genes (Caron et al., 2023). In order to identify high confidence genes regulated by SIN-3, we extended our analysis to genes commonly misregulated in *sin-3(tm1276)* and *sin-3*(*syb2172*) mutant animals that carry a complete loss of function allele obtained by CRISPR-Cas9 (Caron et al., 2023), generating a list of 892 genes (Table S1). Using Worm Cat (Holdorf et al., 2020), within this set we identified a common class of genes with functions related to mitochondria (Figure 1A and Table 1).

Both nuclear and mitochondrial encoded genes contribute to the assembly of mitochondrial respiratory chain complexes (MRC) I-V (Signes and Fernandez-Vizarra, 2018). Five of the 7 MRC complex I subunits encoded by the mitochondrial genome were strongly upregulated in both *sin-3* mutants: *ndub-2*, *ndfl-4, nduo-1, nduo*-2 and *nduo-5* (Figure 1B). By contrast, nuclear encoded MRC subunits identified in our data set were mostly down-regulated (Figure 1B), as were the majority of additional nuclear encoded genes with mitochondria-related functions (31 out of 37, Table 1). These include mitochondrial ribosomal proteins, components of the citric acid cycle, the *tomm-40* translocase and the *coq-3* coenzyme Q3 (Table 1). Comparison of our list of misregulated genes associated with mitochondrial functions to a list of SIN3 targets on chromatin (Beurton et al., 2019) revealed that 23 of

these 37 genes have SIN-3 binding at their promoter region, and the majority (18/23) are downregulated in *sin-3* mutants, including ribosomal protein genes, the t*omm-40* mitochondrial translocase*,* the ATP synthases *atp-1* and *atp-4,* and the cytochrome-C oxidase *cox-7C* (Table S2). SIN-3 may therefore directly promote expression of these genes. Together, our analyses suggest that loss of *sin-3* perturbs the coordinated expression of mitochondrial genes encoded by nuclear and mitochondrial genomes, possibly resulting in mito-nuclear imbalance and affecting mitochondrial homeostasis. Consistent with mitochondrial dysfunction, *sin-3* mutants show reduced fertility, increased sensitivity to oxidative stress, and altered lifespan (Beurton et al., 2019; Caron et al., 2023; Pandey et al., 2018; Sharma et al., 2018), as observed in other mitochondrial mutants (Kropp et al., 2021).

Transmission electron microscopy reveals extensive mitochondrial fragmentation in *sin-3* mutant animals in all tissues examined

Mitochondrial morphology is tightly linked to mitochondrial function, and its steady state is determined by the balance between fission and fusion events that may be disrupted under conditions of mitochondrial stress (Westermann, 2010). To test whether mitochondrial morphology is affected in *sin-3* mutant animals we performed electron microscopy analyses on wildtype and mutant young adults. Mitochondria in the body wall muscles of wild type animals vary in size reflecting dynamic morphological changes, and tend to be cylindrical- or ovular shaped with regular outer membranes and dense cristae throughout each organelle (Figure 2 panel *a,* white arrows). In animals carrying the loss of function allele *sin-3(tm1276),* or the *sin-3(syb2172)* null allele, mitochondria were instead highly fragmented and appeared more numerous, with a stronger effect in *syb2172* animals (Figure 2 panels *b* and *c,* white arrows). For both mutants, highly fragmented mitochondria were visible in all of the tissues examined, including intestine, pharynx, hypodermis, and germline (Figure 2A and Figure S1A). We also observed the presence of enlarged or "giant" mitochondria, most prominent in muscle and intestinal cells, and often containing electron-dense material (Figure 2A panels *b*, *c*, and *e*, Figure 2B panels *a-d,* black arrows) that may indicate iron deposits (Puccio et al., 2001; Schober et al., 2021) (Schiavi et al., 2015) or protein aggregates (Chen et al., 2021) (Al Rawi et al., 2011; Wang et al., 2016; Zhou et al., 2016). Selective autophagy of

mitochondria, or mitophagy, is a process that results in budding off of damaged mitochondria for targeted breakdown, thereby contributing to mitochondrial homeostasis (Onishi et al., 2021). While this process was never observed in wild type, examples of double-membrane autophagosomes were observed in both the hypodermis and germ cells of mutant animals (Figure S1B). Together, these results show that *sin-3* inactivation dramatically alters mitochondrial dynamics and morphology, and reveal increased mitochondrial fission throughout the body of *sin-3* mutant animals, with the most severe phenotypes observed in the null mutant allele.

Time dependent increase in mitochondrial fragmentation in *sin-3* muscle cells

To further examine and quantify changes in mitochondrial morphology in live animals, we used a transgenic strain expressing a red fluorescent protein (RFP) fused at the N terminus to the TOMM-20 translocase of the outer mitochondrial membrane and expressed under the control of a promoter in muscle cells (*myo-3p::20Nter::*wrmScarlet)(Roy et al, 2022), where mitochondria are abundant and easily visible. We used *tm1276* mutant animals because although less fertile than wildtype, they can be maintained as homozygotes, while *syb2172* animals are fully sterile (Caron et al., 2023). In wildtype, the majority of body-wall muscle cells have longitudinally arrayed tubular mitochondria, while a smaller percentage show either elongated mitochondria in an interconnected mesh-like network or fragmented mitochondria (Figure 3A). We arbitrarily classified mitochondrial morphology into three classes-tubular, intermediate, or fragmented- (Regmi et al., 2014), and scored animals falling into each of these at days 1, 6, and 9 of adulthood.

In wild type day one adults, the large majority of mitochondria showed a tubular morphology (Figure 3A and B). In *sin-3* mutants of the same age, we instead mainly observed "intermediate" mitochondrial morphology, with a significant percentage of highly fragmented mitochondria. At day 6, intermediate and fragmented mitochondria also appeared in wild type, while the majority of mitochondria in *sin-3* mutants were highly fragmented. At day 9, mitochondrial fragmentation further increased in *sin-3(tm1276)* mutants, but remained more or less constant in wildtype (Figure 3B). Using a *mex-5p*::tomm-20::mKate2 reporter expressed in the germline, we also observed changes in mitochondrial morphology

in this tissue (Figure S1C). Excessive mitochondrial fragmentation results from an imbalance between fusion and fission that are mediated primarily by two classes of GTPases structurally related to dynamins: mitofusins (MFNs)/Fzo1/FZO-1 and Drp1/DRP-1, respectively (Chen and Chan, 2009; Labrousse et al., 1999; Westermann, 2010). Expression of neither gene was altered in *sin-3* mutants (Caron et al., 2023, Table S1), suggesting that the observed defects in mitochondrial morphology may arise instead as a response to mitochondrial stress.

Muscle fibers degenerate prematurely in *sin-3* mutants

Mitochondrial dysfunction impairs muscle health and causes subsequent muscle wasting, commonly referred to as sarcopenia (Christian and Benian, 2020). Using a muscle myosin reporter *myo-3::*GFP (Mergoud Dit Lamarche et al., 2018) in wildtype young adults sarcomeres appear as straight lines of GFP, and no obvious change was observed up to day 9 (Figure 3C). By contrast, in *sin-3(tm 1276)* mutants at day 9 we observed diffuse GFP fluorescence, suggesting that muscle integrity is affected prematurely in these mutants (Figure 3C). Degradation of muscle proteins may also occur prematurely in these animals (Liang et al., 2014). Because defects in muscle fibers are observed only in older *sin-3* mutant adults, while mitochondrial defects already appear at day 1, these results are consistent with a decline in mitochondrial network structure preceding muscle decline, as previously reported (Etheridge et al., 2015; Gaffney et al., 2018).

Mitochondrial UPR is dampened in the absence of SIN-3

In response to mitochondrial stress, cells trigger the mitochondrial unfolded protein response (UPR^{mt}), a transcriptional response that transmits mitochondrial stress signals to the nucleus to regulate mitochondrial chaperone genes and other factors necessary for the recovery of dysfunctional mitochondria (Lin and Haynes, 2016). Increased mitochondrial fragmentation in *sin-3* mutants suggests that SIN-3 may be required for mitochondrial homeostasis. We therefore asked whether UPR^{mt} is properly activated in *sin-3* mutant animals, using the *hsp-6* chaperone as a reporter (Heussler et al 2022). *sin-3(tm1276)* mutants carrying *hsp-6*::GFP were sterile, so we used RNAi to deplete *sin-3. sin-3*(RNAi) alone had no reproducible effect on *hsp-6::*GFP expression (Figure 4A). Induction of mitochondrial stress by RNAi

knock-down of the NADH ubiquinone oxidoreductase component *nuo-4*, or the mitochondrial ribosomal protein *mrps-5,* resulted in strong *hsp-6*::GFP expression in the intestine, as expected (Houtkooper et al., 2013). Simultaneous depletion of both *sin-3* and *nuo-4,* or *sin-3* and *mrps-5,* significantly decreased GFP expression, but only in older animals at day 6 (Figure 4A). No significant difference in *hsp-6*::GFP induction between *sin-3* and wildtype was observed at day 3 (Figure S2). These results suggest that SIN-3 is required for a full response to mitochondrial stress depending of the age of the animals. Interestingly components of the NuRD chromatin remodeling complex have been shown to relocate to the nucleus upon mitochondrial stress (Zhu et al., 2020) to influence the UPR^{mt}. Using a SIN-3::RFP translational fusion, we observed no obvious change in SIN-3 localization following mitochondrial stress (Figure S3).

Increased oxygen consumption in aged *sin-3* mutant animals

To understand how altered mitochondrial structure following loss of SIN-3 relates to mitochondrial function, we measured oxygen consumption in *sin-3(tm1276)* mutants. In *C. elegans*, oxygen consumption rates (OCRs) as a measure of ETC function can be accurately assessed using a Seahorse Analyzer with intact animals (Koopman et al., 2016; Kropp et al., 2021). Wildtype animals maintained a constant basal OCR from the young adult stage to day 6 of adulthood, although a tendency to reduce basal respiration during aging was apparent, as previously reported (Figure 5A and B, compare YA to D6) (Higashitani et al., 2022; Huang and Lin, 2018). By contrast, as *sin-3* mutants aged, basal OCR dramatically increased, so that at day six of adulthood it was more than 2-fold higher in *sin-3* mutants compared to wild type (Figure 5A, D6).

We next measured maximal respiratory capacity following mitochondrial uncoupling by the addition of carbonyl cyanide-p-trifluoromethoxyphenylhydrazone (FCCP). In *sin-3* young adults, maximal OCR was similar to wild type, but we again observed a significant increase in aged *sin-3* mutants compared to age-matched wildtype (Figure 5B). Moreover, in old *sin-3* mutants the observed increase in basal respiration was proportionally larger than the increase in maximal respiratory capacity (Figure 5A and B). Consequently mitochondrial spare capacity, which characterizes the ability of mitochondria to meet extra energy requirements beyond the basal level (Marchetti et al., 2020), was reduced compared to old wildtype worms (Figure 5C). Increased OCR could be a side effect of partial mitochondrial uncoupling (Demine et al., 2019). We note however that the single mitochondrial uncoupling protein in *C. elegans, ucp-4,* is down- rather than upregulated in both *sin-3* mutants (Table S1), as is the expression of the *ant-*

1.1 and *ant-1.3* ADP/ATP translocators whose activity can also result in mitochondrial uncoupling (Berry et al., 2022; Bertholet et al., 2019). Consistent with depletion of SIN-3 affecting mitochondrial integrity, we observed that levels of conserved electron transport proteins, detected using antibodies against the highly conserved mammalian complex III subunit UQCRC2 and complex II subunit SDHB1, were reproducibly decreased in extracts from *sin-3(tm1276)* animals. Protein abundance of the ATP synthase ATP5 was less affected (Figure 5D and E).

sin-3 inactivation does not alter levels of TCA cycle metabolites, but results in a signature of mitochondrial stress

The above results clearly establish that *sin-3* knock-down or deletion leads to defective mitochondrial function. Because mitochondria are a hub for biosynthetic processes, we used metabolomic analysis to probe for SIN-3-dependent metabolic changes in animals carrying the *sin-3(tm1276)* loss of function allele. We chose this allele because the sterility of *sin-3(syb2172)* null mutants precluded growing the large number of animals required for this type of analysis. We observed no significant change in the abundance of TCA cycle intermediates detected, including succinyl-CoA, alpha-keto-glutaric acid, succinic acid, fumaric acid, and malic acid (Tables S4 and S5, Figures S4 A and B). Although two peaks putatively annotated as glycolytic intermediates glucose-6-P and glucose-1-P showed a significant reduction in *sin-3* mutants, the downstream metabolite fructose-1,6-bis-P showed no difference (Table S4 and Figure S4B). Glucose-1-P is a metabolite of gluconeogenesis and starch and sucrose metabolism. *C. elegans* can store excess energy in the form of trehalose and glycogen (Hanover et al., 2005). However, we detected no significant change in UDP-glucose (an intermediary for glycogen and trehalose synthesis), trehalose-6-P, or trehalose in *sin-3* mutant animals (Table S4 and Figure S4B). Together, these results suggest that the absence of SIN-3 has little or no influence on energy metabolism. This was further corroborated by only minor changes in lipid metabolism intermediates including short-chain acyl-CoA and short-chain acyl-carnitine species (Table S5 and Figure S4A). Nonetheless, it is important to note that metabolite levels are only indicative of changes in metabolic flux, defined as the turnover rate of metabolites through enzymatically controlled pathways (Nielsen, 2003). Increased mitochondrial fragmentation may lead to changes or redirection of metabolic fluxes without altering metabolite levels.

In contrast to the above results, significant changes in amino acid metabolism were detected: aspartic acid levels significantly decreased in *sin-3* mutants, while proline, threonine, lysine, serine, and citrulline increased (Figure 6A and Table S5 and Figure S4C). Interestingly, decreased aspartic acid and increased serine have been shown to be a signature of mitochondrial stress (Quirós et al., 2017). No changes in glutathione (GSH) and glutathione disulfide (GSSG), both associated with oxidative stress, were detected (Table S5 and Figure S4C). An increase in sarcosine and dimethylarginine was also detected (Table S5 and Figure S4C).

SIN-3 is required to maintain polyamine homeostasis

Both serine and sarcosine are connected to one-carbon metabolism, which encompasses both the folate and methionine cycles to generate one-carbon units (methyl groups) that are used for the biosynthesis of important precursors and for methylation reactions (Locasale, 2013). While no changes in folate cycle intermediates folate, 5-methyl tetrahydrofolic (mTHF) or dihydrofolic (DHF) acid were found (Table S5 and figure S4D), a significant decrease in the methionine cycle metabolite S-adenosylmethionine (SAM) was observed (Figure 6B, Table S5 and Figure S4D).

SAM is the major methyl donor in the cell and is critical for the synthesis of phosphatidylcholine, an important component of cellular membranes (Ye et al., 2017), as well as for the methylation of DNA, RNA, and histones through transmethylation (Locasale, 2013). SAM is also connected to polyamine synthesis through the activity of *S*-adenosylmethionine decarboxylase (adoMETDC/*smd-1*) that results in the production of decarboxylated *S*-adenosylmethioninamine (dc-SAM) (Figure 6C). Spermidine synthase (SPDS/*spds-1*), a key enzyme in the pathway, then catalyzes the transfer of an aminopropyl moiety of dcSAM to putrescine, resulting in the formation of spermidine and 5′-methylthioadenosine (MTA). Putrescine is provided by another key enzyme, ornithine decarboxylase (ODC/*odc-1*) (Figure 6C). Interestingly while the abundance of downstream metabolites of the transmethylation pathway, S-adenosyl homocysteine (SAH) and cystathionine, was not altered in *sin-3* mutants (Figure 6B, Table S5 and Figure S4E), both dcSAM and MTA were strongly reduced (Table S5 and Figure S4E). Levels of neither arginine nor ornithine, two precursors of putrescine, nor putrescine itself was altered in s*in-3*

mutants (Figure 6B, Table S5 and Figure S4C), while we detected a large increase in both spermidine and N-Acetyl-spermine, the degradation products of spermine and spermidine, respectively (Figure 6C, Table S5 and Figure S4E). Spermine could not be detected in our analysis. Together, these results suggest that in the absence of SIN-3, the metabolic flux is shifted from transmethylation to polyamine biosynthesis. Consistent with a shift in metabolic flux toward the synthesis of polyamines, the abundance of N-acetylputrescine, a degradation product of putrescine, was unaltered in our analyses (Table S5 and Figure S4D). The abundance of another polyamine, cadaverine, was also increased in *sin-3* mutants (Figure 6D, Table S5 and Figure S4E). Cadaverine is produced by the decarboxylation of lysine, also more abundant in *sin-3* mutants (Figure 6D, Table S5 and Figure S4C). No dedicated lysine decarboxylase has been annotated in *C. elegans* to date, but *odc-1* could potentially fulfill this function (Schaeffer and Donatelli, 1990).

Another lysine catabolite whose abundance increased in *sin-3* mutants is saccharopine, while aminoadipic acid (L-2-Aminoadipate), the metabolite further downstream, showed a slight but not significant increase (Figure 6D, Table S5 and Figure S4C). Because lysine degradation via the formation of saccharopine is confined to the mitochondria (Leandro and Houten, 2020), a potential blockage in its degradation due to defective mitochondria could increase its abundance (Figure 6D).

Transcriptomics analysis reveals deregulation of metabolic pathways

The above metabolic analysis was carried out on *sin-3(tm1276)* mutant animals. Close inspection of the previously published list of genes misregulated in these mutants animals (Beurton et al., 2019) identified candidates whose misexpression correlates with the observed metabolic changes (Figure 6C). The ornithine decarboxylase *odc-1*, which converts ornithine to putrescine (Macrae et al., 1995), was strongly upregulated in *sin-3(tm1276)* mutants (log2FC 1.15, p = 4.09e-06), as was the spermidine synthase *spds-1* (log2FC 2.29, p = 2.88e-19). Regulation of polyamine synthesis is mainly achieved by controlling the activity of ornithine decarboxylase through its inhibitor antizyme, the binding of which disrupts ODC enzymatic activity and targets it for ubiquitin-independent degradation (Coffino, 2001). Significantly, the *C. elegans* homologue of antizyme, *oaz-1*, was significantly downregulated (log2FC -0.86, p = 4.29e-32),

potentially leading to increased ODC-1 activity and spermidine biosynthesis in these mutants. Because *odc-1* may also decarboxylate lysine to produce cadaverin (Schaeffer and Donatelli, 1990), its increased activity could contribute to the observed increase in cadaverin levels. The polyamine oxidase (PAO) *hpo-15* is instead upregulated in *sin-3(tm1276)* mutants (log2FC 1.74, p = 6.56e-08). N-acetylspermine and N-acetylspermidine, metabolites of spermine and spermidine, respectively, are used as substrates by PAO to produce H_2O_2 and either spermidine or putrescine, depending on the starting substrate. An increased *hpo-15* expression may therefore also contribute to both the increase in spermidine levels and increased sensitivity to oxidative stress in *sin-3* mutant animals, as observed in mammalian cells (Jeong et al., 2022). Interestingly, spermidine serves as the sole biosynthetic precursor for hypusination, a post-translational modification that is an integral component of eukaryotic translation initiation factor 5A (eIF5A)(Park et al., 2010). Genes encoding the two enzymes required for hypusination, the deoxyhypusine synthase *dhps-1* and the deoxyhypusine hydroxylase *dohh-1*, were both upregulated in *sin-3(tm1276)* mutants (log2FC 0.7390, p = 7.89e-27 and 0.44, p = 2.60e-18 respectively). Of these genes only *oaz-1* and *hpo-15* are included in the list of genes commonly misregulated in the two *sin-3* alleles (Table 1), most likely reflecting experimental differences between the two transcriptomics analyses (Caron et al., 2023). Altogether our data is consistent with deregulating of specific metabolic genes in *sin-3(tm1276)* mutants contributing to the observed changes in polyamine flux. Whether these changes are a cause or consequence of the observed changes in mitochondrial dynamics and respiration remains to be established.

Discussion

The SIN3 corepressor has been linked to mitochondrial function in several models, but how its loss alters mitochondrial dynamics and metabolism in the context of an entire organism has not been explored. Here, using two different *sin-3* mutant alleles, we show that in *C. elegans* adult animals partial or complete loss of *sin-3* function results in increased expression of genes encoded by the mitochondrial genome and an overall decrease in the expression of nuclear encoded mitochondrial genes, potentially leading to nuclear-mitochondrial imbalance. We show that the altered expression of mitochondrial genes is associated with increased mitochondrial fragmentation in all tissues examined, increased oxygen consumption, and

metabolic changes, including a pronounced shift in metabolic flux from methionine to polyamine biosynthesis. Together our data identify SIN-3 as a key regulator of mitochondrial dynamics and polyamine homeostasis.

Knock-down of SIN3 in different systems results in strikingly similar phenotypes. In yeast, Drosophila cultured cells and *C. elegans,* reduced SIN3 activity is associated with lower ATP levels (Barnes et al., 2010; Pandey et al., 2018), and increased oxidative stress in both Drosophila and *C. elegans* adult animals (Barnes et al., 2014; Sharma et al., 2018). Deregulation of mitochondrial genes was reported following either knock-down or overexpression of SIN3 in cultured Drosophila cells (Barnes et al., 2010; Pile et al., 2003), or conditional *mSin3A* knock-out in primary cell culture (Dannenberg et al., 2005). Our transcriptomics analysis on *sin-3(tm1276)* and *sin-3(syb2178)* mutant animals revealed that expression of respiratory complex I subunits encoded by the mitochondrial genome is strongly increased in both mutants, while expression of nuclear encoded subunits of additional complexes is downregulated. The expression of additional genes with important roles in mitochondrial function, including mitochondrial ribosomal proteins and the *tomm-1* translocase is also significantly decreased in *sin-3* mutants. Importantly, SIN-3 binding on a number of downregulated genes suggests that SIN-3 may positively regulates their expression, as observed for SIN3 in other contexts (Caron et al., 2023; Baymaz et al., 2015; van Oevelen et al., 2010; Zhu et al., 2018).

The nucleus and mitochondria constantly communicate to adjust their activities in order to ensure cellular homeostasis (Ryan and Hoogenraad, 2007), and reducing the expression of a single major ribosomal nuclear protein (MRP) is sufficient to induce a stoichiometric imbalance between nuclear and mitochondrial-DNA encoded ETC subunits, referred to as mitonuclear protein imbalance (Houtkooper 2013). Mitonuclear imbalance leads to mitochondrial stress and activates the UPR^{mt} (Melber and Haynes, 2018). Interestingly, in *C. elegans,* the histone deacetylase *hda-1*, a conserved component of SIN3 complexes (Beurton et al., 2019; Caron et al., 2023), was shown to be required for this stress response (Shao et al., 2020). We observed that expression of the UPR^{mt} reporter *hsp-6* was dampened following induction of mitochondrial stress in *sin-3* knockdown animals, but only in old adults. Therefore, it is likely

that HDA-1 acts in a context other than SIN-3 in the UPR^{mt}, most likely the NuRD histone deacetylase complex (Zhu et al., 2020).

One of the most striking phenotypes we observed is that either reduced SIN-3 function or its complete absence results in a dramatic increase in mitochondrial fragmentation, observed by TEM in all tissues examined, including muscle, intestine, pharynx, hypodermis and germ cells, and through live imaging in muscle cells. The ability to transition between fission/fusion states is essential for mitochondrial function in cellular bioenergetics, regulation of intracellular Ca^{2+}, and cellular stress responses (Wai and Langer, 2016). Fusion allows damaged mitochondria to mitigate stress by mixing contents, while fission contributes to quality control of damaged mitochondria by budding off deteriorating components for targeted breakdown via autophagy or mitophagy. The increased fragmentation we observe is consistent with a defect in the maintenance of mitochondrial homeostasis. We also observed examples of enlarged mitochondria, another hallmark of mitochondrial damage (Vincent et al., 2016), and the accumulation of electron-dense material in mitochondria that may represent iron deposits or misfolded proteins. Similar aggregates were observed by TEM in *C. elegans* following acute heat stress (Chen et al., 2021), in sperm- derived mitochondria before their elimination by mitophagy (Al Rawi et al., 2011; Al Rawi et al., 2011; Wang et al., 2016), and in the mitochondria of worms containing mutations in *eat-3/*OPA1 and *fzo-1/*mfn1 fusion genes (Byrne et al., 2019), supporting a link between their formation and mitochondrial morphological defects. Alternatively, these aggregates may represent iron deposits such as those observed in the mitochondria of a mouse model of Friedrich ataxia (Puccio et al., 2001; Whitnall et al., 2012) and congenital sideroblastic anemia (Ducamp and Fleming, 2019). Interestingly mitochondrial iron overload promotes ROS production, as observed in *sin-3* mutants (Pandey et al., 2018), and is associated with mitochondrial dysfunction and oxidative damage (Ward and Cloonan, 2019). Regardless of the underlying cause, disruption of mitochondria homeostasis, as observed in *sin-3* mutant animals, is likely to have major consequences for mitochondrial health and function.

The rate of oxygen consumption is another measure of mitochondrial activity, and we observed significant differences in respiration in *sin-3(tm1276)* mutants. While neither basal nor maximal oxygen

consumption rates were affected in mutant young adults, both were significantly elevated in older mutants compared to wild type. Conversely, mitochondrial spare respiratory capacity was reduced in these mutants. Spare respiratory capacity can be viewed as a determinant of mitochondrial fitness and correlates with level of mitochondrial plasticity, allowing bioenergetic adaptability in response to pathopsysiological stress conditions (Marchetti et al., 2020). Its decrease in older *sin-3(tm1276)* mutants is consistent with mitochondrial dysfunction in these animals.

Increased basal and maximal oxygen consumption in old *sin-3(tm1276)* animals contrasts with wildtype, in which oxygen consumption has a tendency to decrease with age (Huang and Lin, 2018; Koopman et al., 2016). Interestingly, a similar increase during aging was observed in worms lacking the mitochondrial prohibitin (PHB) complex subunits *phb-1* and *phb-2* (de la Cruz-Ruiz et al., 2021). Like *sin-3* mutants, prohibitin mutants are also short-lived and show severely fragmented mitochondria (Artal-Sanz and Tavernarakis, 2009; Artal-Sanz et al., 2003). PHB plays a prominent role in the response to mitochondrial stress, quality control, biogenesis, and degradation (Hernando-Rodríguez and Artal-Sanz, 2018), and its expression is induced by metabolic stress resulting from mito-nuclear imbalance, but not other cellular stresses (Yoneda et al., 2004). It was suggested that PHB may act as chaperone in respiratory complex assembly (Nijtmans, 2000), with its loss affecting complex integrity. Likewise, imbalance between nuclear- and mitochondrial-encoded subunits in *sin-3* mutants could result in defects in respiratory complex assembly, proton leakage, and dissipation of the proton gradient. In this context, increased oxygen consumption may reflect compensatory activity from properly assembled supercomplexes, or mitochondrial adaptation resulting in an increase in mitochondrial mass (Bennett et al., 2022).

Consistent with mitochondrial fragmentation being generally associated with metabolic dysfunction and disease (Wai and Langer, 2016), metabolomic analysis revealed dramatic changes in the levels of several metabolites in *sin-3(tm1276)* mutants. One of the most striking differences we observed is an increase in the polyamines spermine and cadaverine. Polyamine biosynthesis is tightly controlled, and changes in polyamine levels can have dramatic consequences on physiology, with established links

between polyamine metabolism and human diseases including cancer and diabetes (Madeo et al., 2018). Spermine is a potent free radical scavenger and an important antioxidant (Murray Stewart et al., 2018; Pegg, 2013), and in *C. elegans,* spermidine has been shown to inhibit neurodegeneration and have pro-longevity effects (Yang et al., 2020b). However, spermidine or spermine in excess can also have deleterious consequences on animal physiology (Kumar et al., 2022; Nakanishi and Cleveland, 2021; Pegg, 2013; Til et al., 1997), and SIN-3 inactivation or knock-down in *C. elegans* is associated with sterility, decreased longevity, and increased oxidative stress (Sharma et al., 2018). Our expression profiling suggests that decreased expression of the *oaz-1* antizyme, a critical regulator of polyamine biosynthesis (Coffino, 2001), may be a major contributor to the effect of SIN3 knock-down on polyamine homeostasis.

Among a broad range of functions, spermidine serves as the sole biosynthetic precursor for hypusination, a post-translational modification that is an integral component of eukaryotic translation initiation factor 5A (eIF5A) (Barba-Aliaga and Alepuz, 2022). Polyamine levels are elevated in most cancers, and hypusinated eIF5A is a critical regulator of cell growth (Nakanishi and Cleveland, 2016). More rescently, hypusinated eIF5A was shown to promote expression of mitochondrial proteins in macrophages (Puleston et al., 2019), suggesting that it may also alter mitochondrial activity in both normal and cancer cells. This raises the intriguing possibility that increased spermidine biosynthesis and eIF5A hypusylation in *sin-3* mutants may be part of a mechanism to increase expression of mitochondrial proteins in response to mitochondrial dysfunction.

Further evidence for a shift in metabolic flux towards polyamine biosynthesis comes from the analysis of downstream metabolites in the transmethylation pathway. Conversion of SAM to dcSAM provides necessary amino-propyl groups to sustain polyamine synthesis (Nakanishi and Cleveland, 2021). The methionine salvage pathway (MSP) recycles one carbon unit lost during polyamine synthesis back to the methionine cycle for SAM replenishment. In addition to showing a strong decrease in dcSAM, and a smaller but significant decrease in SAM, *sin-3* mutants also show reduced activity of the salvage pathway, as illustrated by a decrease in levels of the MSP intermediate methyladenosine (Figure 6C). Interestingly,

in Prostate cancer (PCa) cells, which have an intrinsically high polyamine metabolic flux and therefore rely heavily on the methionine salvage pathway, MSP inhibition while maintaining high polyamine flux was shown to be an effective cancer therapy by blocking the ability of the cell to mitigate this stress, leading to cell death (Affronti et al., 2020). In other tumor cell types, by contrast, defects in the MSP were found to increase polyamine levels, highlighting how the stress that is generated by metabolic perturbations is often context-dependent (Nakanishi and Cleveland, 2021). Our study may provide novel insight on the interconnected links between SIN3, methionine metabolism, polyamine biosynthesis, and mitochondrial homeostasis, and point to new lines of investigation.

Materials and Methods

Strains and culture

Strains were cultured on Nematode Growth Medium (NGM) agarose plates with *Escherichia coli* OP50 and incubated at 20°C. The following strains were used (*created for this study, (** from (Beurton et al., 2019);***from (Caron et al., 2023): wild type N2 Bristol, **PFR590 *sin-3(tm1276*) I, ***PHX2172 *sin-3*(syb2172)/hT2[bli-4(e937) let-?(q782) qIs48] I, KAG420 kagIs4[gfp::*myo-3*]V (Mergoud Dit Lamarche et al., 2018); *PFR750 *sin-3(tm1276)* I, kagIs4[*gfp*::*myo-3*]V; EN7714 krSi134[*myo-3p*::*tomm-20*Nter::wrmScarlet] (Roy et al., 2022); PFR754 *sin-3(tm1276)* I; krSi134[*myo-3*p::*tomm-20*Nter::wrmScarlet]; EGD629 egxSi155[*mex-5p::tomm-20*::mKate2::*pie-1* 3'UTR + *unc-119*(+)] II; PFR758 *sin-3(tm1276)*, egxSi155[*mex-5p::tomm-20*::mKate2::pie-1 3'UTR + *unc-119*(+)]II; *PFR669 *sin-3:*:mCherry(*syb521*); oxIs279[*pie-1*p::GFP::H2B + *unc-119*(+)]II; SJ4100 *zcIs13* [*hsp-6p*::GFP + *lin-15*(+)]. PFR750 and PFR754 were obtained by crossing *sin-3(tm1276)* hermaphrodites with GFP::*myo-3* or *myo-3*p::tomm-20Nter::wrmScarlet males, respectively.

Transmission electron microscopy

Worms (young adults) were fixed by HPF with EMPACT-2 (Leica Microsystems) and then freeze substituted in anhydrous acetone containing 1% OsO4, 0.5% glutaraldehyde and 0.25% uranyl acetate for 60 h in a FS system (AFS-2, Leica Microsystems). Larvae were embedded in Epon-Araldite mix (EMS hard formula). To gain better anteroposterior orientation and sectioning, adhesive frames were used (11560294 GENE-FRAME 65 µl, Thermo Fisher Scientific) for flat-embedding, as previously described (Kolotuev et al., 2012). Ultrathin sections were cut on an ultramicrotome (UC7; Leica Microsystems) and collected on formvar-coated slot grids (FCF2010-CU, EMS). Each larva was sectioned in five different places with ≥10 µm between each grid to ensure that different cells were observed. Each grid contained at least 5-10 consecutive sections of 70 nm. TEM grids were observed using a JEM-1400 transmission

electron microscope (JEOL) operated at 120 kV, equipped with a Gatan Orius SC200 camera (Gatan) and piloted by the Digital Micrograph program.

Quantification of muscle mitochondria and imaging of myofilament structure

For mitochondria and myofilament observation in muscle cells, staged worms were mounted on agarose pads in M9 solution containing 10% sodium azide. Muscles in the posterior part of worms were imaged. Z-stack images were acquired using a Zeiss LSM980 inverted confocal microscope with 63× oil immersion objective. Z-stacks were acquired every 0.27µm to image mitochondria and every 0.23µm to image myofilaments. Images shown are projections using max intensity method in Fiji. Quantification of mitochondrial morphology in body wall muscle cells was performed in double blind experiments according to the following criteria: cells containing long interconnected mitochondrial networks were classified as tubular, cells containing a combination of interconnected mitochondrial networks along with smaller fragmented mitochondria were classified as intermediate, and cells with sparse small round mitochondria were classified as fragmented (Regmi et al., 2014).

Activation of UPR^{mt} by RNAi treatment

RNAi bacteria were induced by directly adding 1 mM IPTG directly onto the bacteria lawn 2 hours before the transfer of worms (Shamalnasab et al., 2017). Transgenic animals expressing *hsp-6::*GFP were synchronized by bleaching, and the L1 stage animals obtained transferred to empty vector HT115 or *sin-3(*RNAi) 35mm plates, and allowed to develop to egg-laying adults (P0). 4-6 P0 adults from each RNAi treatment were then individually transferred onto: 1) empty vector control; 2) single RNAi (*sin-3*, *nuo-4*, *mrps-5)* or double RNAi plates (sin-3/*nuo-4*, *sin-3*/*mrps-5)* to induce mitochondrial stress in F1 progeny. *sin-3* RNAi treatment was started in P0 animals to ensure depletion of maternal SIN-3 protein in scored animals. GFP expression was assessed in F1 progeny 5 days after egg lay. For imaging, worms were immobilized using 2.5mM Levamisole in M9 buffer (22mM KH2PO4, 42mM Na2HPO4, 86mM NaCl, 1mM MgSO4). Images were acquired with a Nikon AZ100M microscope.

Oxygen consumption measurements

Worm oxygen consumption was measured using the Agilent Seahorse XFp Analyzer. Animals were synchronized by allowing gravid mothers to lay eggs for 2-3 hours before removing them from plate. Worms (20-30 per well) at the young adult stage or at day 6 of adulthood were transferred into M9-filled Seahorse plates. Working solutions were diluted in M9 at the following final concentrations: Carbonyl cyanide 4-(trifluoromethoxy) phenylhydrazone (FCCP) (Sigma-Aldrich) 250 µM, NaN_3 (Sigma-Aldrich) 400 mM. Oxygen Consumption Rate (OCR) measurements were repeated 8 times in basal conditions, 10 times after FCPP injection (for maximal respiration), and 4 times after NaN_3 injection (no mitochondrial respiration). Each cycle consisted of 3 min mix, 30 second wait, and 3 min measure. Values were normalized per worm. Three independent assays were carried out and the combined data was analyzed by Unpaired t-test, or, when appropriate, Mann-Whitney test, using GraphPad Prism software.

Western blot analysis

Young adult worms were collected in M9 buffer, washed 3 times, pelleted and frozen in dry ice. Pellets were resuspended in TNET buffer (50 mM Tris·HCl (pH 8), 300 mM NaCl, 1 mM EDTA, 0,5% Triton X-100 and cOmplete™ Protease Inhibitor Cocktail [Merck # 11697498001]) and lysed with zirconium beads [Lysing Matrix Y, MP Biomedicals #116960050] using a Precellys24 homogenizer [Ozyme] with the following parameters : 6000 rpm 2x20sec. Homogenates were centrifuged and supernatants aliquoted and frozen at −80◦C. Total protein amount was quantified by the Bradford assay [Bio-Rad]. 10,20,30,40,50 and 80 ug of protein extracts were loaded either on 12% NuPage Novex or 12 % SDS PAGE gels for western blot analysis. After transfer, membranes were incubated overnight with total OXPHOS Rodent WB Antibody Cocktail [Abcam #ab110413] diluted at 1:500 or anti-alpha-tubulin [Abcam #ab18251] diluted at 1:5,000. The next day, membranes were incubated for 1 hour with goat anti-rabbit DyLight™ 800 [Invitrogen # SA5-10036] and IRDye® 680RD goat anti-mouse [LiCOR #926-68070] diluted at 1:10,000. Aquisition was performed on a ChemiDoc MP apparatus [Bio-Rad]. Quantification was carried out using Image J, and each protein signal was normalized to the level of tubulin. Two to three independent biological replicates and three to four technical replicates were used for quantification.

Metabolite extraction and profiling

Embryos derived from bleaching were transferred onto 90 mm plates seeded with 0P50 bacteria and left to develop to the young adult stage. Animals were collected in M9 medium, washed 3 times in 10 ml M9, and pellets quick frozen in liquid nitrogen (Spanier et al., 2021) prior to processing. 8 replicas, each containing approximately 2000 worms, were processed per genotype. All chemicals and solvents were of LC-MS or analytical grade. *C. elegans* samples were thawed on ice and 1 ml of ice-cold H_2O/MeOH/$CHCl_3$ (1/3/1, v/v/v). After suspension in solvent, *C. elegans* animals were transferred to 2 ml MN Bead Tubes Type A (Macherey-Nagel, Düren, Germany) and lysed using a Precellys Bead Beating system with an additional Cryolys cooling module (Bertin Instruments, Montigny-le-Bretonneux, France). After lysis, samples were incubated for 10 minutes in an ice-cold ultrasonic bath, followed by centrifugation at 4°C and 13,000 rpm for 15 minutes. The supernatant was transferred to a fresh reaction tube and evaporated to dryness using a centrifugal evaporator. Proteins were extracted from residue debris pellets and quantified using a BCA kit (Sigma-Aldrich, Taufkirchen, Germany). Metabolite profiling was performed using a Sciex ExionLC AD coupled to a Sciex ZenoTOF 7600 under the control of Sciex OS 3.0 (Sciex, Darmstadt, Germany). Separation was achieved on an Agilent InfinityLab Poroshell 120 HILIC-Z column (2.1 mm x 150 mm, 2.7 µm particle size, PEEK-lined) (Agilent Technologies, Waldbronn, Germany). Different eluents and gradients were applied for positive and negative ionization modes. In positive ionization mode, eluent A consisted of 100% H_2O + 10 mM ammonium formate / 0.1% formic acid, and eluent B consisted of 10% H_2O / 90% ACN + 10 mM ammonium formate / 0.1% formic acid. In negative ionization mode, eluent A consisted of 100% H_2O + 10 mM ammonium acetate / 2.5 µM medronic acid, pH = 9, and eluent A consisted of 15% H_2O / 85% ACN + 10 mm ammonium acetate / 2.5 µM medronic acid, pH = 9. The column temperature was set to 25°C and 50°C for positive and negative ionization modes, respectively, and the flow rate was 0.25 mL/min in both cases. Gradients for both ionization modes are summarized in Table S2. Dried samples were re-dissolved in 50 µL H_2O/ACN (1/3, v/v), and 40 µL were transferred to an autosampler vial and 10 µL to a pooled QC sample. Autosampler temperature was set to 5°C and 5 µl were injected for analysis. In $MS^{1,}$ ions in the m/z range 70 to 1500

were accumulated for 0.1s, and information-dependent acquisition (IDA) of MS^2 was used with a maximum number of 6 candidate ions and a collision energy of 35 eV with a spread of 15 eV. Accumulation time for MS2 was set to 0.025s yielding a total cycle time of 0.299s. ZenoTrapping was enabled with a value of 80000. QC samples were used for conditioning the column and were also injected every ten samples. Automatic calibration of the mass spectrometer in MS^1 and MS^2 mode was performed every five injections using the ESI positive Calibration Solution for the Sciex X500 system or the ESI negative Calibration Solution for the Sciex X500 system (Sciex, Darmstadt, Germany).

Metabolite data analysis

Data analysis was performed in a targeted fashion for identified metabolites (see Tables S4 and S5). Metabolites were identified by comparison to in-house reference standards, publicly available reference spectra, and manual interpretation of fragmentation spectra. Data analysis was performed in Sciex OS 3.0.0.3339 (Sciex, Darmstadt, Germany). Peaks for all metabolites indicated in Tables S4 and S5 were integrated with an XIC width of 0.02 Da and a Gaussian smooth width of 3 points using the MQ4 peak-picking algorithm. Peak areas were exported to a .txt file and normalized according to the protein content of the respective sample. All further processing was performed in R 4.2.1 within RStudio using the following packages: tidyverse (1.3.2), readxl (1.4.1), ggsignif (0.6.4), gghalves (0.1.4), scales (1.2.1) and viridis (0.6.2). Data were plotted using ggplot with gghalves using half box- and half dot-plots. Significance was tested using a Welch test within ggsignif.

Acknowledgments

FP was supported by ANR (Agence Nationale de la Recherche) grant N° 19-CE12-0025-01 and the Centre National de la Recherche Scientifique. MAS was funded through grants from the Ministerio de Ciencia, Innovación y Universidades, the Agencia Estatal de Investigación (AEI) PID 2019-104145GB-I00. GM laboratory receives institutional funding from the Centre National De La Recherche Scientifique and the Université de Rennes. TEM imaging was performed at the Microscopy Rennes imaging Center (Biosit, Rennes, France), a member of the national infrastructure France-BioImaging supported by the French National Research Agency (ANR-10-INBS-04).

Author contributions

PF, FP, GM, MAS and MW conceived and designed experiments, MG, MJRP, ON and MW and CB performed experiments and analyzed the data, FP, MAS and MW wrote the paper.

References

Affronti, H.C., A.M. Rowsam, A.J. Pellerite, S.R. Rosario, M.D. Long, J.J. Jacobi, A. Bianchi-Smiraglia, C.S. Boerlin, B.M. Gillard, E. Karasik, B.A. Foster, M. Moser, J.H. Wilton, K. Attwood, M.A. Nikiforov, G. Azabdaftari, R. Pili, J.G. Phillips, R.A. Casero, and D.J. Smiraglia. 2020. Pharmacological polyamine catabolism upregulation with methionine salvage pathway inhibition as an effective prostate cancer therapy. *Nat Commun*. 11:52. doi:10.1038/s41467-019-13950-4.

Al Rawi, S., S. Louvet-Vallée, A. Djeddi, M. Sachse, E. Culetto, C. Hajjar, L. Boyd, R. Legouis, and V. Galy. 2011. Postfertilization Autophagy of Sperm Organelles Prevents Paternal Mitochondrial DNA Transmission. *Science*. 334:1144–1147. doi:10.1126/science.1211878.

Ali, A.T., L. Boehme, G. Carbajosa, V.C. Seitan, K.S. Small, and A. Hodgkinson. 2019. Nuclear genetic regulation of the human mitochondrial transcriptome. *Elife*. 8:e41927. doi:10.7554/eLife.41927.

Anderson, N.S., and C.M. Haynes. 2020. Folding the Mitochondrial UPR into the Integrated Stress Response. *Trends in Cell Biology*. 30:428–439. doi:10.1016/j.tcb.2020.03.001.

Artal-Sanz, M., and N. Tavernarakis. 2009. Prohibitin couples diapause signalling to mitochondrial metabolism during ageing in C. elegans. *Nature*. 461:793–797. doi:10.1038/nature08466.

Artal-Sanz, M., W.Y. Tsang, E.M. Willems, L.A. Grivell, B.D. Lemire, H. van der Spek, and L.G.J. Nijtmans. 2003. The mitochondrial prohibitin complex is essential for embryonic viability and germline function in Caenorhabditis elegans. *J Biol Chem*. 278:32091–32099. doi:10.1074/jbc.M304877200.

Balasubramanian, M., A.J.M. Dingemans, S. Albaba, R. Richardson, T.M. Yates, H. Cox, S. Douzgou, R. Armstrong, F.H. Sansbury, K.B. Burke, A.E. Fry, N. Ragge, S. Sharif, A. Foster, A. De Sandre-Giovannoli, S. Elouej, P. Vasudevan, S. Mansour, K. Wilson, H. Stewart, S. Heide, C. Nava, B. Keren, S. Demirdas, A.S. Brooks, M. Vincent, B. Isidor, S. Küry, M. Schouten, E. Leenders, W.K. Chung, A. van Haeringen, T. Scheffner, F.-G. Debray, S.M. White, M.I.V. Palafoll, R. Pfundt, R. Newbury-Ecob, and T. Kleefstra. 2021. Comprehensive study of 28 individuals with SIN3A-related disorder underscoring the associated mild cognitive and distinctive facial phenotype. *Eur J Hum Genet*. 29:625–636. doi:10.1038/s41431-020-00769-7.

Bansal, N., G. David, E. Farias, and S. Waxman. 2016. Emerging Roles of Epigenetic Regulator Sin3 in Cancer. *Adv. Cancer Res.* 130:113–135. doi:10.1016/bs.acr.2016.01.006.

Bansal, N., K. Petrie, R. Christova, C.-Y. Chung, B.A. Leibovitch, L. Howell, V. Gil, Y. Sbirkov, E. Lee, J. Wexler, E.V. Ariztia, R. Sharma, J. Zhu, E. Bernstein, M.-M. Zhou, A. Zelent, E. Farias, and S. Waxman. 2015. Targeting the SIN3A-PF1 interaction inhibits epithelial to mesenchymal transition and maintenance of a stem cell phenotype in triple negative breast cancer. *Oncotarget*. 6:34087–34105. doi:10.18632/oncotarget.6048.

Barba-Aliaga, M., and P. Alepuz. 2022. Role of eIF5A in Mitochondrial Function. *IJMS*. 23:1284. doi:10.3390/ijms23031284.

Barnes, V.L., A. Bhat, A. Unnikrishnan, A.R. Heydari, R. Arking, and L.A. Pile. 2014. SIN3 is critical for stress resistance and modulates adult lifespan. *Aging*. 6:645–660. doi:10.18632/aging.100684.

Barnes, V.L., B.S. Strunk, I. Lee, M. Hüttemann, and L.A. Pile. 2010. Loss of the SIN3 transcriptional corepressor results in aberrant mitochondrial function. *BMC Biochem*. 11:26. doi:10.1186/1471-2091-11-26.

Barshad, G., A. Blumberg, T. Cohen, and D. Mishmar. 2018. Human primitive brain displays negative mitochondrial-nuclear expression correlation of respiratory genes. *Genome Res*. 28:952–967. doi:10.1101/gr.226324.117.

Baymaz, H.I., I.D. Karemaker, and M. Vermeulen. 2015. Perspective on unraveling the versatility of 'co-repressor' complexes. *Biochimica et Biophysica Acta (BBA) - Gene Regulatory Mechanisms*. 1849:1051–1056. doi:10.1016/j.bbagrm.2015.06.012.

Bennett, C.F., P. Latorre-Muro, and P. Puigserver. 2022. Mechanisms of mitochondrial respiratory adaptation. *Nat Rev Mol Cell Biol*. 23:817–835. doi:10.1038/s41580-022-00506-6.

Berry, B.J., E. Mjelde, F. Carreno, K. Gilham, E.J. Hanson, E. Na, and M. Kaeberlein. 2022. Preservation of Mitochondrial Membrane Potential is Necessary for Lifespan Extension from Dietary Restriction. Physiology.

Bertholet, A.M., E.T. Chouchani, L. Kazak, A. Angelin, A. Fedorenko, J.Z. Long, S. Vidoni, R. Garrity, J. Cho, N. Terada, D.C. Wallace, B.M. Spiegelman, and Y. Kirichok. 2019. H+ transport is an integral function of the mitochondrial ADP/ATP carrier. *Nature*. 571:515–520. doi:10.1038/s41586-019-1400-3.

Beurton, F., P. Stempor, M. Caron, A. Appert, Y. Dong, R.A.-J. Chen, D. Cluet, Y. Couté, M. Herbette, N. Huang, H. Polveche, M. Spichty, C. Bedet, J. Ahringer, and F. Palladino. 2019. Physical and functional interaction between SET1/COMPASS complex component CFP-1 and a Sin3S HDAC complex in C. elegans. *Nucleic Acids Res*. 47:11164–11180. doi:10.1093/nar/gkz880.

Byrne, J.J., M.S. Soh, G. Chandhok, T. Vijayaraghavan, J.-S. Teoh, S. Crawford, A.E. Cobham, N.M.B. Yapa, C.K. Mirth, and B. Neumann. 2019. Disruption of mitochondrial dynamics affects behaviour and lifespan in Caenorhabditis elegans. *Cell. Mol. Life Sci.* 76:1967–1985. doi:10.1007/s00018-019-03024-5.

Caron, M., V. Robert, L. Gely, A. Adrait, V. Pakulska, Y. Couté, M. Chevalier, C.G. Riedel, C. Bedet, and F. Palladino. 2023. SIN3 acts in distinct complexes to regulate the germline transcriptional program in *C. elegans*. Genetics.

Chaubal, A., and L.A. Pile. 2018. Same agent, different messages: insight into transcriptional regulation by SIN3 isoforms. *Epigenetics Chromatin*. 11:17. doi:10.1186/s13072-018-0188-y.

Chen, H., and D.C. Chan. 2009. Mitochondrial dynamics-fusion, fission, movement, and mitophagy-in neurodegenerative diseases. *Human Molecular Genetics*. 18:R169–R176. doi:10.1093/hmg/ddp326.

Chen, Y., R. Leboutet, C. Largeau, S. Zentout, C. Lefebvre, A. Delahodde, E. Culetto, and R. Legouis. 2021. Autophagy facilitates mitochondrial rebuilding after acute heat stress via a DRP-1–dependent process. *Journal of Cell Biology*. 220:e201909139. doi:10.1083/jcb.201909139.

Christian, C.J., and G.M. Benian. 2020. Animal models of sarcopenia. *Aging Cell*. 19. doi:10.1111/acel.13223.

Coffino, P. 2001. Regulation of cellular polyamines by antizyme. *Nat Rev Mol Cell Biol*. 2:188–194. doi:10.1038/35056508.

de la Cruz-Ruiz, P., B. Hernando-Rodríguez, M.M. Pérez-Jiménez, M.J. Rodríguez-Palero, M.D. Martínez-Bueno, A. Pla, R. Gatsi, and M. Artal-Sanz. 2021. Prohibitin depletion extends lifespan of a TORC2/SGK-1 mutant through autophagy and the mitochondrial UPR. *Aging Cell*. 20:e13359. doi:10.1111/acel.13359.

Dannenberg, J.-H., G. David, S. Zhong, J. van der Torre, W.H. Wong, and R.A. Depinho. 2005. mSin3A corepressor regulates diverse transcriptional networks governing normal and neoplastic growth and survival. *Genes Dev.* 19:1581–1595. doi:10.1101/gad.1286905.

Demine, Renard, and Arnould. 2019. Mitochondrial Uncoupling: A Key Controller of Biological Processes in Physiology and Diseases. *Cells*. 8:795. doi:10.3390/cells8080795.

DiMauro, S., and E.A. Schon. 2003. Mitochondrial Respiratory-Chain Diseases. *N Engl J Med*. 348:2656–2668. doi:10.1056/NEJMra022567.

Ducamp, S., and M.D. Fleming. 2019. The molecular genetics of sideroblastic anemia. *Blood*. 133:59–69. doi:10.1182/blood-2018-08-815951.

Etheridge, T., M. Rahman, C.J. Gaffney, D. Shaw, F. Shephard, J. Magudia, D.E. Solomon, T. Milne, J. Blawzdziewicz, D. Constantin-Teodosiu, P.L. Greenhaff, S.A. Vanapalli, and N.J. Szewczyk. 2015. The integrin-adhesome is required to maintain muscle structure, mitochondrial ATP production, and movement forces in *Caenorhabditis elegans*. *FASEB j.* 29:1235–1246. doi:10.1096/fj.14-259119.

Farias, E.F., K. Petrie, B. Leibovitch, J. Murtagh, M.B. Chornet, T. Schenk, A. Zelent, and S. Waxman. 2010. Interference with Sin3 function induces epigenetic reprogramming and differentiation in breast cancer cells. *Proc. Natl. Acad. Sci. U.S.A.* 107:11811–11816. doi:10.1073/pnas.1006737107.

Fernandez-Vizarra, E., and M. Zeviani. 2021. Mitochondrial disorders of the OXPHOS system. *FEBS Lett*. 595:1062–1106. doi:10.1002/1873-3468.13995.

Gaffney, C.J., A. Pollard, T.F. Barratt, D. Constantin-Teodosiu, P.L. Greenhaff, and N.J. Szewczyk. 2018. Greater loss of mitochondrial function with ageing is associated with earlier onset of sarcopenia in C. elegans. *Aging*. 10:3382–3396. doi:10.18632/aging.101654.

Hanover, J.A., M.E. Forsythe, P.T. Hennessey, T.M. Brodigan, D.C. Love, G. Ashwell, and M. Krause. 2005. A Caenorhabditis elegans model of insulin resistance: altered macronutrient storage and dauer formation in an OGT-1 knockout. *Proc Natl Acad Sci U S A*. 102:11266–11271. doi:10.1073/pnas.0408771102.

Haeussler, S., and B. Conradt. 2022. Methods to Study the Mitochondrial Unfolded Protein Response (UPRmt) in Caenorhabditis elegans. *In* The Unfolded Protein Response. R. Pérez-Torrado, editor. Springer US, New York, NY. 249–259.

Hernando-Rodríguez, B., and M. Artal-Sanz. 2018. Mitochondrial Quality Control Mechanisms and the PHB (Prohibitin) Complex. *Cells*. 7:238. doi:10.3390/cells7120238.

Higashitani, A., M. Teranishi, Y. Nakagawa, Y. Itoh, S. Sudevan, N.J. Szewczyk, Y. Kubota, T. Abe, and T. Kobayashi. 2022. Increased mitochondrial Ca^{2+} contributes to health decline with age and Duchene muscular dystrophy in *C. elegans*. Cell Biology.

Holdorf, A.D., D.P. Higgins, A.C. Hart, P.R. Boag, G.J. Pazour, A.J.M. Walhout, and A.K. Walker. 2020. WormCat: An Online Tool for Annotation and Visualization of *Caenorhabditis elegans* Genome-Scale Data. *Genetics*. 214:279–294. doi:10.1534/genetics.119.302919.

Houtkooper, R.H., L. Mouchiroud, D. Ryu, N. Moullan, E. Katsyuba, G. Knott, R.W. Williams, and J. Auwerx. 2013. Mitonuclear protein imbalance as a conserved longevity mechanism. *Nature*. 497:451–457. doi:10.1038/nature12188.

Huang, S.-H., and Y.-W. Lin. 2018. Bioenergetic Health Assessment of a Single Caenorhabditis elegans from Postembryonic Development to Aging Stages via Monitoring Changes in the Oxygen Consumption Rate within a Microfluidic Device. *Sensors*. 18:2453. doi:10.3390/s18082453.

Jeong, H.D., J.H. Kim, G.E. Kwon, and S.-T. Lee. 2022. Expression of Polyamine Oxidase in Fibroblasts Induces MMP-1 and Decreases the Integrity of Extracellular Matrix. *IJMS*. 23:10487. doi:10.3390/ijms231810487.

Kolotuev, I., D.J. Bumbarger, M. Labouesse, and Y. Schwab. 2012. Targeted Ultramicrotomy. *In* Methods in Cell Biology. Elsevier. 203–222.

Koopman, M., H. Michels, B.M. Dancy, R. Kamble, L. Mouchiroud, J. Auwerx, E.A.A. Nollen, and R.H. Houtkooper. 2016. A screening-based platform for the assessment of cellular respiration in Caenorhabditis elegans. *Nat Protoc*. 11:1798–1816. doi:10.1038/nprot.2016.106.

Kropp, P.A., J. Wu, M. Reidy, S. Shrestha, K. Rhodehouse, P. Rogers, M.N. Sack, and A. Golden. 2021. Allele-specific mitochondrial stress induced by Multiple Mitochondrial Dysfunctions Syndrome 1 pathogenic mutations modeled in Caenorhabditis elegans. *PLoS Genet*. 17:e1009771. doi:10.1371/journal.pgen.1009771.

Kumar, V., R.K. Mishra, D. Ghose, A. Kalita, P. Dhiman, A. Prakash, N. Thakur, G. Mitra, V.D. Chaudhari, A. Arora, and D. Dutta. 2022. Free spermidine evokes superoxide radicals that manifest toxicity. *eLife*. 11:e77704. doi:10.7554/eLife.77704.

Labrousse, A.M., M.D. Zappaterra, D.A. Rube, and A.M. van der Bliek. 1999. C. elegans Dynamin-Related Protein DRP-1 Controls Severing of the Mitochondrial Outer Membrane. *Molecular Cell*. 4:815–826. doi:10.1016/S1097-2765(00)80391-3.

Latypova, X., M. Vincent, A. Mollé, O.A. Adebambo, C. Fourgeux, T.N. Khan, A. Caro, M. Rosello, C. Orellana, D. Niyazov, D. Lederer, M. Deprez, Y. Capri, P. Kannu, A.C. Tabet, J. Levy, E. Aten, N. den Hollander, M. Splitt, J. Walia, L.L. Immken, P. Stankiewicz, K. McWalter, S. Suchy, R.J.

Louie, S. Bell, R.E. Stevenson, J. Rousseau, C. Willem, C. Retiere, X.-J. Yang, P.M. Campeau, F. Martinez, J.A. Rosenfeld, C. Le Caignec, S. Küry, S. Mercier, K. Moradkhani, S. Conrad, T. Besnard, B. Cogné, N. Katsanis, S. Bézieau, J. Poschmann, E.E. Davis, and B. Isidor. 2021. Haploinsufficiency of the Sin3/HDAC corepressor complex member SIN3B causes a syndromic intellectual disability/autism spectrum disorder. *The American Journal of Human Genetics*. 108:929–941. doi:10.1016/j.ajhg.2021.03.017.

Leandro, J., and S.M. Houten. 2020. The lysine degradation pathway: Subcellular compartmentalization and enzyme deficiencies. *Molecular Genetics and Metabolism*. 131:14–22. doi:10.1016/j.ymgme.2020.07.010.

Lewis, M.J., J. Liu, E.F. Libby, M. Lee, N.P.S. Crawford, and D.R. Hurst. 2016. SIN3A and SIN3B differentially regulate breast cancer metastasis. *Oncotarget*. 7:78713–78725. doi:10.18632/oncotarget.12805.

Liang, V., M. Ullrich, H. Lam, Y.L. Chew, S. Banister, X. Song, T. Zaw, M. Kassiou, J. Götz, and H.R. Nicholas. 2014. Altered proteostasis in aging and heat shock response in C. elegans revealed by analysis of the global and de novo synthesized proteome. *Cell. Mol. Life Sci.* 71:3339–3361. doi:10.1007/s00018-014-1558-7.

Lin, Y.-F., and C.M. Haynes. 2016. Metabolism and the UPR mt. *Molecular Cell*. 61:677–682. doi:10.1016/j.molcel.2016.02.004.

Lionaki, E., I. Gkikas, I. Daskalaki, M.-K. Ioannidi, M.I. Klapa, and N. Tavernarakis. 2022. Mitochondrial protein import determines lifespan through metabolic reprogramming and de novo serine biosynthesis. *Nat Commun*. 13:651. doi:10.1038/s41467-022-28272-1.

Locasale, J.W. 2013. Serine, glycine and one-carbon units: cancer metabolism in full circle. *Nat Rev Cancer*. 13:572–583. doi:10.1038/nrc3557.

Luz, A.L., J.P. Rooney, L.L. Kubik, C.P. Gonzalez, D.H. Song, and J.N. Meyer. 2015. Mitochondrial Morphology and Fundamental Parameters of the Mitochondrial Respiratory Chain Are Altered in Caenorhabditis elegans Strains Deficient in Mitochondrial Dynamics and Homeostasis Processes. *PLoS One*. 10:e0130940. doi:10.1371/journal.pone.0130940.

Macrae, M., R.H. Plasterk, and P. Coffino. 1995. The ornithine decarboxylase gene of Caenorhabditis elegans: cloning, mapping and mutagenesis. *Genetics*. 140:517–525. doi:10.1093/genetics/140.2.517.

Madeo, F., T. Eisenberg, F. Pietrocola, and G. Kroemer. 2018. Spermidine in health and disease. *Science*. 359:eaan2788. doi:10.1126/science.aan2788.

Marchetti, P., Q. Fovez, N. Germain, R. Khamari, and J. Kluza. 2020. Mitochondrial spare respiratory capacity: Mechanisms, regulation, and significance in non-transformed and cancer cells. *FASEB j.* 34:13106–13124. doi:10.1096/fj.202000767R.

Matilainen, O., P.M. Quirós, and J. Auwerx. 2017. Mitochondria and Epigenetics - Crosstalk in Homeostasis and Stress. *Trends Cell Biol*. 27:453–463. doi:10.1016/j.tcb.2017.02.004.

Melber, A., and C.M. Haynes. 2018. UPRmt regulation and output: a stress response mediated by mitochondrial-nuclear communication. *Cell Res*. 28:281–295. doi:10.1038/cr.2018.16.

Mercer, T.R., S. Neph, M.E. Dinger, J. Crawford, M.A. Smith, A.-M.J. Shearwood, E. Haugen, C.P. Bracken, O. Rackham, J.A. Stamatoyannopoulos, A. Filipovska, and J.S. Mattick. 2011. The human mitochondrial transcriptome. *Cell*. 146:645–658. doi:10.1016/j.cell.2011.06.051.

Mergoud Dit Lamarche, A., L. Molin, L. Pierson, M.-C. Mariol, J.-L. Bessereau, K. Gieseler, and F. Solari. 2018. UNC-120/SRF independently controls muscle aging and lifespan in Caenorhabditis elegans. *Aging Cell*. 17:e12713. doi:10.1111/acel.12713.

Murray Stewart, T., T.T. Dunston, P.M. Woster, and R.A. Casero. 2018. Polyamine catabolism and oxidative damage. *Journal of Biological Chemistry*. 293:18736–18745. doi:10.1074/jbc.TM118.003337.

Nakanishi, S., and J.L. Cleveland. 2021. Polyamine Homeostasis in Development and Disease. *Medical Sciences*. 9:28. doi:10.3390/medsci9020028.

Nielsen, J. 2003. It Is All about MetabolicFluxes. *J Bacteriol*. 185:7031–7035. doi:10.1128/JB.185.24.7031-7035.2003.

Nijtmans, L.G.J. 2000. Prohibitins act as a membrane-bound chaperone for the stabilization of mitochondrial proteins. *The EMBO Journal*. 19:2444–2451. doi:10.1093/emboj/19.11.2444.

van Oevelen, C., C. Bowman, J. Pellegrino, P. Asp, J. Cheng, F. Parisi, M. Micsinai, Y. Kluger, A. Chu, A. Blais, G. David, and B.D. Dynlacht. 2010. The Mammalian Sin3 Proteins Are Required for Muscle Development and Sarcomere Specification. *Molecular and Cellular Biology*. 30:5686–5697. doi:10.1128/MCB.00975-10.

Onishi, M., K. Yamano, M. Sato, N. Matsuda, and K. Okamoto. 2021. Molecular mechanisms and physiological functions of mitophagy. *EMBO J*. 40:e104705. doi:10.15252/embj.2020104705.

Pandey, R., M. Sharma, and D. Saluja. 2018. SIN-3 as a key determinant of lifespan and its sex dependent differential role on healthspan in Caenorhabditis elegans. *Aging*. 10:3910–3937. doi:10.18632/aging.101682.

Park, M.H., K. Nishimura, C.F. Zanelli, and S.R. Valentini. 2010. Functional significance of eIF5A and its hypusine modification in eukaryotes. *Amino Acids*. 38:491–500. doi:10.1007/s00726-009-0408-7.

Pegg, A.E. 2013. Toxicity of Polyamines and Their Metabolic Products. *Chem. Res. Toxicol.* 26:1782–1800. doi:10.1021/tx400316s.

Pile, L.A., P.T. Spellman, R.J. Katzenberger, and D.A. Wassarman. 2003. The SIN3 Deacetylase Complex Represses Genes Encoding Mitochondrial Proteins. *Journal of Biological Chemistry*. 278:37840–37848. doi:10.1074/jbc.M305996200.

Puccio, H., D. Simon, M. Cossée, P. Criqui-Filipe, F. Tiziano, J. Melki, C. Hindelang, R. Matyas, P. Rustin, and M. Koenig. 2001. Mouse models for Friedreich ataxia exhibit cardiomyopathy, sensory nerve defect and Fe-S enzyme deficiency followed by intramitochondrial iron deposits. *Nat Genet*. 27:181–186. doi:10.1038/84818.

Puleston, D.J., M.D. Buck, R.I. Klein Geltink, R.L. Kyle, G. Caputa, D. O'Sullivan, A.M. Cameron, A. Castoldi, Y. Musa, A.M. Kabat, Y. Zhang, L.J. Flachsmann, C.S. Field, A.E. Patterson, S. Scherer,

F. Alfei, F. Baixauli, S.K. Austin, B. Kelly, M. Matsushita, J.D. Curtis, K.M. Grzes, M. Villa, M. Corrado, D.E. Sanin, J. Qiu, N. Pällman, K. Paz, M.E. Maccari, B.R. Blazar, G. Mittler, J.M. Buescher, D. Zehn, S. Rospert, E.J. Pearce, S. Balabanov, and E.L. Pearce. 2019. Polyamines and eIF5A Hypusination Modulate Mitochondrial Respiration and Macrophage Activation. *Cell Metabolism*. 30:352-363.e8. doi:10.1016/j.cmet.2019.05.003.

Quirós, P.M., A. Mottis, and J. Auwerx. 2016. Mitonuclear communication in homeostasis and stress. *Nat Rev Mol Cell Biol*. 17:213–226. doi:10.1038/nrm.2016.23.

Quirós, P.M., M.A. Prado, N. Zamboni, D. D'Amico, R.W. Williams, D. Finley, S.P. Gygi, and J. Auwerx. 2017. Multi-omics analysis identifies ATF4 as a key regulator of the mitochondrial stress response in mammals. *J Cell Biol*. 216:2027–2045. doi:10.1083/jcb.201702058.

Reeve, A.K., K.J. Krishnan, and D. Turnbull. 2008. Mitochondrial DNA Mutations in Disease, Aging, and Neurodegeneration. *Annals of the New York Academy of Sciences*. 1147:21–29. doi:10.1196/annals.1427.016.

Regmi, S.G., S.G. Rolland, and B. Conradt. 2014. Age-dependent changes in mitochondrial morphology and volume are not predictors of lifespan. *Aging*. 6:118–130. doi:10.18632/aging.100639.

Richter-Dennerlein, R., S. Oeljeklaus, I. Lorenzi, C. Ronsör, B. Bareth, A.B. Schendzielorz, C. Wang, B. Warscheid, P. Rehling, and S. Dennerlein. 2016. Mitochondrial Protein Synthesis Adapts to Influx of Nuclear-Encoded Protein. *Cell*. 167:471-483.e10. doi:10.1016/j.cell.2016.09.003.

Rolland, S., and B. Conradt. 2022. Genetic screen identifies non-mitochondrial proteins involved in the maintenance of mitochondrial homeostasis. *MicroPubl Biol*. 2022. doi:10.17912/micropub.biology.000562.

Rolland, S.G., S. Schneid, M. Schwarz, E. Rackles, C. Fischer, S. Haeussler, S.G. Regmi, A. Yeroslaviz, B. Habermann, D. Mokranjac, E. Lambie, and B. Conradt. 2019. Compromised Mitochondrial Protein Import Acts as a Signal for UPRmt. *Cell Reports*. 28:1659-1669.e5. doi:10.1016/j.celrep.2019.07.049.

Ryan, M.T., and N.J. Hoogenraad. 2007. Mitochondrial-nuclear communications. *Annu Rev Biochem*. 76:701–722. doi:10.1146/annurev.biochem.76.052305.091720.

Schaeffer, J.M., and M.R. Donatelli. 1990. Characterization of a high-affinity membrane-associated ornithine decarboxylase from the free-living nematode Caenorhabditis elegans. *Biochem J*. 270:599–604. doi:10.1042/bj2700599.

Schiavi, A., S. Maglioni, K. Palikaras, A. Shaik, F. Strappazzon, V. Brinkmann, A. Torgovnick, N. Castelein, S. De Henau, B.P. Braeckman, F. Cecconi, N. Tavernarakis, and N. Ventura. 2015. Iron-Starvation-Induced Mitophagy Mediates Lifespan Extension upon Mitochondrial Stress in C. elegans. *Current Biology*. 25:1810–1822. doi:10.1016/j.cub.2015.05.059.

Schober, F.A., D. Moore, I. Atanassov, M.F. Moedas, P. Clemente, Á. Végvári, N.E. Fissi, R. Filograna, A.-L. Bucher, Y. Hinze, M. The, E. Hedman, E. Chernogubova, A. Begzati, R. Wibom, M. Jain, R. Nilsson, L. Käll, A. Wedell, C. Freyer, and A. Wredenberg. 2021. The one-carbon pool controls mitochondrial energy metabolism via complex I and iron-sulfur clusters. *Sci. Adv.* 7:eabf0717. doi:10.1126/sciadv.abf0717.

Scoville, D.W., H.A. Cyphert, L. Liao, J. Xu, A. Reynolds, S. Guo, and R. Stein. 2015. MLL3 and MLL4 Methyltransferases Bind to the MAFA and MAFB Transcription Factors to Regulate Islet β-Cell Function. *Diabetes*. 64:3772–3783. doi:10.2337/db15-0281.

Shamalnasab, M., M. Dhaoui, M. Thondamal, E.B. Harvald, N.J. Færgeman, H. Aguilaniu, and P. Fabrizio. 2017. HIF-1–dependent regulation of lifespan in Caenorhabditis elegans by the acyl-CoA–binding protein MAA-1. *Aging*. 9:1745–1769. doi:10.18632/aging.101267.

Shao, L.-W., Q. Peng, M. Dong, K. Gao, Y. Li, Y. Li, C.-Y. Li, and Y. Liu. 2020. Histone deacetylase HDA-1 modulates mitochondrial stress response and longevity. *Nat Commun*. 11:4639. doi:10.1038/s41467-020-18501-w.

Sharma, M., R. Pandey, and D. Saluja. 2018. ROS is the major player in regulating altered autophagy and lifespan in sin-3 mutants of C. elegans. *Autophagy*. 14:1239–1255. doi:10.1080/15548627.2018.1474312.

Signes, A., and E. Fernandez-Vizarra. 2018. Assembly of mammalian oxidative phosphorylation complexes I–V and supercomplexes. *Essays in Biochemistry*. 62:255–270. doi:10.1042/EBC20170098.

Spanier, B., A. Laurençon, A. Weiser, N. Pujol, S. Omi, A. Barsch, A. Korf, S.W. Meyer, J.J. Ewbank, F. Palladino, S. Garvis, H. Aguilaniu, and M. Witting. 2021. Correction to: Comparison of lipidome profiles of Caenorhabditis elegans—results from an inter-laboratory ring trial. *Metabolomics*. 17:33. doi:10.1007/s11306-021-01784-5.

Taanman, J.-W. 1999. The mitochondrial genome: structure, transcription, translation and replication. *Biochimica et Biophysica Acta (BBA) - Bioenergetics*. 1410:103–123. doi:10.1016/S0005-2728(98)00161-3.

Tian, Y., G. Garcia, Q. Bian, K.K. Steffen, L. Joe, S. Wolff, B.J. Meyer, and A. Dillin. 2016. Mitochondrial Stress Induces Chromatin Reorganization to Promote Longevity and UPR mt. *Cell*. 165:1197–1208. doi:10.1016/j.cell.2016.04.011.

Til, H.P., H.E. Falke, M.K. Prinsen, and M.I. Willems. 1997. Acute and subacute toxicity of tyramine, spermidine, spermine, putrescine and cadaverine in rats. *Food and Chemical Toxicology*. 35:337–348. doi:10.1016/S0278-6915(97)00121-X.

To, T.-L., A.M. Cuadros, H. Shah, W.H.W. Hung, Y. Li, S.H. Kim, D.H.F. Rubin, R.H. Boe, S. Rath, J.K. Eaton, F. Piccioni, A. Goodale, Z. Kalani, J.G. Doench, D.E. Root, S.L. Schreiber, S.B. Vafai, and V.K. Mootha. 2019. A Compendium of Genetic Modifiers of Mitochondrial Dysfunction Reveals Intra-organelle Buffering. *Cell*. 179:1222-1238.e17. doi:10.1016/j.cell.2019.10.032.

Vincent, A.E., Y.S. Ng, K. White, T. Davey, C. Mannella, G. Falkous, C. Feeney, A.M. Schaefer, R. McFarland, G.S. Gorman, R.W. Taylor, D.M. Turnbull, and M. Picard. 2016. The Spectrum of Mitochondrial Ultrastructural Defects in Mitochondrial Myopathy. *Sci Rep*. 6:30610. doi:10.1038/srep30610.

Wai, T., and T. Langer. 2016. Mitochondrial Dynamics and Metabolic Regulation. *Trends Endocrinol Metab*. 27:105–117. doi:10.1016/j.tem.2015.12.001.

Wang, Y., Y. Zhang, L. Chen, Q. Liang, X.-M. Yin, L. Miao, B.-H. Kang, and D. Xue. 2016. Kinetics and specificity of paternal mitochondrial elimination in Caenorhabditis elegans. *Nat Commun*. 7:12569. doi:10.1038/ncomms12569.

Ward, D.M., and S.M. Cloonan. 2019. Mitochondrial Iron in Human Health and Disease. *Annu Rev Physiol*. 81:453–482. doi:10.1146/annurev-physiol-020518-114742.

Wei, W., and G. Ruvkun. 2020. Lysosomal activity regulates *Caenorhabditis elegans* mitochondrial dynamics through vitamin B12 metabolism. *Proc. Natl. Acad. Sci. U.S.A.* 117:19970–19981. doi:10.1073/pnas.2008021117.

Westermann, B. 2010. Mitochondrial fusion and fission in cell life and death. *Nat Rev Mol Cell Biol*. 11:872–884. doi:10.1038/nrm3013.

Whitnall, M., Y. Suryo Rahmanto, M.L.-H. Huang, F. Saletta, H.C. Lok, L. Gutiérrez, F.J. Lázaro, A.J. Fleming, T.G. St Pierre, M.R. Mikhael, P. Ponka, and D.R. Richardson. 2012. Identification of nonferritin mitochondrial iron deposits in a mouse model of Friedreich ataxia. *Proc Natl Acad Sci U S A*. 109:20590–20595. doi:10.1073/pnas.1215349109.

Witteveen, J.S., M.H. Willemsen, T.C.D. Dombroski, N.H.M. van Bakel, W.M. Nillesen, J.A. van Hulten, E.J.R. Jansen, D. Verkaik, H.E. Veenstra-Knol, C.M.A. van Ravenswaaij-Arts, J.S.K. Wassink-Ruiter, M. Vincent, A. David, C. Le Caignec, J. Schieving, C. Gilissen, N. Foulds, P. Rump, T. Strom, K. Cremer, A.M. Zink, H. Engels, S.A. de Munnik, J.E. Visser, H.G. Brunner, G.J.M. Martens, R. Pfundt, T. Kleefstra, and S.M. Kolk. 2016. Haploinsufficiency of MeCP2-interacting transcriptional co-repressor SIN3A causes mild intellectual disability by affecting the development of cortical integrity. *Nat Genet*. 48:877–887. doi:10.1038/ng.3619.

Yang, R., Y. Li, Y. Wang, J. Zhang, Q. Fan, J. Tan, W. Li, X. Zou, and B. Liang. 2022. NHR-80 senses the mitochondrial UPR to rewire citrate metabolism for lipid accumulation in Caenorhabditis elegans. *Cell Reports*. 38:110206. doi:10.1016/j.celrep.2021.110206.

Yang, X., S.M. Graff, C.N. Heiser, K.-H. Ho, B. Chen, A.J. Simmons, A.N. Southard-Smith, G. David, D.A. Jacobson, I. Kaverina, C.V.E. Wright, K.S. Lau, and G. Gu. 2020a. Coregulator Sin3a Promotes Postnatal Murine β-Cell Fitness by Regulating Genes in Ca2+ Homeostasis, Cell Survival, Vesicle Biosynthesis, Glucose Metabolism, and Stress Response. *Diabetes*. 69:1219–1231. doi:10.2337/db19-0721.

Yang, X., M. Zhang, Y. Dai, Y. Sun, Y. Aman, Y. Xu, P. Yu, Y. Zheng, J. Yang, and X. Zhu. 2020b. Spermidine inhibits neurodegeneration and delays aging via the PINK1-PDR1-dependent mitophagy pathway in C. elegans. *Aging*. 12:16852–16866. doi:10.18632/aging.103578.

Ye, C., B.M. Sutter, Y. Wang, Z. Kuang, and B.P. Tu. 2017. A Metabolic Function for Phospholipid and Histone Methylation. *Molecular Cell*. 66:180-193.e8. doi:10.1016/j.molcel.2017.02.026.

Yoneda, T., C. Benedetti, F. Urano, S.G. Clark, H.P. Harding, and D. Ron. 2004. Compartment-specific perturbation of protein handling activates genes encoding mitochondrial chaperones. *Journal of Cell Science*. 117:4055–4066. doi:10.1242/jcs.01275.

Zhou, Q., H. Li, H. Li, A. Nakagawa, J.L.J. Lin, E.-S. Lee, B.L. Harry, R.R. Skeen-Gaar, Y. Suehiro, D. William, S. Mitani, H.S. Yuan, B.-H. Kang, and D. Xue. 2016. Mitochondrial endonuclease G

mediates breakdown of paternal mitochondria upon fertilization. *Science*. 353:394–399. doi:10.1126/science.aaf4777.

Zhu, D., X. Wu, J. Zhou, X. Li, X. Huang, J. Li, J. Wu, Q. Bian, Y. Wang, and Y. Tian. 2020. NuRD mediates mitochondrial stress-induced longevity via chromatin remodeling in response to acetyl-CoA level. *Sci Adv*. 6:eabb2529. doi:10.1126/sciadv.abb2529.

Zhu, F., Q. Zhu, D. Ye, Q. Zhang, Y. Yang, X. Guo, Z. Liu, Z. Jiapaer, X. Wan, G. Wang, W. Chen, S. Zhu, C. Jiang, W. Shi, and J. Kang. 2018. Sin3a–Tet1 interaction activates gene transcription and is required for embryonic stem cell pluripotency. *Nucleic Acids Research*. 46:6026–6040. doi:10.1093/nar/gky347.

Figure 1. Loss of *sin-3* alters the expression of mitochondrial genes (A) WormCat visualization of categories enriched in genes commonly misregulated in *sin-3(tm1276)* and *sin-3(syb2172)* mutants. The legend for bubble charts is indicated on the right, with size referring to the number of genes in each category and color referring to the p-value. (B) Respiratory complex subunits commonly misregulated in *sin-3(tm1276)* and *sin-3(syb2172)* mutants are indicated, along with their mammalian counterparts. Subunits encoded by the mitochondrial genome are shown in bold.

Figure 2. TEM microscopy of mitochondria in *sin-3* mutant animals

Transverse sections captured with electron microscopy of mitochondria from the body wall muscles, intestine, pharynx and germline of young adult wild type, *sin-3(tm1276)* and *sin-3*(*syb2172*) mutant animals. Images are representative of a total of 6 animals imaged for wild type, 4 for *sin-3*(*syb2172*) and 5 for *sin-3*(*syb2172*). Further examples for each genotype are displayed in Supplementary Figure 1. White arrows indicate examples of individual mitochondria, black arrows examples enlarged mitochondria with densely stained aggregates. Scale bars are indicated for each image.

Figure 3. Altered mitochondria morphology and microfilament structure in *sin-3(tm1276)* muscle cells. (A) Representative confocal images of mitochondria morphology in body wall muscles expressing *myo-3p::tomm-20*Nter*::*wrmScarlet in wildtype and *sin-3(tm1276)* mutant animals. Images were taken at day 1, 6 or 9 of adulthood. Scale bar: 10µm. (B) Quantification of animals with the indicated muscle mitochondria phenotypes at day 1, 6 or 9 of adulthood. Total number of worms scored for each condition is indicated above bars. Phenotypes are described in Materials and Methods. (C) Representative confocal images of myofilament structure in body wall muscles expressing GFP*::myo-3* in wildtype or *sin-3(tm1276)* mutant animals. Images were taken at day 1, 6 or 9 of adulthood. Scale bar: 10µm.

Figure 4. Loss of *sin-3* dampens the response to mitochondrial stress. (A) Images of wildtype or *sin-3*(RNAi) animals expressing *hsp-6p::GFP* reporter under basal conditions, or following mitochondrial stress induced by RNAi knock-down of mitochondrial genes *nuo-4* and *mrps-5*. Parent worms were grown on HT115 control or *sin-3* RNAi from hatch until the adult stage. F1 offspring were then grown from

hatch on control, *nuo-4* or *mrps-5* single RNAi, or *sin-3*, *sin-3* + *nuo-4*, and *sin-3* + *mrps-5* double RNAi. GFP expression was measured 5 days after eggs were laid. Scale bar: 300µm. (B) Quantification of *hsp-6p::*GFP expression. Data is representative of one of two independent experiments with 30 animals per condition each. Significance was calculated using Mann-Whitney test, P-value * < 0.05, **** < 0.0001.

Figure 5. Oxygen consumption rate (OCR) and abundance of mitochondrial respiratory chain subunits in *sin-3(tm1276)* mutants. (A) Basal OCR of wild type and *sin-3* mutants at the young adult (YA) stage and at day 6 of adulthood (D6). (B) Maximal OCR of wild type and *sin-3* mutants at the YA stage and at D6 of adulthood. (C) Spare respiratory capacity of wild type and *sin-3* mutants at the YA stage and at D6 of adulthood. Significance was calculated using unpaired *t*-test or, when appropriate, Mann-Whitney test, P-value * < 0.05, **** < 0.0001. (D) Western blot showing SDHB-1 (complex II), CTC-1 (complex IV), and ATP-2 (complex V) protein levels in total protein extracts from wildtype and *sin-3(tm1276)* L4-young adult worms detected by fluorescence. (F) Levels of each protein were quantified with Image J and normalized to tubulin levels. Bar plot represents the mean of two to three independent biological replicates; error bars correspond to SD.

Figure 6. Metabolic alterations in *sin-3(tm1276)* mutant animals and their related pathways. Changes in amino acid metabolites (A) and polyamine-related metabolites (B) in *sin-3(tm1276)* mutants at the young adult stage. Welch test, P-value * < 0.05, ** < 0.01, *** < 0.005. (C) Schematic representation of biosynthetic pathway for arginine-derived polyamines. (D) Biosynthetic pathway of cadaverine and lysine degradation. Arrows and colors in (C) and (D) indicate significant changes for metabolites and metabolic genes (blue = down, red = up). Specific pathways and reactions that take place in the mitochondria are shaded in gray.

Table 1. List of genes with mitochondrial function commonly misregulated in both *sin-3(syb2172)* and *sin-3(tm1276)* germlines. The list of all commonly misregulated genes was generated by crossing the set of genes obtained for each allele with a FDR <0.05 following DESeq2 analysis (Table S1), and the list of mitochondrial genes extracted from WormCat.

Supplementary information

Figure S1. Mitochondrial defects in *sin-3* mutants. (A) fragmented or enlarged mitochondria in *sin-3* mutants (arrows). (B) Arrows indicates double membrane structure of autophagosomes in hypodermis

(left) and germ cells (right) of *sin-3(tm1276)* animals. (C) Representative confocal images of mitochondria morphology in germ cells from wildtype or *sin-3(tm1276)* mutants expressing *mex-5p::tomm-20*::mKate2::*pie-1*mKate fluorescent protein targeted to the mitochondrial outer membrane. Mitochondrial morphology is shown at day 1 or 6 of adulthood. Scale bar: 20µm.

Figure S2. *hsp-6*p*::GFP* in day 3 adults. Images of day 3 control or *sin-3*(RNAi) animals expressing *hsp-6*p*::GFP* reporter under basal conditions, or following mitochondrial stress induced by RNAi knock-down of mitochondrial genes *nuo-4* and *mrps-5.*

Figure S3. SIN-3::RFP localization is not altered following induction of mitochondrial stress. Representative confocal images of mCherry-SIN-3 expression in intestinal cells, germline, and neurons of L4 stage animals following RNAi knock-down of *mrps-5*. Worms were fed control or *mrps-5* RNAi from the first larval stage until the L4 stage. Scale bar: 20µm.

Figure S4. Boxplots of normalized peak areas from QC, N2 and *sin-3* samples of: (A) Acyl-CoA and carnitine metabolites; (B) TCA cycle and related metabolites; (C) amino acids and related metabolites; (D) other metabolites; (E) SAM and polyamine metabolites. P-values were calculated using a Welch-test. QC; quality control.

Table S1. List of genes commonly misregulated in *sin-3(tm1276)* and *sin-3(syb2172)* mutant germlines. The list was generated by crossing the lists of all genes with a FDR <0.05 after DESeq2 analysis for each allele (Caron et al., 2023).

Table S2. List of mitochondrial genes with SIN3 promoter peaks and commonly misregulated in *sin-3* mutants. List was generated using bedtools intersect to identify the overlap between the list of commonly misregulated mitochondrial genes (from Wormcat analysis, Table 1) and the list of SIN-3 ChIP-seq peaks at promoter regions (Beurton et al., 2019).

Table S2. LC-MS gradients used for positive and negative metabolomics analysis.

Table S3. Table of metabolites detected in positive ionization mode, including m/z and RT. Values represent the protein normalized peak areas. Columns W indicates the relative standard deviation in the QC samples (pooled sample), Column X indicates the log2 fold-change between N2 and sin-3, Column Y indicates the p-value of a Welch-test.

Table S4 Table of metabolites detected in negative ionization mode, including m/z and RT. Values represent the protein normalized peak areas. Columns W indicates the relative standard deviation in the QC samples (pooled sample), Column X indicates the log2 fold-change between N2 and sin-3, Column Y indicates the p-value of a Welch-test.

Figure 1

A. **categories enriched in genes commonly misregulated in *sin-3(tm1276)* and *sin-3(syb2172)***

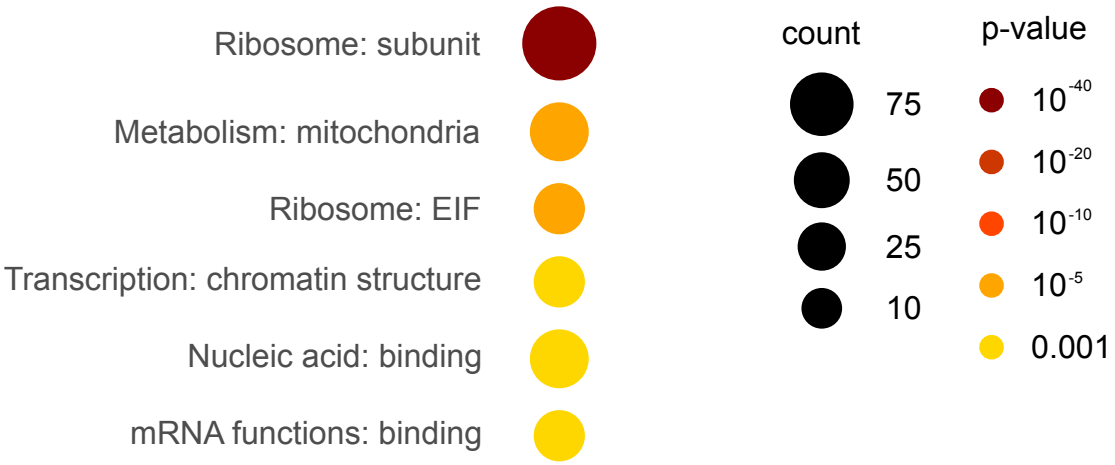

B.

mitochondrial complex	**subunit identity**	**mammalian homologue**	**misregulation in *sin-3 mutant animals***
complex I	***ndub-2***	NDUFB2	UP
	ndfl-4	NADH dehydrogenase	UP
	nduo-1	MT-ND1	UP
	nduo-2	NADH dehydrogenase	UP
	nduo-5	MT-ND5	UP
	Y54F10AM.5	NDUFA8	UP
complex III	***ucr-2.1***	UQCRC2	UP
	ucr-2.3	UQCRC2	DOWN
	cyc-2.1	CYCS	DOWN
complex IV	*cox-7C*	COX7C	DOWN
complex V	*atp-1*	ATP5F1A	DOWN
	R53.4	ATP5MF	DOWN
	atp-4	ATP5PF	DOWN
	Y82E9BR.3	ATP5MC1	DOWN

Figure 2

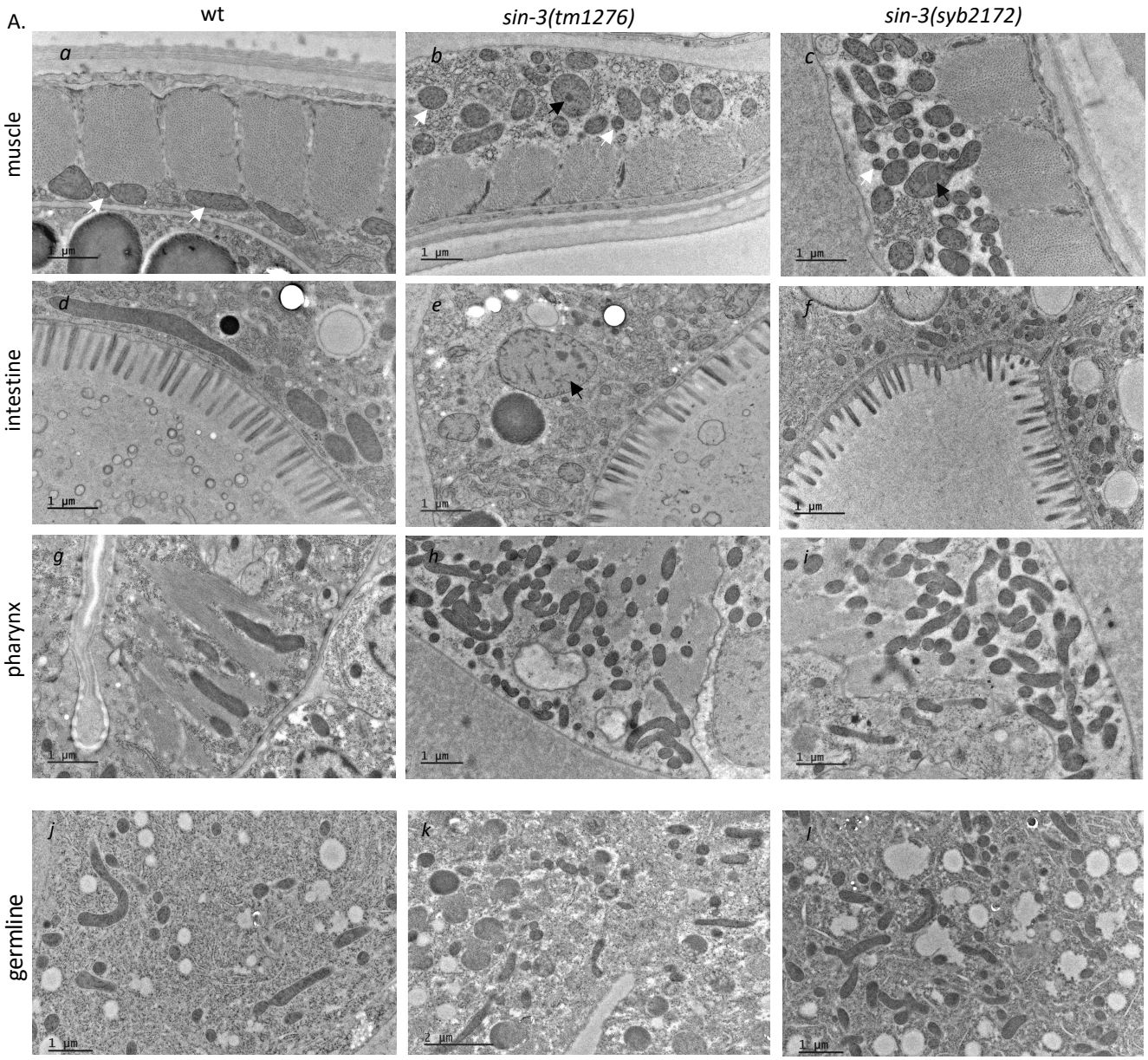
A.
wt
sin-3(tm1276)
sin-3(syb2172)
muscle
intestine
pharynx
germline
a
b
c
d
e
f
g
h
i
j
k
l
1 µm
2 µm

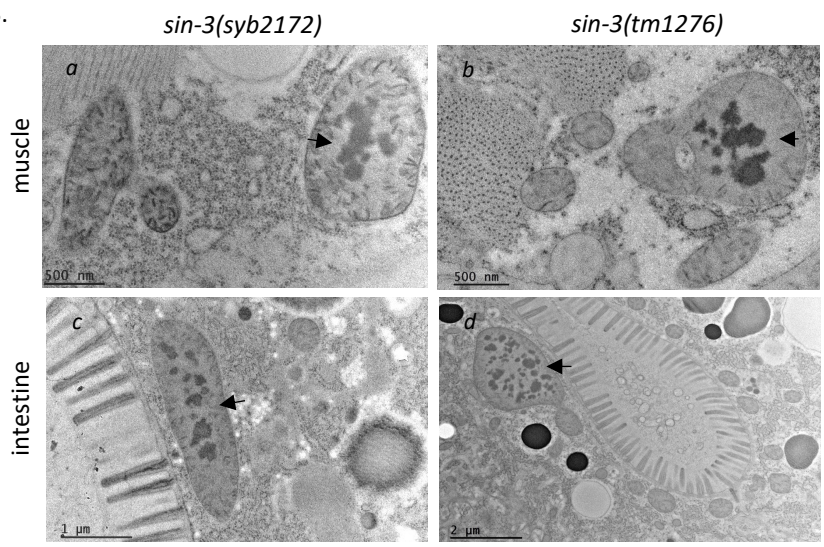
B.
sin-3(syb2172)
sin-3(tm1276)
muscle
intestine
a
b
c
d
500 nm
1 µm
2 µm

Figure 3

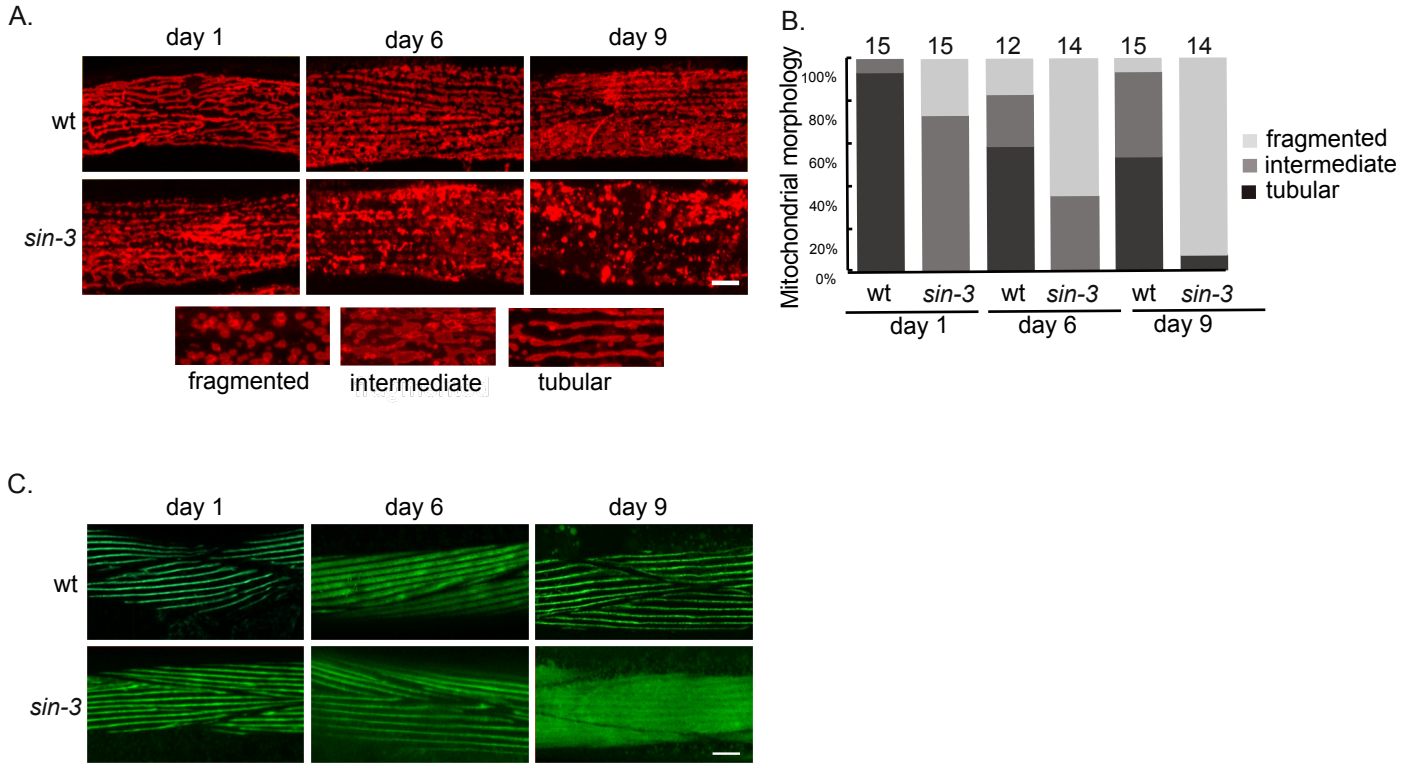
A.
day 1
day 6
day 9
wt
sin-3
fragmented
intermediate
tubular
B.
15
15
12
14
15
14
Mitochondrial morphology
100%
80%
60%
40%
20%
0%
fragmented
intermediate
tubular
wt
sin-3
wt
sin-3
wt
sin-3
day 1
day 6
day 9
C.
day 1
day 6
day 9
wt
sin-3

Figure 4

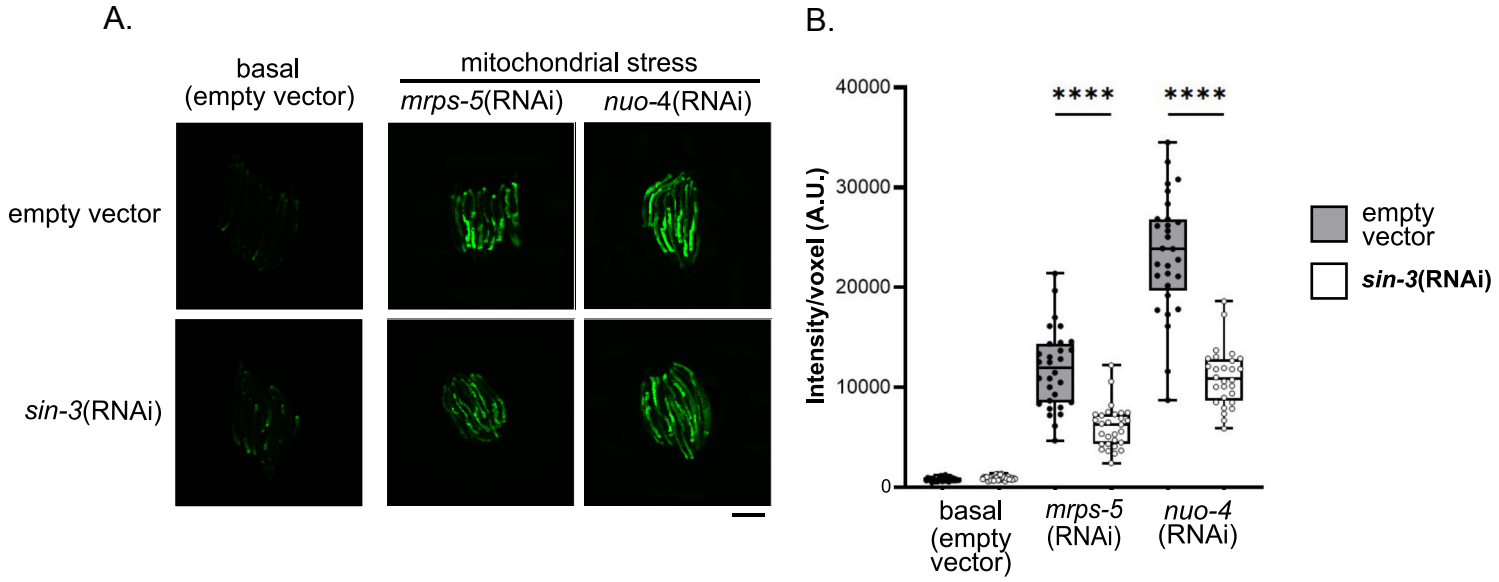
A.
basal
(empty vector)
mitochondrial stress
mrps-5(RNAi)
nuo-4(RNAi)
empty vector
sin-3(RNAi)
B.
Intensity/voxel (A.U.)
40000
30000
20000
10000
0
****
****
basal
(empty
vector)
mrps-5
(RNAi)
nuo-4
(RNAi)
empty
vector
sin-3(RNAi)

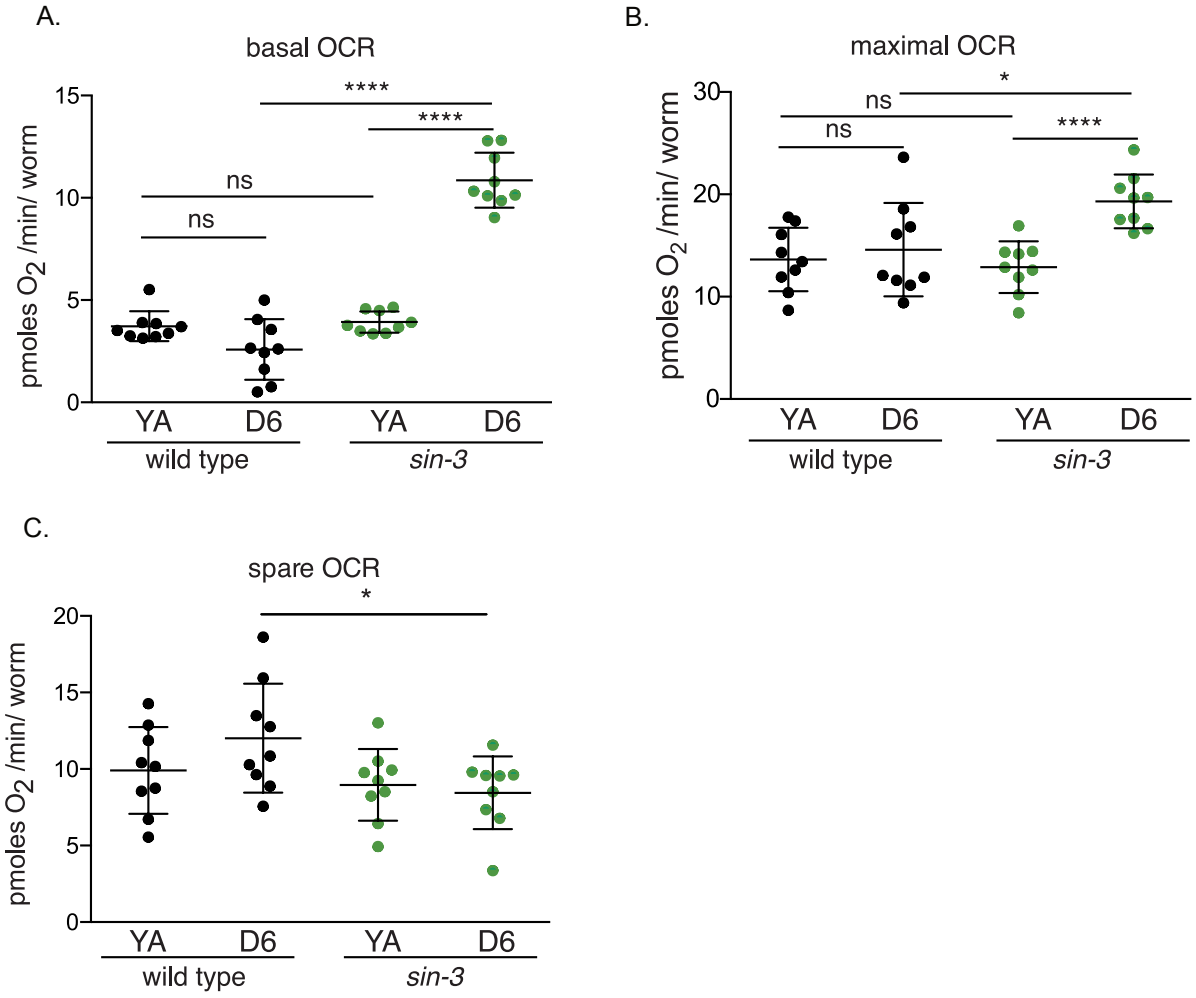
A.
basal OCR
pmoles O2 /min/ worm
15
10
5
0
****
****
ns
ns
YA
D6
YA
D6
wild type
sin-3
B.
maximal OCR
pmoles O2 /min/ worm
30
20
10
0
*
ns
ns
****
YA
D6
YA
D6
wild type
sin-3
C.
spare OCR
pmoles O2 /min/ worm
20
15
10
5
0
*
YA
D6
YA
D6
wild type
sin-3

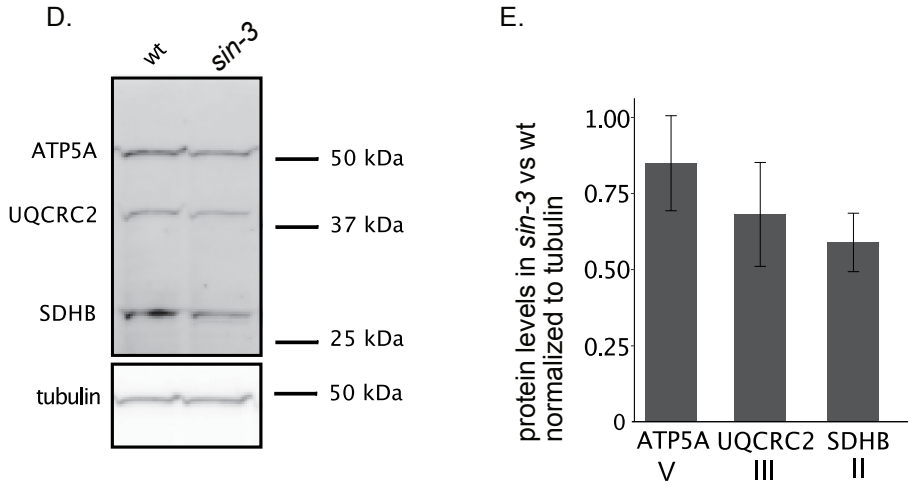
D.
wt
sin-3
ATP5A
UQCRC2
SDHB
tubulin
50 kDa
37 kDa
25 kDa
50 kDa
E.
protein levels in sin-3 vs wt normalized to tubulin
1.00
0.75
0.50
0.25
0
ATP5A
V
UQCRC2
III
SDHB
II

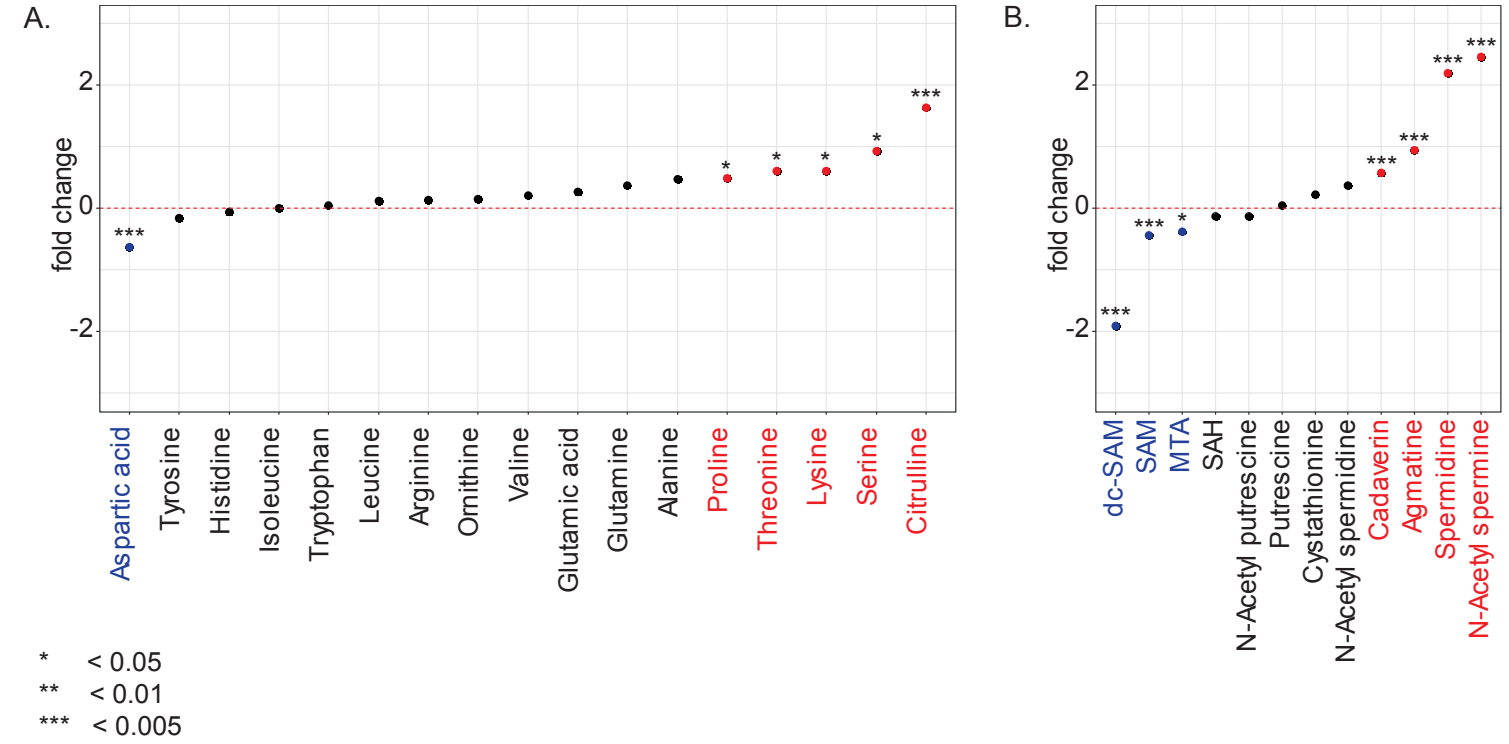
A.
fold change
2
0
-2
Aspartic acid
Tyrosine
Histidine
Isoleucine
Tryptophan
Leucine
Arginine
Ornithine
Valine
Glutamic acid
Glutamine
Alanine
Proline
Threonine
Lysine
Serine
Citrulline
B.
dc-SAM
SAM
MTA
SAH
N-Acetyl putrescine
Putrescine
Cystathionine
N-Acetyl spermidine
Cadaverin
Agmatine
Spermidine
N-Acetyl spermine
* < 0.05
** < 0.01
*** < 0.005

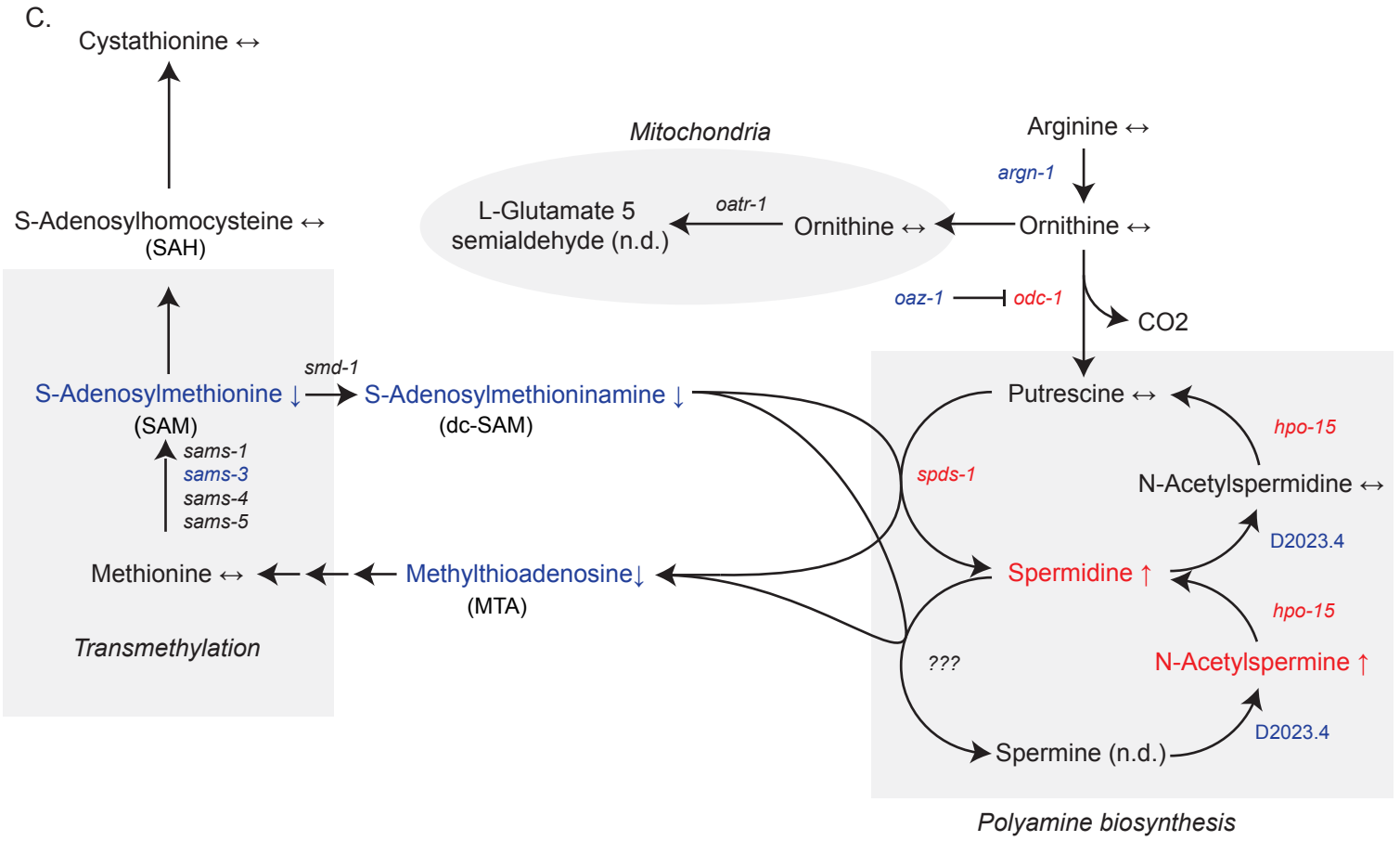
C.
Cystathionine ↔
S-Adenosylhomocysteine ↔
(SAH)
S-Adenosylmethionine ↓
(SAM)
smd-1
S-Adenosylmethioninamine ↓
(dc-SAM)
sams-1
sams-3
sams-4
sams-5
Methionine ↔
Methylthioadenosine↓
(MTA)
Transmethylation
Mitochondria
L-Glutamate 5
semialdehyde (n.d.)
oatr-1
Ornithine ↔
Arginine ↔
argn-1
Ornithine ↔
oaz-1
odc-1
CO2
Putrescine ↔
spds-1
hpo-15
N-Acetylspermidine ↔
D2023.4
Spermidine ↑
hpo-15
???
N-Acetylspermine ↑
D2023.4
Spermine (n.d.)
Polyamine biosynthesis

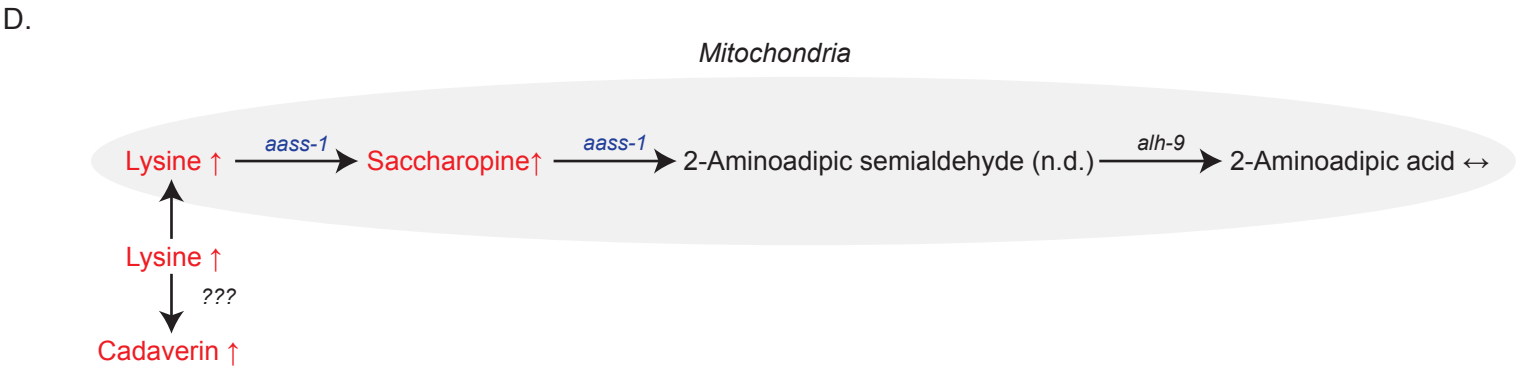
D.
Mitochondria
Lysine ↑
aass-1
Saccharopine↑
aass-1
2-Aminoadipic semialdehyde (n.d.)
alh-9
2-Aminoadipic acid ↔
Lysine ↑
???
Cadaverin ↑

Table 1

sequence_ID	**category**	**misregulation in *sin-3(syb2172)***
F54C9.6	Metabolism: mitochondria: chaperone	DOWN
C35D10.5	Metabolism: mitochondria: chaperone	DOWN
F25H9.7	Metabolism: mitochondria: citric acid cycle	DOWN
F59B8.2	Metabolism: mitochondria: citric acid cycle	DOWN
C50F7.4	Metabolism: mitochondria: citric acid cycle	DOWN
F23H11.3	Metabolism: mitochondria: citric acid cycle	DOWN
ndub-2	**Metabolism: mitochondria: complex I**	**UP**
MTCE.4	**Metabolism: mitochondria: complex I**	**UP**
MTCE.11	**Metabolism: mitochondria: complex I**	**UP**
MTCE.16	**Metabolism: mitochondria: complex I**	**UP**
MTCE.35	**Metabolism: mitochondria: complex I**	**UP**
Y54F10AM.5	Metabolism: mitochondria: complex I	UP
VW06B3R.1	Metabolism: mitochondria: complex III	UP
E04A4.7	Metabolism: mitochondria: complex III	DOWN
T24C4.1	Metabolism: mitochondria: complex III	DOWN
F26E4.6	Metabolism: mitochondria: complex IV	DOWN
H28O16.1	Metabolism: mitochondria: complex V	DOWN
R53.4	Metabolism: mitochondria: complex V	DOWN
T05H4.12	Metabolism: mitochondria: complex V	DOWN
Y82E9BR.3	Metabolism: mitochondria: complex V	DOWN
F13B9.8	Metabolism: mitochondria: morphology	UP
Y71G12B.24	Metabolism: mitochondria: protease	UP
C25A1.13	Metabolism: mitochondria: ribosome	DOWN
T13H5.5	Metabolism: mitochondria: ribosome	DOWN
T21B10.1	Metabolism: mitochondria: ribosome	DOWN
Y48C3A.10	Metabolism: mitochondria: ribosome	DOWN
F56D1.3	Metabolism: mitochondria: ribosome	DOWN
T14B4.2	Metabolism: mitochondria: ribosome	DOWN
T20F5.3	Metabolism: mitochondria: ribosome	DOWN
Y37E3.8	Metabolism: mitochondria: ribosome	DOWN
F32A7.4	Metabolism: mitochondria: RNA methyltransfer	DOWN
C18E9.6	Metabolism: mitochondria: translocase	DOWN
Y67H2A.4	Metabolism: mitochondria: transporter	DOWN
Y57G11C.11	Metabolism: mitochondria: ubiquinone	DOWN
K08E3.7	Metabolism: mitochondria: unassigned	DOWN
F27D4.1	Metabolism: mitochondria: unassigned	DOWN
K12G11.3	Metabolism: mitochondria: unassigned	DOWN
T06D8.6	Metabolism: mitochondria: unassigned	DOWN
ZK1010.2	Metabolism: mitochondria: unassigned	DOWN
T14G11.3	Metabolism: mitochondria: unassigned	UP
C27H6.9	Metabolism: mitochondria: unassigned	DOWN
F32A7.4	Metabolism: mitochondria: unassigned	DOWN

Figure S1

A.

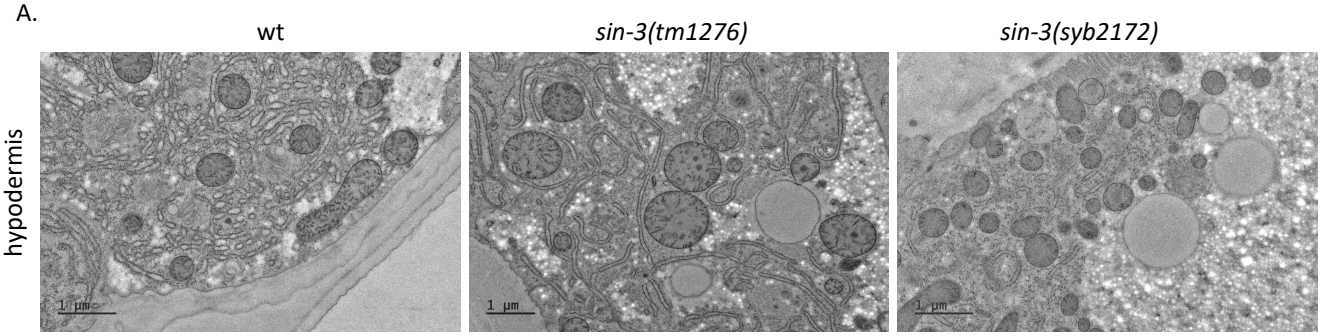

B.

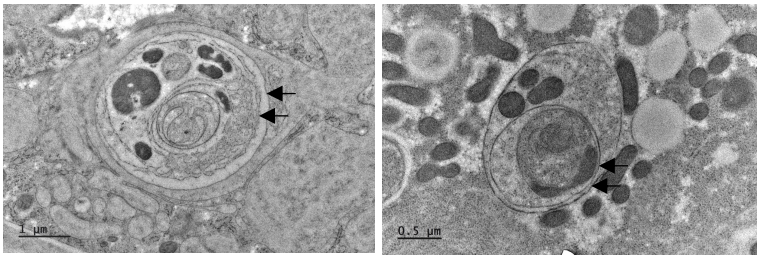

C.

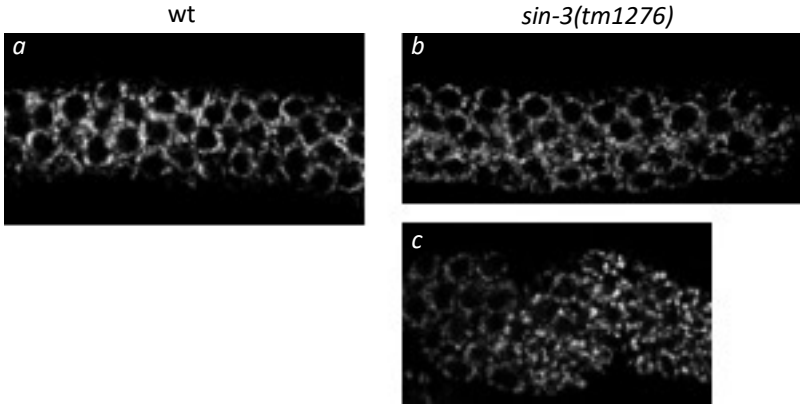

Figure S2

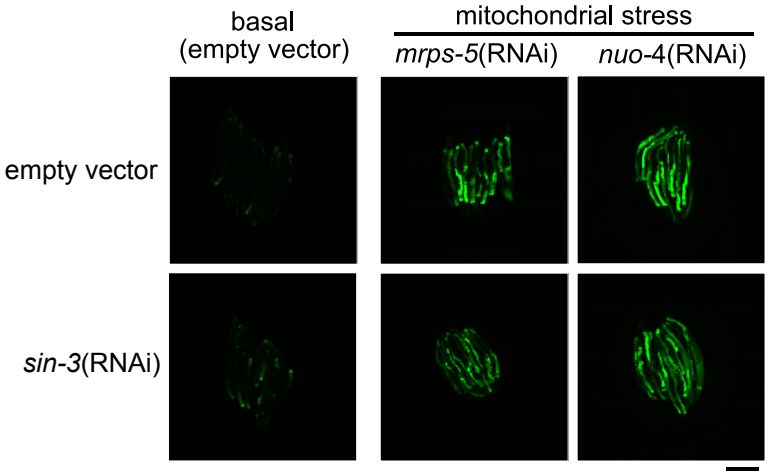
basal
(empty vector)
mitochondrial stress
mrps-5(RNAi)
nuo-4(RNAi)
empty vector
sin-3(RNAi)

Figure S3

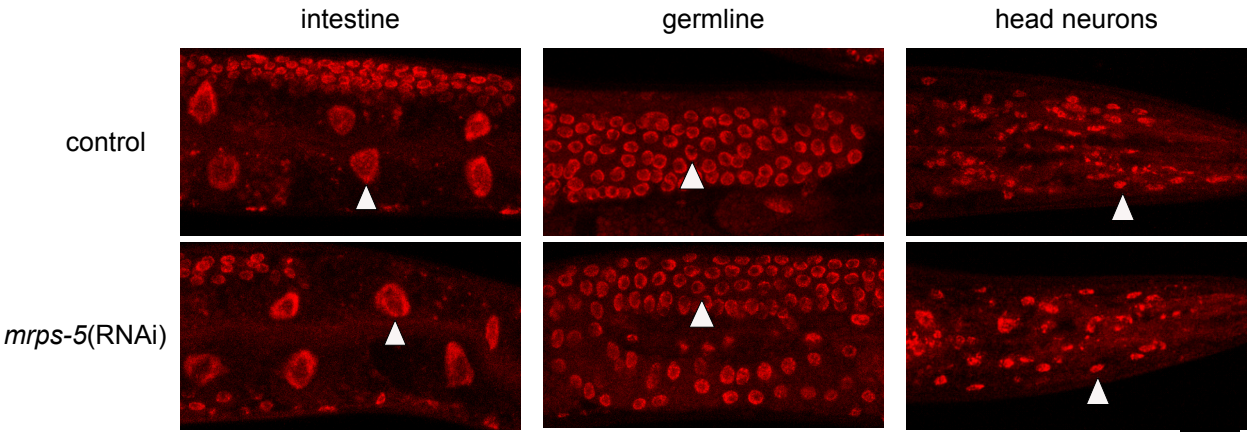

Figure S4A; CoAs and carnitines

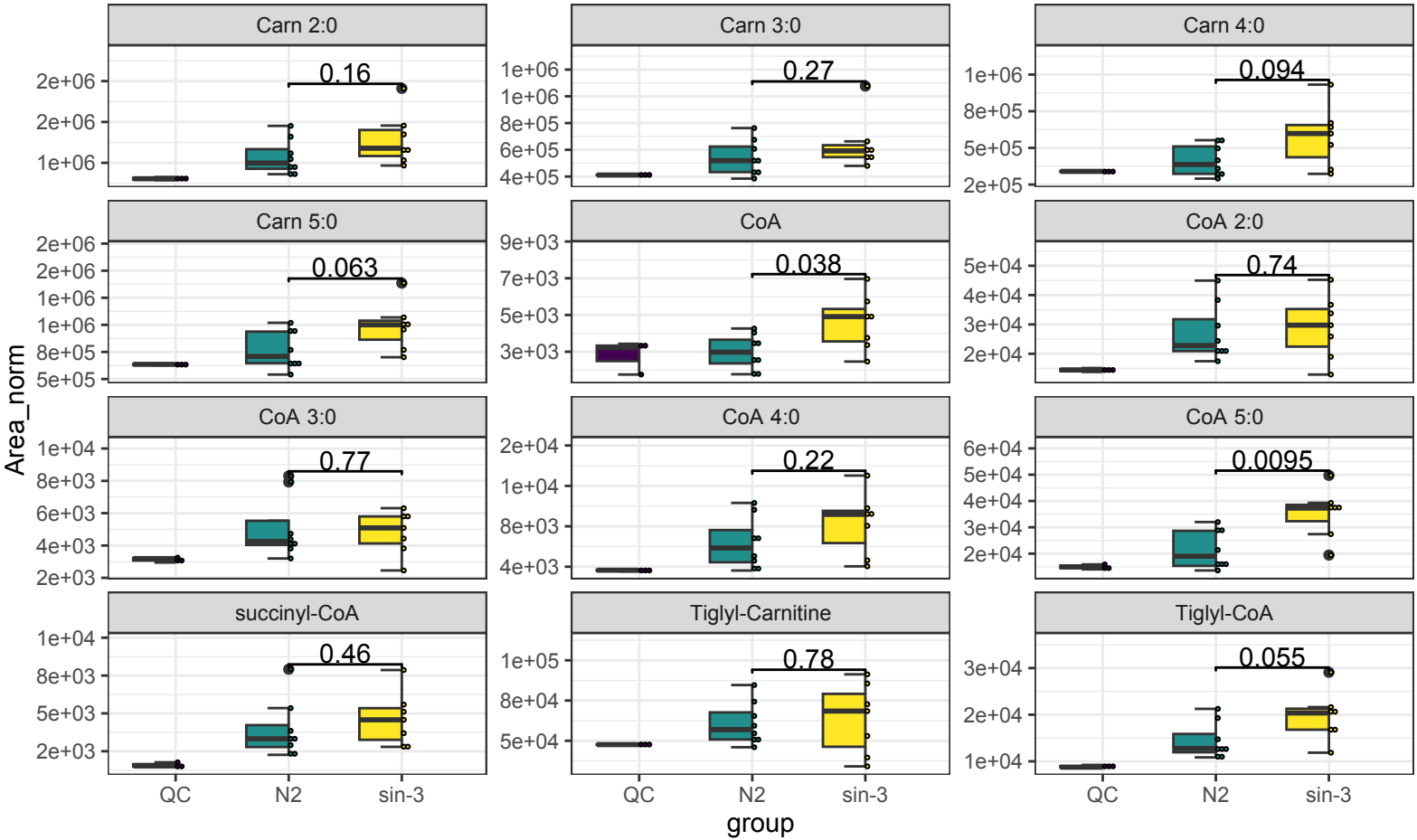

Figure S4B; TCA and others

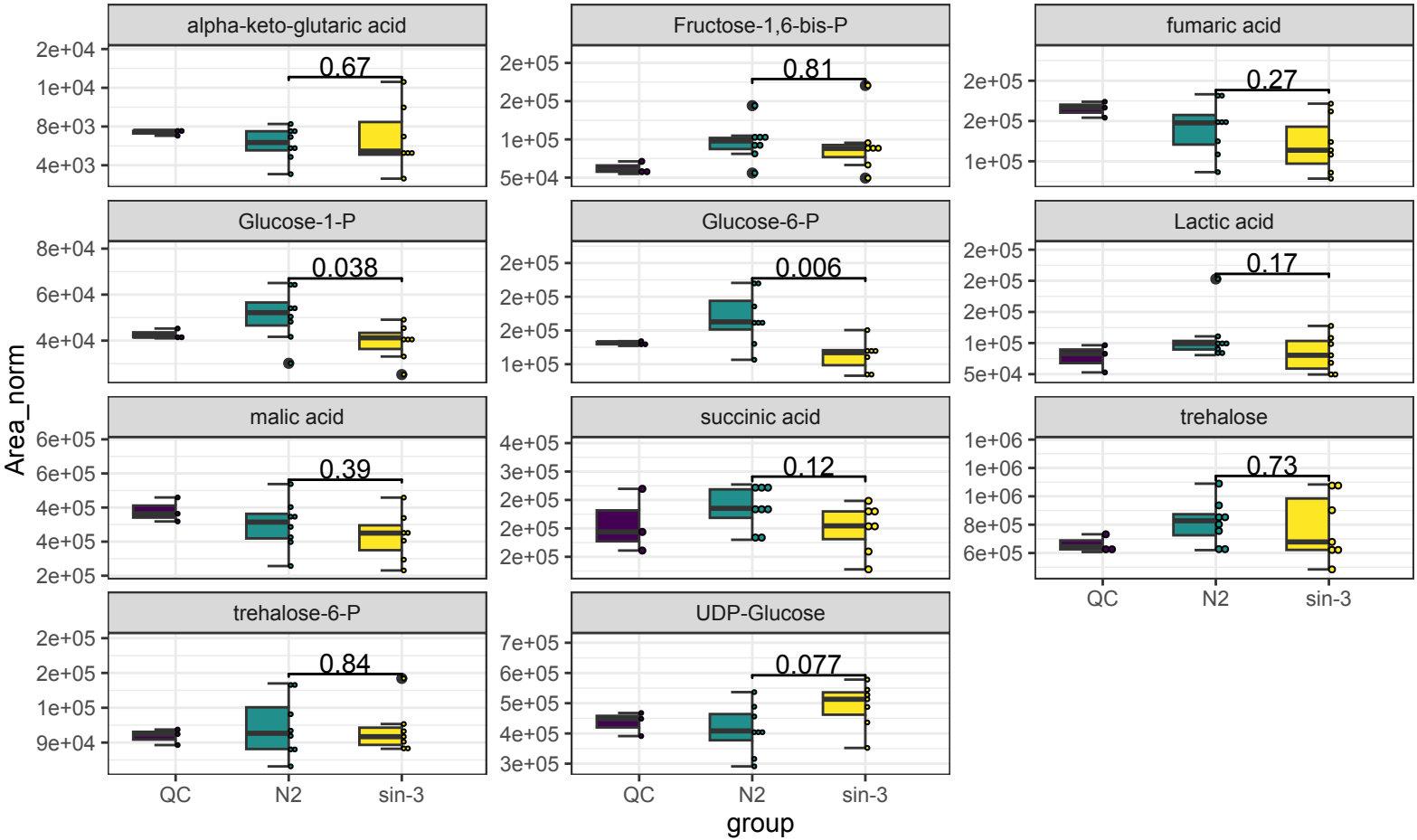

Figure S4C; amino acid and related

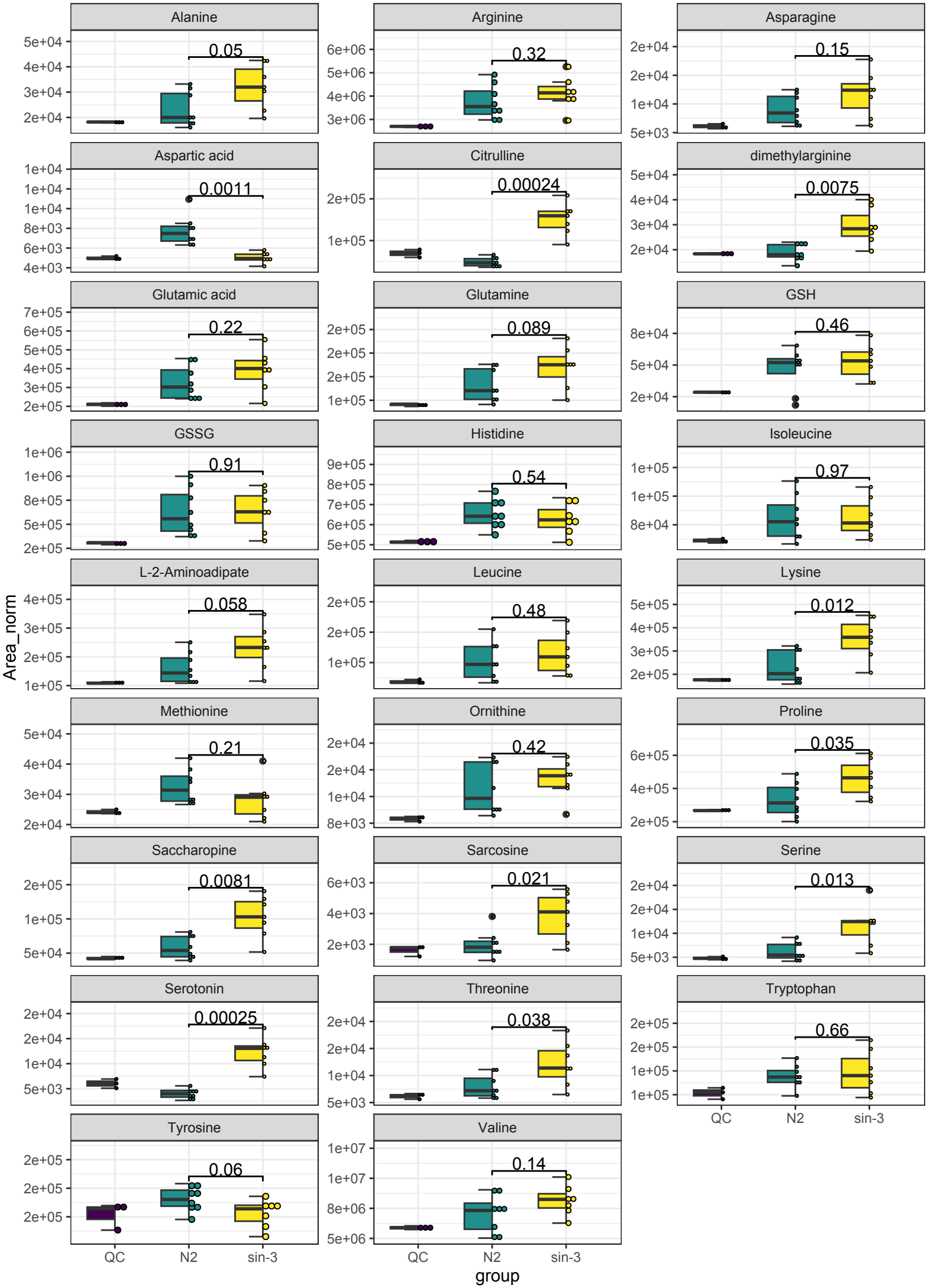

Figure S4D; other metabolites

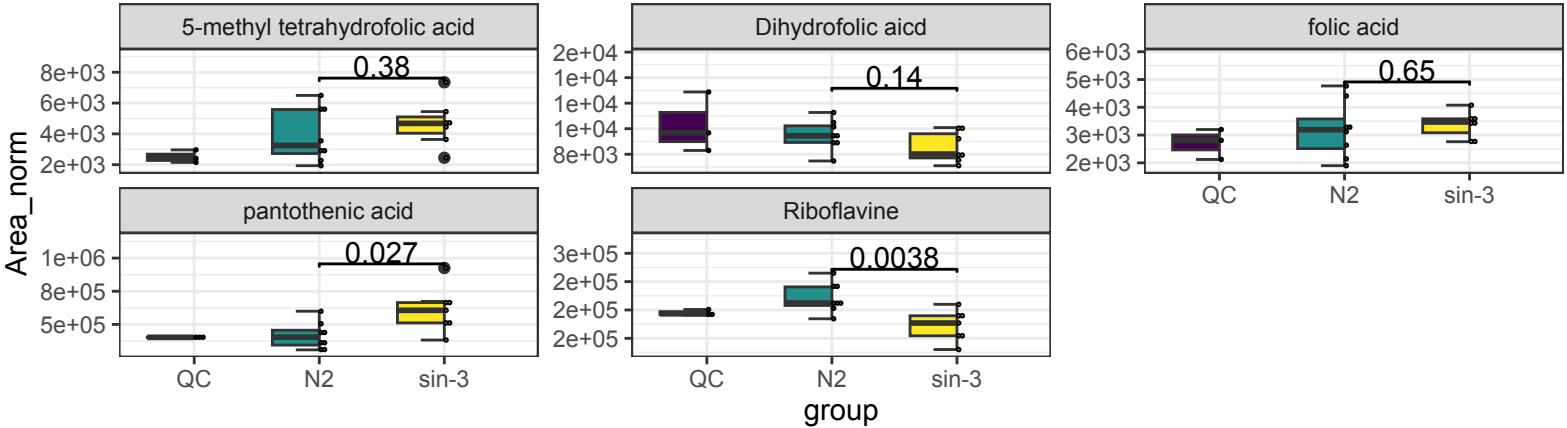

Figure S4E; SAM and polyamines

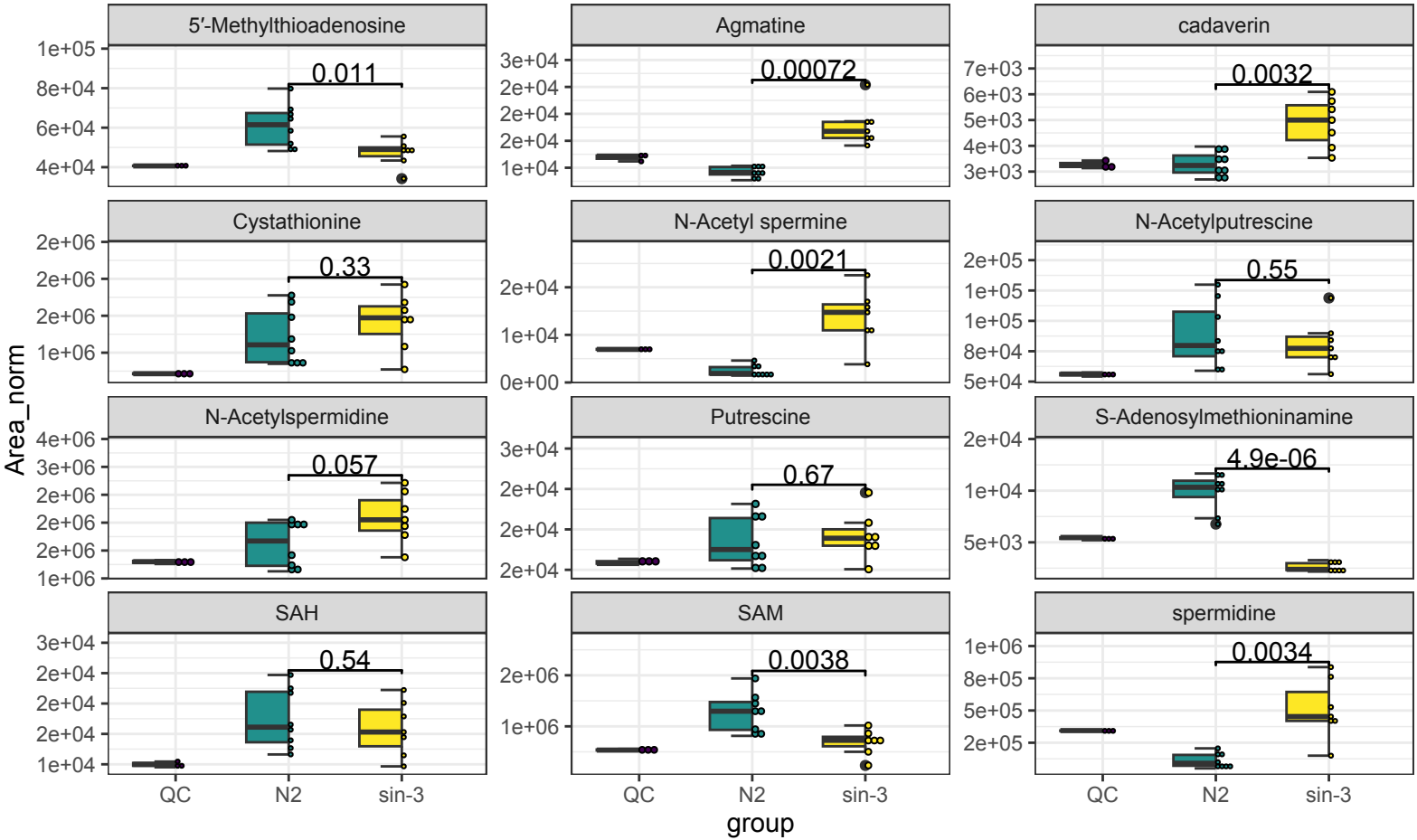

Table S1 : List of significant commonly misregulated genes in *sin-3(tm1276)* and *sin-3(syb21 72)* compared to wild-type

id_gene	gene_name	Log2.FC_tm	padj_tm1276	Log2.FC_syb	padj_syb2172
WBGene00000	act-2	-0.7337908935	4.6777629160	-1.3402953390	0.00388591688508462
WBGene00000	agt-1	-0.5074901861	2.2471986508	-1.3241776459	0.000298497174038359
WBGene00000	agt-2	-0.5693187693	3.2229899386	-0.8925756648	0.0363039359761594
WBGene00000	alh-8	-0.8871072606	3.2512867891	-1.0480043824	0.000941745667591152
WBGene00000	apc-10	-1.3101957701	4.3810443309	-2.0494584607	2.78971557688454e-07
WBGene00000	apc-11	-0.3589899004	1.7461620344	-1.1518369501	0.00378024821546395
WBGene00000	arf-3	-0.2073248196	4.2385913681	-0.7832594046	0.0396665340979832
WBGene00000	arx-7	-0.4237311310	1.4169793737	-1.4853415957	0.000629068370943816
WBGene00000	asp-1	-1.1439227516	0.0070392156	1.9633212522	0.0402998074998023
WBGene00000	asp-6	-1.3206931081	0.0065410198	2.9998061931	0.0119879695899209
WBGene00000	bli-4	-0.8585983354	1.9027740050	-1.2224593886	0.000129397405920671
WBGene00000	bpl-1	-1.3999098793	5.5058664536	-2.3117290683	1.97362331745253e-10
WBGene00000	ccf-1	-0.3599930022	1.5459843331	-0.6978171117	0.0442907004844807
WBGene00000	cdd-2	-0.8113385697	6.3865066050	-1.6386297869	3.31185720168559e-05
WBGene00000	cdk-1	-0.1592949382	0.0002992521	-0.7680852667	0.0337165143815552
WBGene00000	cdk-5	-0.5833238832	1.3801606288	-1.0913610946	0.000903237471222072
WBGene00000	cey-2	-0.6733215617	1.5700492576	-1.9271667090	1.0420981813283e-06
WBGene00000	cey-3	-0.3387835175	4.9310470973	-1.3713276095	0.000179216214333118
WBGene00000	cgh-1	-0.3717875748	0.0057237951	-1.2954968683	8.00021391507808e-05
WBGene00000	chp-1	-0.1511256723	0.0116949242	-0.9872204511	0.00754173239372364
WBGene00000	clh-6	-0.2427904167	1.8712661756	-0.8702924870	0.0465138372032017
WBGene00000	coq-3	-0.2246779888	0.0015724725	-1.0493901119	0.0233759444726421
WBGene00000	cpb-1	-1.8109856009	5.0314156873	-1.7551213789	0.000292439353591756
WBGene00000	cpn-1	-0.9708363551	7.8863110980	-1.3373542433	0.00274369066672906
WBGene00000	crn-2	-0.4353830356	8.6080892246	-0.9538047627	0.0434236144179205
WBGene00000	cul-1	-0.9128845631	6.9424928069	-0.7292892218	0.043906502119357
WBGene00000	cul-5	-0.8863130371	3.2195335421	-1.1204560253	0.0033531951019102
WBGene00000	cyn-5	-0.3182618676	1.9909270866	-1.0295372387	0.00723497380251161
WBGene00000	cyn-7	-0.4210380440	7.4749138189	-1.1067966082	0.02375596895563
WBGene00000	cyn-10	-0.7261455461	1.1899076571	-1.3073272412	0.00219544124564106
WBGene00000	cyn-12	-0.6042960662	1.2483490299	-1.0876181795	0.0076207331370829
WBGene00000	hsp-90	-0.6388899726	3.6320870766	-1.1007139090	0.0173374876563467
WBGene00000	daf-25	-0.4194945366	6.8361972336	-0.8186805715	0.0465138372032017
WBGene00000	dbr-1	-0.8294941257	3.7644594303	-1.0684207604	0.00242437861275097
WBGene00000	dhs-11	-0.6805876527	2.8716528845	-1.3896285706	0.000268972261359105

WBGene00000	dhs-12	-1.4379477228	2.7960223819	-2.1503922821	9.70332770424679e-07
WBGene00001	dnc-2	-0.6674191931	2.2272846123	-1.1069358404	0.00262843922352046
WBGene00001	dnj-17	-1.0315362601	8.3385682268	-0.8155077036	0.0474925382769167
WBGene00001	dnj-19	-0.5613004052	2.0171113408	-0.7680322304	0.0430134412966845
WBGene00001	eef-2	-0.4388652776	2.1634932679	-1.3580958772	0.000789757293431072
WBGene00001	eef-1A.1	-0.6240433084	3.4319756153	-1.4473476432	0.00356305659172655
WBGene00001	eif-3.G	-0.3782749036	3.9686728579	-0.9846433199	0.0107665712442118
WBGene00001	eif-3.K	-0.3485575364	2.4520370689	-1.0353506253	0.00355483757279993
WBGene00001	elb-1	-0.4605590273	1.4231022422	-0.8868568727	0.029792358284338
WBGene00001	emo-1	-0.6941068448	5.8126929036	-1.0475027280	0.00536349951241789
WBGene00001	qars-1	-0.5048482349	3.9842759685	-1.0314160255	0.00316729511205931
WBGene00001	exl-1	-1.2593020110	4.2664734374	-1.4494594178	0.00089446647563869
WBGene00001	fbp-1	-0.4604296898	2.0758425313	-1.2440536630	0.00162191545186003
WBGene00001	fem-2	-0.5543916935	1.5779667829	-0.9963951934	0.00330240458741758
WBGene00001	fkb-1	-0.9165824389	2.8595502654	-1.0931924668	0.0321753128310218
WBGene00001	frm-10	-1.0454608694	8.7209391281	-1.3366946651	0.00262843922352046
WBGene00001	fum-1	-1.5729436556	5.6763212785	-1.7551863864	1.0420981813283e-06
WBGene00001	gln-6	-0.6173531983	9.6868572065	-1.1989267488	0.00112019944442587
WBGene00001	gna-2	-0.5041856027	2.0886056703	-0.8275668483	0.0116603908719766
WBGene00001	gpd-4	-0.9806284855	1.0894149170	-1.1805851953	0.0218364924533932
WBGene00001	gst-1	-0.3377534117	2.8227854668	-1.2472131894	0.000390481151327125
WBGene00001	hil-4	-0.1250670382	0.0149370295	-1.1345489792	0.00809816817866127
WBGene00001	hil-5	-0.5148861366	1.3117087075	-1.5101345023	5.32190669710519e-05
WBGene00001	him-5	-0.9643073232	1.0539857312	-1.3069079294	0.0145394758785685
WBGene00001	him-6	-0.7432588933	2.3051074668	-0.9426179148	0.00622535664943638
WBGene00001	him-14	-1.0609457528	5.6588696803	-1.2521427405	0.00350810133964749
WBGene00001	his-35	-0.9651596104	5.4422261131	-1.7065463547	7.16906857710512e-05
WBGene00001	C50F4.6	-0.8067511484	1.5980197957	-1.5907415455	1.04848973078758e-06
WBGene00001	his-37	-0.8155011572	1.2050953930	-1.7201528837	1.7408386620663e-06
WBGene00001	his-48	-0.5571205497	6.1163611875	-1.7386376088	0.0178821293999925
WBGene00001	his-59	-0.8935714087	3.1405607809	-2.0966537003	1.53330988297995e-06
WBGene00001	his-60	-0.8866623142	5.7805917329	-2.7282152167	1.41501011006282e-13
WBGene00001	his-61	-0.9038038228	5.7248314144	-2.4433133862	9.03744198071171e-05
WBGene00001	his-62	-0.9172401706	1.6070908179	-2.9157638696	1.65204800580944e-11
WBGene00001	his-63	-0.2180722657	0.0147780938	-1.9787675305	0.00231355529884879
WBGene00002	icd-1	-0.2288583599	5.6235155193	-1.0107304741	0.0433529837227188
WBGene00002	ife-3	-0.4076657628	1.2880294737	-1.0748219721	0.00162191545186003
WBGene00002	iff-1	-0.3462929443	5.7613774166	-1.7258843845	9.88795158767315e-05

WBGene00002	ile-1	-0.8654400816	1.8109723251	-1.0207042888	0.00136329489293447
WBGene00002	inx-14	-0.8988255879	1.0407711066	-2.1124269707	1.61990188885901e-12
WBGene00002	klp-10	-0.1464900257	0.0147885897	-1.2056839658	0.000622639997514217
WBGene00002	klp-16	-0.5885222183	5.4558422659	-1.1566351277	0.00437687905729372
WBGene00002	kars-1	-0.3167119557	7.8485025541	-0.9142205630	0.0144548481156194
WBGene00002	lap-2	-1.4053324887	1.0750228588	-1.8229049964	2.17325367568778e-09
WBGene00002	lat-1	-0.1967085498	1.8093003056	0.9396027736	0.0112437461973556
WBGene00002	lig-1	-0.6079772488	1.3537598196	-0.8235740368	0.0116603908719766
WBGene00003	lin-36	-0.6254649049	4.8230406702	-1.2967176993	0.0336672285262766
WBGene00003	lip-1	-0.7115827410	1.6292208652	-1.2341964768	0.00558748894629725
WBGene00003	lsm-1	-0.3417173615	3.9245755791	-1.0598765006	0.008865975072662
WBGene00003	mec-15	-0.2295755098	4.0297040220	-0.8215955770	0.0148951764508183
WBGene00003	mxl-1	-0.5388407371	7.8275553041	-0.9711798880	0.00597326454241204
WBGene00003	mxl-2	-0.5393565462	3.4676362753	-1.2268979900	0.000749009360469706
WBGene00003	ndx-6	-1.0319850623	1.2816030900	-1.5694954390	0.00491233666167212
WBGene00003	nhr-61	-0.9925145010	8.4935118857	-1.1981595270	0.0173238639391292
WBGene00003	npp-16	-0.4455928347	1.8531743469	-0.8848234443	0.0402998074998023
WBGene00003	ntl-2	-0.6882065484	1.5334262074	-0.8735861070	0.0243900038821214
WBGene00003	pab-1	-0.3339409934	2.7068749034	-1.3551435446	0.00187001525247731
WBGene00003	pas-1	-0.2623983344	1.0232978342	-0.9205474162	0.00677370412473355
WBGene00003	pas-2	-0.6069178869	1.3804406865	-1.0171138248	0.0136490014199656
WBGene00003	pbs-3	-0.5899410603	1.3150710082	-0.8344276693	0.0223806327271981
WBGene00003	pbs-7	-0.3535193198	6.6217295391	-0.8821034924	0.0156574305595428
WBGene00003	pdr-1	-0.5576817916	4.0575677010	-0.7335878719	0.0463171456168638
WBGene00004	plp-1	-0.7432968811	3.8677538039	-1.1600299410	0.000267187769893407
WBGene00004	pms-2	-0.7669307935	4.9123826835	-0.9934945553	0.0207387346240917
WBGene00004	stam-1	-1.1463001873	3.6613381358	-0.9420714553	0.00725539903713165
WBGene00004	sin-3	-1.0532992737	3.1038429569	-10.630972264	4.8522884794687e-31
WBGene00004	pqn-51	-0.6961635962	1.1206666066	-0.8657252768	0.0164796048661349
WBGene00004	psr-1	-0.4413432710	1.1936327305	-0.8892430936	0.00908265097152629
WBGene00004	puf-5	-0.6335012321	2.4772822100	-1.0418004738	0.00595323709087748
WBGene00004	puf-10	-0.4553258804	4.9857248266	-0.8905655287	0.0454929174258304
WBGene00004	rab-6.1	-0.8632007402	2.5581596407	-1.2989039273	0.000126432142977859
WBGene00004	ran-1	-0.0970982897	0.0085010407	-1.0555008946	0.00985659341951121
WBGene00004	rbx-1	-0.5069107471	1.1424488300	-0.8548074721	0.0494474158666274
WBGene00004	rde-4	-0.2540430478	1.7684604548	-0.7615112145	0.0321753128310218
WBGene00004	rec-1	-0.7542881720	4.5165455960	-1.1563917120	0.0214213514035014
WBGene00004	rfc-3	-0.3573178074	1.6872252018	-0.9653577680	0.00204518906207917

WBGene00004	rfs-1	-0.8534184100	3.9145513497	-2.3379747838	0.0169530127113724
WBGene00004	rme-2	-0.4625018934	1.5062840506	-1.3077178694	1.85524941163152e-05
WBGene00004	rla-0	-0.4083455261	8.0077306538	-1.6401879249	0.00108793603484848
WBGene00004	rla-1	-0.3932678808	2.8992289121	-2.1394382648	1.94680928232503e-05
WBGene00004	rla-2	-0.2330882339	5.2745005176	-1.1568857916	0.00953480849473906
WBGene00004	rpl-1	-0.3804133921	1.9729830284	-1.6932607257	0.000689030759008703
WBGene00004	rpl-2	-0.3700555942	1.2117831212	-1.2202383874	0.0156468961960255
WBGene00004	rpl-3	-0.3294480168	3.7276067183	-1.4556824908	0.00470154847198345
WBGene00004	rpl-4	-0.3622434460	7.8281827094	-1.3902556610	0.00369637835521812
WBGene00004	rpl-6	-0.2708104065	4.6538605452	-1.4577076530	0.00595323709087748
WBGene00004	rpl-7	-0.2481825612	4.9218361615	-1.2705487617	0.0150329335626997
WBGene00004	rpl-7A	-0.3247485131	2.4313217166	-1.6514520042	0.000651782091240334
WBGene00004	rpl-9	-0.6739577912	3.5572850255	-1.8588451135	5.23344157137434e-05
WBGene00004	rpl-10	-0.4369016013	2.5390871050	-1.4817045911	0.00294785822294085
WBGene00004	rpl-11.1	-0.3769524823	7.3153874686	-1.5071279023	0.00256401156083131
WBGene00004	rpl-12	-0.2938576649	3.7452473223	-1.5937970132	0.00116343402047996
WBGene00004	rpl-13	-0.3016035061	2.4729009056	-1.4344772951	0.00645439812875181
WBGene00004	rpl-14	-0.4715140939	4.2341010851	-1.5699932357	0.000958347340252515
WBGene00004	rpl-15	-0.3774457435	8.5957987735	-1.4510327325	0.00768576189551562
WBGene00004	rpl-16	-0.3318900813	7.0063422339	-1.4690798572	0.00539452957835146
WBGene00004	rpl-17	-0.3782002740	3.0699281401	-1.4843369007	0.00534762234784027
WBGene00004	rpl-18	-0.4521054339	4.8220196990	-1.4236226782	0.00388591688508462
WBGene00004	rpl-19	-0.4021779037	6.1949177265	-1.5351761901	0.0024790258954136
WBGene00004	rpl-20	-0.3215015728	3.2190374072	-1.5435452679	0.00215491874653192
WBGene00004	rpl-21	-0.4687972004	4.7387629116	-1.7766481118	0.000336985098138496
WBGene00004	rpl-22	-0.3808321265	2.4817002633	-1.6960506568	0.000133307543909504
WBGene00004	rpl-23	-0.1706133376	0.0061330386	-1.4816191824	0.00353409625586477
WBGene00004	rpl-24.1	-0.3254967732	1.8557772896	-1.5754443836	0.00263876395481626
WBGene00004	rpl-25.2	-0.5462434042	6.6495366415	-1.9330320763	1.20231853332228e-05
WBGene00004	rpl-26	-0.2992506342	8.4892576284	-1.4257370654	0.0039835275127462
WBGene00004	rpl-27	-0.2583045780	7.1635550474	-1.7090125081	0.0002890451114692
WBGene00004	rpl-28	-0.4788453989	2.5745767373	-1.8621309397	3.3054287899841e-05
WBGene00004	rpl-29	-0.4322833769	2.2930263149	-1.5425365234	0.00185435322591254
WBGene00004	rpl-30	-0.3710573047	7.1724306738	-1.4897670125	0.00128421156701525
WBGene00004	rpl-31	-0.3321938383	1.3114516515	-1.7126013896	0.000183374429730536
WBGene00004	rpl-32	-0.5333899366	4.3810852644	-1.8468371200	0.000118714794143051
WBGene00004	rpl-33	-0.3438038436	2.9040222508	-1.4530021316	0.00471864363186537
WBGene00004	rpl-34	-0.3883493205	7.1176623062	-1.5882137546	0.00103691264406009

WBGene00004	rpl-35	-0.4074353098	6.5748880996	-1.6417385048	0.000609852746924961
WBGene00004	rpl-36	-0.4456718816	7.0820972295	-1.7771999833	0.000254238044499091
WBGene00004	rpl-38	-0.2928807931	1.3737374650	-1.5577345510	0.00193076697382952
WBGene00004	rpl-39	-0.5540409542	8.5285770963	-1.5044532819	0.00294492304896226
WBGene00004	rpl-36.A	-0.3725950875	2.9015780671	-1.5846622280	0.000762435275597351
WBGene00004	rpl-43	-0.4515092511	3.0851189726	-1.6327215266	0.000689030759008703
WBGene00004	rpn-7	-0.3910406748	8.1014571188	-0.8482889124	0.043156163420299
WBGene00004	rps-0	-0.3983893109	2.9027289726	-1.7089598964	0.000499516337434342
WBGene00004	rps-1	-0.3864440134	3.5652088315	-1.3415200368	0.00664951028719712
WBGene00004	rps-2	-0.4400148164	1.1750864907	-1.4921060663	0.00190697006507797
WBGene00004	rps-3	-0.3935082217	8.6068525655	-1.5516041935	0.00124182782482806
WBGene00004	rps-4	-0.4074181351	1.7314623305	-1.5424429826	0.00102379428314494
WBGene00004	rps-5	-0.4539836897	4.6651990542	-1.6177178026	0.00162191545186003
WBGene00004	rps-6	-0.3816209657	1.9437111799	-1.4133075781	0.00351398392465421
WBGene00004	rps-7	-0.3700926017	2.8386142415	-1.5993393193	0.00113733838842422
WBGene00004	rps-8	-0.6469713667	8.6370801570	-1.9487690363	8.48708236411893e-05
WBGene00004	rps-9	-0.4484421675	1.4216531526	-1.7762333460	0.000234933118014274
WBGene00004	rps-10	-0.4155159035	5.9055542044	-1.6358715202	0.000867385463938174
WBGene00004	rps-11	-0.5508690208	5.5401754301	-1.7993471689	0.000116830216264568
WBGene00004	rps-12	-0.5309881268	3.0980813049	-1.7633760575	5.80777911736705e-05
WBGene00004	rps-13	-0.3696235906	1.5844551122	-1.5421879680	0.0013203911812113
WBGene00004	rps-14	-0.5550313878	7.4114390760	-1.9682518130	3.3054287899841e-05
WBGene00004	rps-15	-0.4209598649	8.6872404037	-1.6072294472	0.000714919184242183
WBGene00004	rps-16	-0.5245532836	7.0263697042	-2.0533369478	8.44127148142459e-06
WBGene00004	rps-17	-0.3909382258	4.0914698194	-1.4830265442	0.00283066552464399
WBGene00004	rps-18	-0.3274262870	4.7402347794	-1.5580871678	0.00189260944960837
WBGene00004	rps-19	-0.4574747485	8.6105071432	-1.7090277256	0.000163958780800124
WBGene00004	rps-20	-0.3425099074	3.9755370059	-1.3695529463	0.00230390817754383
WBGene00004	rps-21	-0.4514337455	9.8552331082	-1.6694605304	0.000369930480878299
WBGene00004	rps-22	-0.3821669989	2.6237082793	-1.6267329478	0.000394154325503377
WBGene00004	rps-23	-0.5358477568	7.6000838970	-1.8391539485	0.000145937036737947
WBGene00004	rps-24	-0.1467249447	0.0302477597	-1.2249248329	0.0161451716418977
WBGene00004	rps-25	-0.5691245147	2.0886056703	-1.7808991830	0.000340957907800636
WBGene00004	rps-26	-0.4147188594	1.6636349457	-1.5717559979	0.000622639997514217
WBGene00004	rps-27	-0.4214481707	2.2890959325	-1.6557272939	0.000269748600157396
WBGene00004	rps-28	-0.3812345578	1.1784973439	-1.7849871467	0.00032445021679883
WBGene00004	rps-29	-0.3751809554	4.2843285834	-1.7376920320	0.000446587150055289
WBGene00004	rps-30	-0.3284020336	1.0573035318	-1.4027205985	0.00132144705165653

WBGene00004	rpt-1	-0.3232675248	2.2434666428	-0.8602071108	0.00723677364366282
WBGene00004	rpt-5	-0.5067849047	2.8439954747	-0.9514379329	0.0223806327271981
WBGene00004	rars-2	-0.9299439249	3.3252307092	-0.9874426635	0.00539452957835146
WBGene00004	sip-1	-0.3189010699	0.0031192105	-1.3400297289	0.00573886886712709
WBGene00004	skr-1	-0.9997938584	3.4997327317	-1.2008684631	0.000145937036737947
WBGene00004	skr-2	-0.6761795588	1.2320794765	-1.1811492515	0.00559280336363835
WBGene00004	smn-1	-0.7898092908	5.6880804928	-1.3756007072	5.62711545793835e-05
WBGene00004	smo-1	-0.2214775801	2.3217466233	-0.8953538452	0.0398296893164544
WBGene00004	spd-3	-0.2982160428	0.0092015218	-0.9526573477	0.0423296157548056
WBGene00004	spe-5	-1.0427953308	3.6020906321	-1.1558171363	0.0128213883420574
WBGene00005	F26F4.8	-0.8052724264	3.1341042812	-1.4596761892	0.000153390482255783
WBGene00005	sars-1	-0.5383416301	2.6355016642	-0.9773968581	0.00491233666167212
WBGene00006	tac-1	-0.2314730787	1.9301293696	-1.1175471383	0.000972056743744006
WBGene00006	fut-3	-1.5561401514	3.5700372990	-2.5119906050	3.38313618532338e-16
WBGene00006	ant-1.1	-0.4573381921	4.2025527253	-1.5295122736	0.000121181955763698
WBGene00006	tag-115	-0.4556054970	2.1992705782	-1.3165816197	0.000549694814527833
WBGene00006	acl-3	-0.5669494652	4.8631364744	-1.1632204035	0.00128421156701525
WBGene00006	thk-1	-0.1926838722	0.0064046603	-0.7022660407	0.0485777920031503
WBGene00006	ubc-6	-0.6359945834	4.8006338081	-1.2214483782	0.00497240446106148
WBGene00006	ubc-9	-0.5475199363	1.3718059033	-1.1816026646	0.000549694814527833
WBGene00006	ubc-18	-0.6783898994	1.1151895302	-1.0175219274	0.00885639537461736
WBGene00006	ubh-2	-0.8049419798	6.6138042703	-1.4292058231	0.0002890451114692
WBGene00006	ubh-3	-0.9403449242	4.0114262131	-1.3558415712	5.80387754337262e-05
WBGene00006	ubl-1	-0.3168629102	7.3415218088	-1.4030656053	0.00205184539342337
WBGene00006	ubq-2	-0.3981012661	8.2886201643	-1.5201320652	0.00118945466690309
WBGene00006	ulp-3	-0.5316494095	2.1587873524	-1.0867616093	0.0485202274827325
WBGene00006	unc-54	-0.5328330847	0.0401812736	1.1335144891	0.0176109583884111
WBGene00006	vig-1	-0.2959724087	1.2492863828	-1.0832350834	0.000649083160055533
WBGene00007	mdt-8	-0.4194669582	3.3802691479	-0.8078610486	0.0335837708426836
WBGene00007	mdt-18	-0.6825107349	1.0480560598	-1.0422739955	0.0115552719636781
WBGene00007	mdt-22	-0.6541662931	2.0807953530	-1.1897511660	0.000179216214333118
WBGene00007	mdt-29	-0.4446348723	1.2199995383	-0.8013734554	0.0452974243984957
WBGene00007	B0001.5	-0.3419594194	3.1178245047	-1.0156659540	0.00474556665655936
WBGene00007	trx-2	-2.0887552798	7.5123985806	-1.7771565630	1.27082934119061e-05
WBGene00007	B0035.3	-0.4005754857	5.7867479690	-0.8962216851	0.00942429983180476
WBGene00007	acly-2	-0.7281197961	2.0586707836	-0.7133770607	0.0365753756603351
WBGene00007	C05C10.2	-0.9433879290	1.1803831387	-0.9168286285	0.00718173560036619
WBGene00007	cdc-48.1	-0.1687610200	7.2998564705	-0.7739779846	0.0296206393086034

WBGene00007	algn-6	-0.7971684283	6.8034140713	-1.0952687003	0.00640912669776512
WBGene00007	pptr-2	-0.7375225359	2.6861015881	-1.0430103727	0.00100173661445288
WBGene00007	C14B1.8	-0.3155857172	1.7635594524	-1.0902775933	0.0021394879293794
WBGene00007	C18D11.3	-0.1195011026	0.0430836926	-0.9200560415	0.040615685318781
WBGene00007	tomm-40	-0.5264361143	1.7256869831	-0.7628456574	0.033754881545758
WBGene00007	tram-1	-0.8076938919	2.2172906247	-1.1239410128	0.0093802098399202
WBGene00007	C24F3.2	-1.4858708171	7.2863207846	-1.9443490351	6.32866611528839e-08
WBGene00007	qns-1	-1.2266151514	2.5352692090	-1.3965694009	1.66278899885084e-05
WBGene00007	clec-87	-0.6356347213	1.1313846575	-1.1714386254	0.00501386450942347
WBGene00007	mrpl-34	-0.1904034156	0.0039132199	-0.9012533153	0.0398296893164544
WBGene00007	C25G4.2	-0.4412477432	1.6945880036	-1.4079441480	0.000770969507008345
WBGene00007	spe-44	-1.2522617747	1.8646719467	-1.4861207563	0.000651782091240334
WBGene00007	C26D10.3	-0.7826703895	1.2181655542	-1.7833490351	0.000903237471222072
WBGene00007	C27B7.5	-0.4372256134	8.5791535086	-1.0081147186	0.00677370412473355
WBGene00007	tofu-1	-0.3059916797	1.8131129007	-0.9779249716	0.00449720293366652
WBGene00007	C29A12.1	-0.9908218767	1.1809306492	-1.3729037361	3.54156571913312e-05
WBGene00007	C30H6.9	-0.7039602655	7.7527515165	-1.1431172231	0.00636986770451487
WBGene00007	C35A5.8	-0.7765746188	5.6671985698	-0.9112682975	0.0100151084487745
WBGene00008	sfxn-1.4	-1.7512250898	7.4986966318	-2.8136619861	0.000116830216264568
WBGene00008	C49C3.7	-1.1269090558	1.4192181563	-1.4695566147	0.000353928006283995
WBGene00008	ril-1	-0.4906487918	4.3909827285	-0.8422557799	0.033754881545758
WBGene00008	C55A6.1	-0.9387095893	3.2071270317	-1.6594352234	1.75400422059934e-08
WBGene00008	C56A3.4	-0.6811823326	3.0241019245	-1.0556104617	0.00103219645283455
WBGene00008	D1054.3	-0.6038385572	2.7164228678	-1.7361372844	3.07788940615176e-09
WBGene00008	F01G4.5	-0.4388919831	1.3538986267	-1.3745725484	0.00289114599560019
WBGene00008	F02E9.5	-0.7619556453	4.8440360057	-1.7265824456	1.46519193149496e-05
WBGene00008	gfat-1	-0.5611847781	2.3867493160	-1.2153827655	0.00319524488216138
WBGene00008	F07H5.10	-0.6885729039	1.1748905824	-1.3157201525	0.000124181031519663
WBGene00008	dsb-1	-0.5783131946	8.9287428108	-0.7722800320	0.0463171456168638
WBGene00008	F10B5.2	-0.3811282175	5.8302742659	-0.9538947276	0.0258679652651789
WBGene00008	pch-2	-1.5270260432	7.4809972521	-1.9511252445	1.66367469370274e-07
WBGene00008	dylt-1	-0.3437059623	1.1649729011	-0.9054526540	0.013608461639879
WBGene00008	eef-1G	-0.3998451517	2.2597720025	-1.5021924325	0.000100727501279383
WBGene00008	elli-1	-0.4355634140	2.6878622789	-0.8415947979	0.0154523121407801
WBGene00009	hint-1	-0.5915276806	1.0113960014	-0.8744866967	0.0353087416934608
WBGene00009	pfd-6	-0.3224391163	1.3543373103	-1.2296071529	0.000322350607850862
WBGene00009	gfat-2	-0.4594620784	5.1029519054	-1.0754912597	0.00643204948490271
WBGene00009	F22B5.10	-0.2691763466	1.8901643471	-0.8434912559	0.0169233036117202

WBGene00009	F22D6.2	-0.2892825258	3.1296373623	-0.6950026320	0.0437544571524835
WBGene00009	F23B12.4	-1.1894529641	3.6820746903	-2.1880784225	0.0456233515442048
WBGene00009	ndk-1	-0.5641154420	8.9133529412	-1.6848575933	0.000205564210550367
WBGene00009	F25H9.7	-0.5492533349	1.9798320856	-1.2691994664	0.00124982886905589
WBGene00009	cox-7C	-0.7851126825	6.0010663306	-1.0726602970	0.0103104356701034
WBGene00009	F27D4.1	-1.2751067877	1.6202251059	-1.2129652291	0.000133307543909504
WBGene00009	F30F8.1	-0.5432579572	9.4971124560	-1.1101663233	0.0161518182402066
WBGene00009	F31C3.3	-0.7318656297	2.0308078699	-1.0396672613	0.00379708600337224
WBGene00009	psf-2	-0.6881635577	4.6904891888	-1.6006291136	5.23344157137434e-05
WBGene00009	F32A7.4	-0.8973804502	3.1668106536	-1.3305551413	0.000340957907800636
WBGene00009	tbc-3	-0.9517081694	1.3024874677	-1.1877037643	0.00164273934511792
WBGene00009	F32D8.5	-0.7103876404	1.6847515716	-1.7315179268	2.78971557688454e-07
WBGene00009	F32D8.14	-0.4001241104	2.4065931368	-1.0042711448	0.00355483757279993
WBGene00009	marb-1	-0.6808749329	3.7244325448	-1.0308646768	0.0184425133577051
WBGene00009	F35G12.7	-1.2718197184	2.0309198654	-1.7583554180	9.07077462671283e-07
WBGene00009	F40F8.1	-0.6557124468	4.7605435016	-1.1572065423	0.000450766117250963
WBGene00009	xbx-6	-0.9027417787	5.7912387622	-1.5386183602	3.24555459924065e-06
WBGene00009	aagr-3	-0.4835563219	1.0632970816	-0.8435984851	0.02598056971727
WBGene00009	F43G6.3	-0.7887784615	4.6879683899	-2.0812738597	1.74603546934847e-07
WBGene00009	egg-3	-0.3666296442	5.9766185642	0.7623823118	0.0432109890811548
WBGene00009	F44G4.1	-0.3344606479	7.8765707121	-0.8723923033	0.0124380346774357
WBGene00009	F44G4.2	-0.4717225958	1.9814144362	-1.1359373822	0.00123881112648002
WBGene00009	F44G4.3	-0.9523312889	2.5569131256	-1.4929426417	0.00815576152222132
WBGene00009	F46B6.12	-0.4203514805	5.0941187521	-0.8707885297	0.0262867713947236
WBGene00009	F49C12.9	-0.7833726172	4.7990975735	-1.8683892351	5.83330330439036e-11
WBGene00009	F49C12.11	-0.3270955994	2.2045576758	-1.1958323936	0.00294492304896226
WBGene00009	F49C12.12	-0.5668485735	2.2094101864	-1.0798222647	0.0331096221507528
WBGene00009	vha-17	-0.8833398887	2.5197517846	-1.5558250615	0.000607456725515455
WBGene00009	gcsh-2	-1.1540309769	3.8459919775	-2.4526437322	1.66714033278636e-13
WBGene00009	kbrl-1	-1.0341766245	1.1934406282	-1.3629047578	0.0089347942925171
WBGene00009	ogr-2	-2.3004264996	1.2169142485	-2.1859431606	0.000213129492314089
WBGene00010	bcs-1	-0.3022414348	1.1384254462	-0.9893890330	0.00506681649534184
WBGene00010	F54D5.7	-0.4828423207	1.5149573430	-0.7507310804	0.0461749028997023
WBGene00010	vha-14	-0.2536654791	2.7115152254	-0.6915195339	0.0454929174258304
WBGene00010	F57A10.4	-0.8859906303	4.2973897456	-1.1762634227	0.0281160137391156
WBGene00010	pot-2	-0.7735719677	2.1126376028	-1.3402216854	0.000958347340252515
WBGene00010	F57F5.1	-1.0765404398	0.0003458020	2.0650189582	0.0364512076140284
WBGene00010	F58A4.2	-1.8286745478	6.5292526081	-2.7138007267	1.18152069329156e-12

WBGene00010	F58A4.6	-0.6115773840	7.5806236413	-1.3028290016	0.000935725912547021
WBGene00010	rbm-17	-0.2390840649	0.0002616896	-0.8905416563	0.0332656119558407
WBGene00010	F58H1.3	-0.5631400184	2.8489624451	-1.2898098780	0.00450375172201545
WBGene00010	idh-1	-0.8078370198	2.1114896102	-0.8880986145	0.00895635473259128
WBGene00010	H19N07.3	-0.3512539291	0.0226437656	-1.1886058128	0.0161451716418977
WBGene00010	atp-1	-0.4419912086	8.6622808809	-1.0883778038	0.00437687905729372
WBGene00010	enu-3.6	-1.0323672015	9.9527439227	-2.0450308938	4.58962259640861e-05
WBGene00010	K01G5.8	-0.2381704544	0.0035929059	-0.9184963340	0.0223151767303369
WBGene00010	rack-1	-0.3811215248	9.8058012413	-1.4001266298	0.00360746772975649
WBGene00010	cdc-48.3	-0.8701636974	2.5796956277	-1.2759944052	0.00545753427217956
WBGene00010	ath-1	-1.0755450059	1.3001210330	-1.3072188785	0.00092440542526763
WBGene00010	vacl-14	-1.3365613875	3.6261531674	-1.0634259299	0.0024790258954136
WBGene00010	scbp-2	-0.9931831887	3.2997836661	-1.7971311671	0.0118123134770021
WBGene00010	dut-1	-0.3659860409	8.4687219177	-0.7392087473	0.0372327044948143
WBGene00010	K07C5.3	-0.3888306999	3.8060785956	-0.7457148888	0.0412620104466134
WBGene00010	dbn-1	-0.4802692674	6.7113012021	-0.7674629562	0.0286823030911631
WBGene00010	K08E3.5	-0.5623750080	8.5874517363	-0.7943690759	0.0336778002262491
WBGene00010	K08E4.2	-0.8680623530	1.1549137611	-1.6972746438	0.000111854824934051
WBGene00010	K08F4.3	-0.4515678516	1.9515916629	-1.7388219232	2.26635683089548e-08
WBGene00010	aipl-1	-1.2290300813	2.1281209507	-1.4586606714	1.04848973078758e-06
WBGene00010	trpp-6	-0.1901924785	0.0112935315	-0.7493638886	0.0423961764505718
WBGene00010	sodh-1	-1.2261338548	0.0004697212	-2.9936148734	0.00157921715493894
WBGene00010	M01F1.3	-0.2785660579	1.4847781986	-1.0441231872	0.0119879695899209
WBGene00010	M110.3	-0.5447498729	5.9766674736	-1.1732097581	0.0128272093808894
WBGene00010	R01H10.7	-0.6394986035	7.2681308568	-1.3418129210	0.00168516076425543
WBGene00011	R05H5.3	-0.5012004694	4.7292367306	-1.2135240613	0.00979700011909909
WBGene00011	R05H5.4	-1.8168783661	5.5833775605	-1.6145801075	0.000653977949136587
WBGene00011	R05H5.5	-1.9201798544	6.0076349182	-1.8614192293	0.0027895859221073
WBGene00011	arrd-13	-1.2641694458	1.1958960015	-1.1550032912	0.00273177042703495
WBGene00011	cpg-3	-0.4146628504	1.4738771280	-1.5332574385	0.000352530084109221
WBGene00011	adsl-1	-0.3995945390	7.5167303738	-0.7541825795	0.0473193699012478
WBGene00011	ztf-15	-0.8017513408	5.9570924934	-0.8685533008	0.0219922527615037
WBGene00011	R07H5.8	-1.1497821624	8.4958040996	-1.3214051167	8.44127148142459e-06
WBGene00011	rbm-3.2	-0.6690063715	3.2936958100	-1.7767689110	0.000457131841034829
WBGene00011	gkow-1	-0.6057732963	2.6572062572	-0.7449825760	0.0467334672360067
WBGene00011	R53.4	-0.2202769992	1.1476011525	-0.9715645943	0.0332656119558407
WBGene00011	R74.8	-0.3585322177	2.4696934661	-0.7525830315	0.0325318905054985
WBGene00011	allo-1	-1.1335785511	6.0357193278	-1.3826643408	4.49779203958323e-05

WBGene00011	R186.3	-0.4641227786	3.0220018998	-0.9622262687	0.00989402234545058
WBGene00011	hrde-2	-0.4292890068	3.2835665795	-1.1539056107	0.00103219645283455
WBGene00011	T03F6.3	-0.8276579464	3.3238226568	-1.5210589026	1.6216592557174e-06
WBGene00011	T05B9.1	-0.1782414408	3.3033027589	-0.7959909162	0.0243138899128504
WBGene00011	rmd-1	-0.4135262556	3.1138904300	-1.4213679549	9.01310911531528e-06
WBGene00011	pdha-1	-0.5212875202	3.7102180403	-1.0025024889	0.00292542072350632
WBGene00011	gpcp-2	-2.0207236784	0	-1.7656417776	3.69496504494446e-08
WBGene00011	cchl-1	-0.3563622074	9.8647661184	-0.8058468736	0.0204303981800394
WBGene00011	umps-1	-1.1072567848	1.7410510820	-1.5608666892	9.55535219717875e-06
WBGene00011	sds-22	-0.5000434351	6.0304350408	-1.3680361326	2.52583743459589e-05
WBGene00011	T09A5.15	-0.5000619919	0.0012324174	-1.9719376368	0.00897654577886356
WBGene00011	T10C6.6	-0.7322621015	6.7428429512	-1.0484980711	0.00511247369619112
WBGene00011	T12G3.4	-1.3815803598	1.0078264132	-2.1155394815	2.01871975550886e-06
WBGene00011	mrps-18B	-0.8432093915	4.3479447137	-0.9892989212	0.0122456032813657
WBGene00011	gtf-2H2C	-0.4152325148	1.3473577757	-0.8210022570	0.0257935778433515
WBGene00011	T20D3.5	-0.8133543959	1.3055734811	-0.9979583334	0.0154518252417962
WBGene00011	mrpl-50	-0.1414246863	0.0168981478	-0.9845180643	0.00739247315611174
WBGene00011	erh-1	-0.1852913826	0.0031173682	-0.7940099336	0.0243138899128504
WBGene00011	ctf-8	-0.3930476357	0.0003215992	-1.2087228110	0.000207815563577541
WBGene00012	dkf-2	-0.2267166726	0.0001314799	0.9580136230	0.00924849189475974
WBGene00012	ebp-2	-0.7893579946	1.3543078897	-0.9717962945	0.0166422659830224
WBGene00012	adbp-1	-0.9405922344	2.3656215931	-1.1864851469	0.0161451716418977
WBGene00012	W01D2.1	-0.3000410725	5.0640328269	-1.5812734808	0.00157921715493894
WBGene00012	osta-3	-0.3539266365	6.7626162963	-0.8870789312	0.0100767602737566
WBGene00012	W01G7.4	-0.3942368688	3.2940223166	-1.2025145249	0.00050856030341505
WBGene00012	W02B12.11	-0.5908768659	3.1636667851	-0.8567347953	0.0243138899128504
WBGene00012	W07G4.3	-1.5475617317	4.2705213667	-1.6089383190	4.62190058821177e-05
WBGene00012	Y11D7A.7	-2.0072527163	4.1093964004	-1.9051573512	0.00100173661445288
WBGene00012	Y17G7B.21	-0.5094305294	4.8549416187	-1.3984016707	0.0269444824229092
WBGene00012	Y18D10A.11	-0.4587301103	1.2136594903	-1.4402627358	2.51064728013099e-05
WBGene00012	car-1	-0.3747943413	0.0167989560	-0.8464287280	0.0291838371309107
WBGene00012	cec-7	-0.3695392846	1.2427556527	-1.1238800167	0.00276905205630985
WBGene00012	Y39B6A.37	-0.2811130407	6.8587149274	-0.8752206036	0.0296206393086034
WBGene00012	Y41E3.8	-0.5475481823	8.6387744843	-1.1150674933	0.0168205811972573
WBGene00012	Y43E12A.3	-0.8635984119	3.4015784651	-1.7978704739	4.71144492096621e-05
WBGene00012	mrpl-20	-0.1421943328	0.0475653611	-1.0816017030	0.0336672285262766
WBGene00013	cept-2	-1.6047156024	1.7986228230	-1.5998202900	0.00217151044409565
WBGene00013	Y49A3A.3	-0.9183725840	8.3184315627	-0.9587082900	0.0369209930932115

WBGene00013	Y53H1B.2	-0.6233469971	0.0284400933	2.5840193417	1.66488265312191e-05
WBGene00013	Y54G9A.5	-0.8114311843	1.0343918552	-1.6189945068	2.34011410893036e-07
WBGene00013	bub-3	-0.4485346493	2.1511795058	-0.8244226570	0.0170958384865374
WBGene00013	Y57G11C.8	-1.0192290657	7.2160233597	-2.0966361873	0.000422686938373154
WBGene00013	Y57G11C.36	-2.4713082915	1.4371164363	-2.6979641932	2.59794690993153e-14
WBGene00013	fars-2	-0.5171478603	1.5557331811	-1.1215995332	0.00139555742596482
WBGene00013	Y62E10A.13	-0.3134633615	3.7179187708	-0.8620963397	0.0305254502373799
WBGene00013	ule-5	-1.6094132039	0.0123245118	6.2857815922	1.80372556890977e-07
WBGene00013	Y67H2A.2	-0.2763433167	3.2053056244	-1.3185028101	0.000684897301178945
WBGene00013	micu-1	-0.6657002657	7.5385929469	-0.9693980331	0.0178115489770295
WBGene00013	kdp-1	-0.1243183307	0.0497230328	-0.9519931418	0.0155184979937502
WBGene00013	Y75B8A.18	-0.5579031233	2.5032377908	-1.2262224486	0.000205564210550367
WBGene00013	bath-36	-0.3370610028	0.0061809049	-1.3187364468	0.00134096442093109
WBGene00013	Y87G2A.18	-0.9270177866	4.9290863993	-1.0983711178	0.0283902055649011
WBGene00013	Y105E8A.14	-0.1283727711	0.0324539487	-1.0867969912	0.0121827370881007
WBGene00013	Y106G6H.14	-0.2292033737	0.0056123103	-0.7647056501	0.0357022951838369
WBGene00013	ZK287.7	-0.5311457715	2.2803548517	-0.9565891926	0.0261894168811472
WBGene00014	riok-3	-0.4536584092	6.6921295050	-0.9974083281	0.00506681649534184
WBGene00014	ZK643.2	-0.7944352241	9.0383093569	-0.9629729015	0.0110532723345955
WBGene00014	gdh-1	-0.6325820352	5.2541991511	-0.7441263183	0.0445570152615297
WBGene00014	chpf-1	-0.4935422765	3.9537966699	-1.0286710904	0.00598048819140576
WBGene00014	ZK856.11	-0.5018604379	1.5825793629	-1.2363233887	0.00177514678549764
WBGene00014	clpp-1	-0.7412954311	6.7615649591	-1.1187636939	0.00276901369474864
WBGene00014	ZK1010.2	-0.1647328013	0.0164627960	-0.9916063361	0.00474556665655936
WBGene00014	ZK1320.9	-0.9668023110	1.2570705420	-0.9271411037	0.0145923950011764
WBGene00014	C06A1.4	-0.2676950401	8.6545931295	-0.7837600362	0.0200811112092543
WBGene00014	F56D5.4	-0.8396566090	8.3449638413	-1.5403556601	0.0261252586228313
WBGene00014	ZK637.6	-1.3613854990	1.3625881610	-1.9055148611	1.78334142028818e-06
WBGene00015	B0205.8	-0.6276551006	0.0001122942	-0.9306068179	0.0312371879423459
WBGene00015	B0238.9	-0.8303227933	2.4170906324	-1.0098649568	0.00530316637230017
WBGene00015	natc-2	-0.4078630107	9.1325745551	-0.9026140805	0.00908195216272628
WBGene00015	cpg-2	-0.4851018241	7.6793526966	-1.0898282627	0.0465138372032017
WBGene00015	B0304.2	-0.6894900423	3.7581304138	-1.0899299474	0.00216338447887046
WBGene00015	arle-14	-0.3742523276	3.7258906575	-0.8677645976	0.0179408245694232
WBGene00015	B0336.13	-0.2505110654	0.0004146922	-1.1111787063	0.000871900460474218
WBGene00015	cdc-26	-0.3326188450	5.9579735573	-0.8938169368	0.0242354245041834
WBGene00015	C01B12.8	-1.3002002397	1.9295358771	-1.6039153104	7.58581909918408e-05
WBGene00015	ddi-1	-0.4491623878	4.7370211059	-0.9044096528	0.00807211411071431

WBGene00015	C01G8.1	-0.2532326861	9.0129725192	-1.2687337757	3.31185720168559e-05
WBGene00015	ivd-1	-0.7684977694	2.0228172663	-0.8806047842	0.0129349286410967
WBGene00015	snpn-1	-0.5810797893	4.3510958734	-1.0255233726	0.0106033449406399
WBGene00015	C04E6.11	-0.6237402425	3.4571785473	-0.7735318417	0.0481286646478953
WBGene00015	C06A5.6	-0.5771773245	3.9786672047	-1.0700424020	0.00103219645283455
WBGene00015	sams-3	-0.2049445593	0.0003992857	-1.5625705931	6.3694466229515e-07
WBGene00015	C07H6.2	-1.0320199470	6.0331066472	-1.4063290517	0.0337368089204015
WBGene00015	C09E7.7	-0.7844950501	6.3471138734	-1.4545368804	0.00841726100453489
WBGene00015	C11D2.7	-0.8427442863	8.8913192249	-1.1930563039	0.000903237471222072
WBGene00015	C13F10.5	-0.2361045210	0.0024699689	-0.9327570622	0.0189396424832857
WBGene00015	C16A11.3	-0.2826908479	0.0001262755	-0.9443555945	0.0303131756710447
WBGene00015	C18F10.7	-1.3677162581	8.8355375992	-1.2492222052	0.000111676552334899
WBGene00016	mdt-26	-1.0359444605	9.5858728167	-1.2617699943	0.00459640898935717
WBGene00016	ift-43	-1.0658862161	9.3487214147	-2.6902234421	0.00200107317870346
WBGene00016	elpc-4	-0.4299420326	8.3028137838	-1.0403901053	0.0069037543072462
WBGene00016	mesp-1	-0.6004598443	8.4517580399	-1.1396533208	0.00413441580878045
WBGene00016	mob-4	-0.7312094227	1.6641796538	-0.7775439472	0.0275903896523023
WBGene00016	hpo-27	-1.4699032366	3.7487844279	-0.8769432641	0.0303866056542812
WBGene00016	C35D10.5	-1.0231797336	9.8996408826	-1.0187475154	0.0145584411311045
WBGene00016	C35D10.10	-0.8315724446	3.0235153332	-1.2339766910	0.00102379428314494
WBGene00016	C37A2.7	-0.2553533484	2.9098997045	-1.4463545132	0.00256792105080881
WBGene00016	C42C1.8	-0.7196205922	4.3388568296	-1.3954806364	1.97337966950321e-05
WBGene00016	C42C1.13	-0.4259750861	4.1393904798	-0.9520135187	0.0262867713947236
WBGene00016	arch-1	-0.7781922496	9.6632862755	-2.0195852158	1.19273295195317e-06
WBGene00016	C45G9.2	-0.4135397183	2.1988532744	-0.9232624068	0.0248382742211052
WBGene00016	C50C3.1	-0.7597625340	3.4621437273	-0.9347972731	0.0139236874261562
WBGene00016	sucg-1	-0.8704790301	1.5895386659	-0.7982933948	0.0490785725796147
WBGene00016	C53H9.2	-0.2482098824	0.0004330242	-1.5186378033	0.000168371087637383
WBGene00016	madf-6	-0.8624516816	2.2368226433	-1.4300746172	0.000549694814527833
WBGene00016	C56C10.7	-0.3181187517	6.0355191396	-0.7539504091	0.0301985736874914
WBGene00016	epg-5	-0.2742774638	0.0065683188	-1.2074408635	0.0050242906408362
WBGene00017	D1007.10	-0.6056355356	1.6091862858	-1.1086419909	0.0155992455340687
WBGene00017	D2024.5	-0.2379770213	1.4269042861	-0.7611120184	0.0353087416934608
WBGene00017	glrx-3	-0.2472883938	5.8775078037	-0.9713493614	0.00263774656986395
WBGene00017	ppfr-2	-0.6506856480	2.3460285903	-0.9657036521	0.0093802098399202
WBGene00017	maco-1	-1.5346000423	6.0589154009	-1.5100107941	0.000147132736403807
WBGene00017	D2096.7	-0.4206611208	5.4487988672	-1.2212749808	0.00630463673704035
WBGene00017	cyc-2.1	-0.4758094814	1.1393820378	-1.1052489013	0.00754173239372364

WBGene00017	tofu-6	-0.5172414119	2.4784098253	-0.8559678048	0.00738368517951859
WBGene00017	EEED8.3	-2.5823481574	1.7712071507	-1.9747339387	2.44286985405309e-11
WBGene00017	EEED8.13	-3.7626922224	5.3810701440	-3.0282752567	0.000209131983178942
WBGene00017	EEED8.14	-4.0138917672	0	-2.3474867547	2.99239547764308e-08
WBGene00017	E_BE45912.2	-0.4759190904	0.0003151156	-1.3762077954	0.0248342126466234
WBGene00017	aldo-2	-0.5223016864	4.2009827982	-1.5184324892	1.0460442912599e-06
WBGene00017	F07F6.7	-1.1689430578	6.2399129713	-2.0241874922	0.00284025348926687
WBGene00017	F10E9.7	-0.9259628709	3.2072592882	-1.0757615958	0.0129154452124318
WBGene00017	F14D2.11	-1.2352313426	6.1341969984	-1.5947267373	0.00500289730536609
WBGene00017	F14D2.14	-0.4459178221	0.0002452130	-1.2144385871	0.0299521577536132
WBGene00017	pid-1	-0.5618108612	6.7743509363	-1.1324845978	0.00180557581903888
WBGene00017	tofu-2	-0.6968863461	1.0073263270	-1.4932528361	1.03073966602003e-05
WBGene00017	polk-1	-0.5203977585	1.7036326236	-0.8549399543	0.017057526997178
WBGene00017	F23H11.2	-0.8565466207	5.5269953287	-1.2398302825	0.0116427887769126
WBGene00017	sucl-2	-0.4717186082	2.1162413262	-0.8287484405	0.0152204464533136
WBGene00017	crls-1	-0.5325977458	1.2156240391	-1.0053996340	0.00656268717028767
WBGene00017	F25B5.5	-0.3598070224	1.6950730382	-1.0978318275	0.00126254757190248
WBGene00017	F25B5.6	-0.7193508970	6.8035957872	-1.1551945298	0.00290486678286092
WBGene00017	F26F4.6	-0.2198832675	0.0019356570	-0.8918022728	0.0139440228697523
WBGene00017	F26F4.9	-0.4743290257	3.8445976997	-1.2188659593	0.000390481151327125
WBGene00017	F26F4.12	-0.1583246121	0.0276809189	-1.2053229015	0.000665917845674207
WBGene00017	kbp-2	-0.4215871829	6.5363924856	-1.1464823870	0.00677370412473355
WBGene00017	neg-1	-1.0112136620	1.3055679924	-0.8917007140	0.0235556494463057
WBGene00017	F32D1.7	-0.6114758747	2.0908766677	-0.9161214487	0.0127285525894454
WBGene00017	cec-4	-0.8616108182	1.8345740239	-0.9254739856	0.02598056971727
WBGene00018	ztf-28	-2.6918189450	1.5574853044	-1.3969454271	0.000510854549622812
WBGene00018	F37A4.1	-0.5118467469	2.2721417406	-0.8827341897	0.0162618944506573
WBGene00018	F37A4.2	-0.3993221749	7.7950641154	-1.4939265971	2.05276210072155e-05
WBGene00018	mpdu-1	-0.8863482592	1.4476331501	-1.6911840149	5.34559173032201e-05
WBGene00018	F40A3.3	-0.7968116548	8.7926462320	-1.0561377905	0.00895635473259128
WBGene00018	mage-1	-0.5816986056	1.0680470461	-0.8966694168	0.0244783720413201
WBGene00018	F41G3.6	-0.7286689297	1.0226732734	-1.0637679187	0.000618548436802115
WBGene00018	exos-8	-0.2774625425	5.7862861999	-1.5089575233	1.91616686475813e-06
WBGene00018	F42A9.8	-0.8830911502	4.8372195160	-1.3065539445	0.0311577370372484
WBGene00018	F43E2.1	-0.1755549273	0.0390474422	-0.9943257334	0.0342244440990075
WBGene00018	F44E7.5	-1.7377625503	1.2066239095	-2.8122259267	2.73911497924593e-08
WBGene00018	skpt-1	-0.5261001567	1.0129536449	-1.6474786750	7.92918249265342e-08
WBGene00018	oef-1	-0.2448715984	6.4377461919	-1.0630626866	0.00262856802218715

WBGene00018	F49E8.6	-0.4406310050	0.0038908557	-1.1658817004	0.0170106070434896
WBGene00018	F52C12.2	-0.6207762716	2.2250700557	-1.1206214577	0.0106033449406399
WBGene00018	vha-18	-1.2016439116	2.7034577052	-1.5341265991	6.3694466229515e-07
WBGene00018	F53F10.2	-0.7561187290	1.1463408225	-0.9372137102	0.011456584182127
WBGene00018	pst-2	-0.2137414934	0.0021612732	-0.9129991224	0.0465138372032017
WBGene00018	eef-1B.1	-0.5565578931	8.0229617196	-1.6739623293	0.000112574325495644
WBGene00018	wago-2	-0.7553149902	5.1300861478	-0.8695607857	0.0430134412966845
WBGene00018	zhp-1	-0.6865486532	5.1705761591	-1.0695830344	0.0115028859114922
WBGene00018	mrps-16	-0.2617870155	0.0004314056	-1.1688860834	0.0186127178510814
WBGene00018	F56D2.2	-0.6850955922	1.6987358451	-0.8910479806	0.0188072328511341
WBGene00019	F59A7.8	-2.2129447879	3.2823070246	-2.9887330124	9.20261700414605e-12
WBGene00019	H14A12.3	-1.7966953316	4.6367347521	-2.8872273145	1.27673630128777e-11
WBGene00019	ahcy-1	-0.3877513302	6.5638795562	-1.0531435476	0.0169441344162188
WBGene00019	K03B4.1	-0.4552153373	1.5030115417	-1.0911489177	0.00221361802153402
WBGene00019	K03B4.2	-0.4717855419	1.0740528858	-0.8832892220	0.00803374610352617
WBGene00019	K04C2.3	-0.5437330760	7.8214175509	-1.0321290382	0.00531767608699746
WBGene00019	acdh-3	-0.5455772758	4.0136417742	-0.9139812773	0.0145082457050912
WBGene00019	K06B9.2	-0.8820112005	0.0249916222	-1.8607686114	0.0300271386046165
WBGene00019	tos-1	-0.1770434150	0.0326837299	-0.8644775163	0.0243138899128504
WBGene00019	K07E8.7	-1.5902362944	2.1723891267	-2.0522272036	6.53319000782299e-06
WBGene00019	K07H8.9	-0.4164960250	1.6964361743	-1.8135996804	1.53330988297995e-06
WBGene00019	K08D12.3	-0.3688577055	0.0026993517	-1.1797341002	0.00136467290642108
WBGene00019	K09H9.7	-1.8051930443	1.8955680879	-1.7705279521	0.00388591688508462
WBGene00019	clec-88	-0.2675263518	6.0108546947	-0.7447068959	0.0223806327271981
WBGene00019	K11D12.12	-1.2663432387	6.6192163892	-1.4380369434	0.0233323892972349
WBGene00019	K12H4.2	-0.3979009347	8.9391365003	-1.1561678363	0.00933478753881291
WBGene00019	K12H4.3	-0.2153549296	0.0002550847	-1.1446190828	0.00050285466026984
WBGene00019	spcs-3	-0.3580867218	4.2986850776	-1.5472129541	1.09514906507189e-06
WBGene00019	M02B7.2	-0.5197910489	5.4602354559	-1.0821189290	0.0337165143815552
WBGene00019	algn-14	-0.2376397582	0.0001921181	-1.2042446637	0.0312371879423459
WBGene00019	egg-2	-0.4201297815	2.2699829141	-0.7533867050	0.0461749028997023
WBGene00019	R02D3.8	-1.1659362112	1.1678434627	-1.4744426610	0.000824068172363266
WBGene00019	R02F2.1	-0.6920139976	1.6079060319	-0.9314457990	0.0078656359497159
WBGene00019	R05F9.6	-1.1135775774	4.7186398914	-1.2321732561	0.000144314865322779
WBGene00019	sti-1	-0.7538059190	3.0986634845	-1.2561571441	0.00708274462531474
WBGene00020	R12C12.7	-1.0369314668	3.3745052656	-1.6336109945	0.000123049391069684
WBGene00020	egg-5	-0.8737967164	1.4896645444	-1.2313654263	0.00503912163069302
WBGene00020	kbp-1	-0.7711880060	6.0111546462	-1.2074522070	0.00553924671861108

WBGene00020	T02G5.7	-0.2361901302	8.9372720838	-0.7009713638	0.044022646510514
WBGene00020	T02G5.11	-3.9975466995	1.3484377734	-3.0698517492	0.0166430563819311
WBGene00020	atp-4	-0.3471443367	1.1821120435	-0.8575003875	0.033154286463503
WBGene00020	tag-261	-0.1997171901	0.0040813730	-0.9876120596	0.0079717549655951
WBGene00020	T08B2.11	-2.1672401826	5.7006926803	-3.0029656029	1.52254313225766e-08
WBGene00020	cerk-1	-0.5368392228	6.7634405082	-0.9949977564	0.00268598678908732
WBGene00020	T12F5.2	-0.7640267506	2.8116559468	-1.5990052372	4.45383950996644e-05
WBGene00020	ssup-72	-0.3632443555	1.4504837956	-0.9202512830	0.0298449485909544
WBGene00020	mrps-18.C	-0.2455631598	0.0020192569	-0.9309296633	0.031153239395208
WBGene00020	T14B4.3	-0.3613826303	1.3383810150	-0.8964511321	0.00623810332288005
WBGene00020	T19H12.2	-0.4095072133	3.5798294672	-1.0626690956	0.00291156215625154
WBGene00020	mrrf-1	-1.4154546489	8.2064263184	-1.6801258388	0.0212807746566505
WBGene00020	pygl-1	-0.9071629588	1.2439698522	-1.1610329024	0.000110414404197634
WBGene00020	T23B3.1	-0.9847039625	8.7068543477	-1.0588938134	0.00351398392465421
WBGene00020	ucr-2.3	-0.4799078956	7.0212863748	-0.8018193383	0.0373779614830297
WBGene00020	T24C4.5	-0.5698066004	6.0711399199	-1.2527880006	0.0011759418423118
WBGene00020	T24H7.3	-0.4655912422	1.2941182879	-0.8905520342	0.0158736979154305
WBGene00020	T26A5.8	-0.4569180313	7.7299605048	-1.4971795460	4.21085398307813e-05
WBGene00020	W02D7.6	-0.7245636682	6.8269444828	-1.6067232274	2.55212689430524e-07
WBGene00020	sna-1	-0.4807256916	1.4989440040	-1.0187295844	0.00212159820835683
WBGene00021	W03F9.2	-0.4000957333	8.1510657613	-1.0490169675	0.0334676409985324
WBGene00021	W03G9.2	-0.7139553255	6.2343209601	-0.9325040228	0.0203341362737953
WBGene00021	W07E6.5	-0.3087877870	0.0322551602	-1.6974311070	1.27082934119061e-05
WBGene00021	zip-11	-1.7604287586	4.9287971001	-3.1856886391	8.29822266521554e-10
WBGene00021	cdc-37	-0.8686190271	8.7432378082	-1.0638616748	0.00119903939876447
WBGene00021	W09B6.4	-0.4890737669	1.9753514855	-1.5853284451	0.0136099493059425
WBGene00021	W09C3.4	-0.5490803337	2.2041509794	-0.9172647172	0.0185909049680459
WBGene00021	Y17G9B.4	-0.7966602214	5.7569944155	-1.4261303013	0.00106497933438308
WBGene00021	Y23H5A.2	-1.0945016717	9.1152197231	-2.3811841452	7.36218723704568e-09
WBGene00021	Y34F4.5	-0.7026731061	0.0001722193	-2.6436506051	1.51565881698569e-06
WBGene00021	Y37E3.8	-0.4188115407	1.0771766830	-1.7154742692	0.000787164040166247
WBGene00021	Y37E11B.6	-0.4059580613	0.0003323120	-1.3571301192	0.000715657494382445
WBGene00021	trap-3	-0.4540699505	4.5844389568	-0.9620114642	0.0445570152615297
WBGene00021	Y41D4A.6	-0.4801431771	1.1721179223	-1.4579073104	0.000320486715448534
WBGene00021	Y41D4B.4	-0.4876519151	1.8273480328	-1.0537044472	0.0309502660531166
WBGene00021	Y48G1A.1	-0.8682530282	9.1116342104	-1.3234509649	0.0344894948241989
WBGene00021	Y48G1A.2	-0.9116787850	6.4610882719	-1.6867620249	9.62941544957265e-08
WBGene00021	Y48G8AL.7	-1.2318560494	3.8151022526	-1.8470530799	0.000647797193650177

WBGene00021	Y51F10.2	-0.1532859989	0.0047143709	-0.8393745030	0.0137536777166226
WBGene00021	Y52E8A.2	-0.6999644707	6.8495039883	-0.9175905085	0.033401244700199
WBGene00021	fbxc-45	-0.8995547434	2.0419500404	-1.0971471779	0.0423961764505718
WBGene00021	Y57E12AL.1	-0.5591954646	1.0236591696	-1.0460755530	0.000805580688094815
WBGene00021	Y57E12AM.1	-0.5515624020	1.0567917582	-1.1167966137	0.00332591574427685
WBGene00022	Y65B4A.8	-1.4296755999	3.7040115636	-1.9891685626	5.5309454276613e-05
WBGene00022	icd-2	-0.2508764850	1.3906534786	-1.2167154033	0.0229703867155608
WBGene00022	Y67D2.7	-0.5588214542	4.7079067502	-0.8959477818	0.0178975239152386
WBGene00022	Y69A2AR.32	-1.2348929808	5.4285726732	-1.8395945715	9.92604209534234e-06
WBGene00022	Y71F9B.6	-0.7634766859	7.1537967464	-1.6117175204	0.00224760130662034
WBGene00022	chaf-2	-0.5596415546	1.8002338798	-0.7479035899	0.0387574681577992
WBGene00022	Y71H2AM.9	-0.5325021017	1.5674117072	-1.0008822446	0.0298449485909544
WBGene00022	Y73B3A.9	-1.0145573303	7.9767176066	-2.1327823672	0.00352998412119056
WBGene00022	sqd-1	-0.3193374761	4.5309513101	-0.7617651899	0.0203341362737953
WBGene00022	acp-6	-0.9318708008	0.0001363725	3.7927656358	0.0252140795219324
WBGene00022	Y73B6BL.29	-0.9171191916	2.1986679830	-1.2065648803	0.0405802317934255
WBGene00022	Y73E7A.1	-1.0584553818	2.0705818541	-1.0611264213	0.00935324407502791
WBGene00022	Y82E9BR.3	-0.4838325719	5.2288316424	-0.8514628158	0.0441661636313187
WBGene00022	Y110A2AR.1	-0.4685410720	6.8519581500	-1.0821439495	0.00101619099710174
WBGene00022	ZC317.7	-4.6509867740	6.3553188505	-1.3963910584	0.0288845729948923
WBGene00022	ZC477.3	-0.3984987408	9.1617541909	-0.8517179520	0.0384223473069214
WBGene00022	rde-8	-0.6572012435	3.0126591718	-0.9859816522	0.00904663019082651
WBGene00022	acl-9	-0.5279475497	1.0892980662	-0.7044703950	0.0413361410622778
WBGene00022	npp-24	-0.4596797763	1.1633101005	-0.7731626199	0.0236839577576897
WBGene00022	ZK177.8	-0.6690989055	5.9954305698	-0.8732796890	0.00974430804973334
WBGene00022	tofu-7	-0.2492342207	4.4728742118	-0.8982578877	0.0274793045827988
WBGene00022	fubl-2	-0.4771055795	1.5189125214	-0.7636612748	0.0437482643927757
WBGene00022	**oaz-1**	**-0.8578390169**	**1.2179384805**	**-1.0105455302**	**0.00210421422518981**
WBGene00022	ZK484.6	-1.1154321047	0.0033693276	-2.7831903664	0.000787164040166247
WBGene00022	tag-307	-0.6022710765	3.9173490138	-0.8932012418	0.0175943731149859
WBGene00022	fahd-1	-1.2928599743	2.3324809550	-1.6424922525	0.0120983277433306
WBGene00022	ZK688.5	-1.6504803602	0	-2.0009152804	2.09669906748304e-11
WBGene00022	ZK688.9	-0.4941641307	1.2946681575	-0.9561099286	0.00839079332258292
WBGene00022	cin-4	-1.4693017344	4.1095712411	-2.3880927951	1.3523787616686e-12
WBGene00022	ZK1236.1	-1.2390463702	3.0194472831	-0.9154054185	0.0376430255149683
WBGene00022	ZK1248.11	-0.4493983985	5.7641061861	-1.2892168142	0.000169389591623116
WBGene00022	ZK1248.15	-1.8058982048	1.4119587009	-1.3091731401	0.000953639281157841
WBGene00022	ZK1248.19	-1.4539176580	1.0120775760	-1.1718843545	0.0376430255149683

WBGene00022	CD4.10	-0.3866483261	0.0001036294	-1.2878317745	0.0298449485909544
WBGene00023	rpl-41.2	-0.5033065577	5.8456832969	-1.7026958246	0.000386142291953241
WBGene00023	F14D2.15	-0.8324231182	1.8835511312	-1.0739673328	0.0261252586228313
WBGene00043	F32E10.9	-2.4700672180	7.2781643624	-3.8509759364	1.89325550357446e-05
WBGene00044	T01G1.4	-0.3616939399	9.1604914267	-0.8245783421	0.0437482643927757
WBGene00044	tag-229	-0.5232140351	4.0573888788	-0.9895855705	0.0162618944506573
WBGene00044	Y57G11C.51	-1.1961131799	6.5822152055	-1.7772982527	6.37005321944363e-05
WBGene00044	rad-8	-0.5764270118	7.4641976544	-0.8657215025	0.0103104356701034
WBGene00044	tag-280	-0.8622471201	7.0380928104	-1.6327550150	0.00276901369474864
WBGene00044	ZK688.11	-1.5478345391	1.6804275106	-2.7258451743	1.67298835968004e-13
WBGene00077	C27H6.9	-0.7956612734	6.0736623312	-1.5921547068	4.0176869867396e-05
WBGene00138	F58H1.8	-0.5762370040	3.0961815311	-1.1189594131	0.0103104356701034
WBGene00185	K11H3.8	-0.4920384274	4.8700661770	-0.9967414023	0.0408117353667565
WBGene00194	C53A5.16	-0.6998274363	3.3035033059	-1.3100937155	0.0249786768895591
WBGene00206	Y80D4G.1	-1.2127096203	1.9591239151	-1.9344894204	0.00474556665655936
WBGene00219	Y54G2A.73	-0.5989044867	3.8306542635	-1.7555539182	0.0039092944050503
WBGene00219	C06A1.12	-0.3262577191	0.0011566124	-0.8386970234	0.0430134412966845
WBGene00255	B0511.19	-0.1989622757	0.0027421370	-0.9970915119	0.00864605053815648
WBGene00271	T10E9.14	-0.9849243213	1.7412500742	-1.4656060100	0.0233558884336998
WBGene00271	D2089.8	-0.8304200042	3.7709873629	-2.0074685114	0.0161451716418977
WBGene00000	akt-2	1.1020782965	6.0569455632	2.1060266075	0.0284191845169195
WBGene00000	amx-1	0.5181813609	1.1943404238	1.6795571830	0.00783279954694634
WBGene00000	anc-1	0.8599211381	1.0425489310	1.2067675374	0.0442907004844807
WBGene00000	apl-1	0.7621579618	1.7219104179	1.4940605770	0.0199340180016796
WBGene00000	ark-1	0.4888538738	7.2176177241	1.0489781159	0.00971459101435518
WBGene00000	atf-5	0.4334275041	0.0472530754	1.3852991760	0.00953480849473906
WBGene00000	atf-6	0.5826578405	4.7775910231	1.5383363077	0.024159501943747
WBGene00000	ccg-1	0.7636046523	0.0001564242	1.4478239687	0.00413441580878045
WBGene00000	cdc-14	0.1244535507	0.0078732571	0.8122329540	0.0170106070434896
WBGene00000	cdh-4	0.5790201601	2.1232065475	1.2888998807	0.00231355529884879
WBGene00000	cpi-1	1.1687228057	6.7671410689	3.6304190998	3.57146439038755e-14
WBGene00000	cnt-1	0.3543465844	1.3886276833	1.3165892741	0.0377483985724088
WBGene00000	crn-4	0.7747891883	2.1879337965	1.1361653164	0.024165383077767
WBGene00000	dao-3	0.3853441770	0.0384945609	-1.6559192391	0.0260030250996233
WBGene00000	dhs-14	0.6900431078	0.0327499559	4.7622859434	0.00380541493777915
WBGene00000	dhs-21	1.6635270496	2.9372371314	3.0643484766	0.000499516337434342
WBGene00001	dnj-27	0.6381905054	6.6931193980	2.0617480318	0.000689030759008703
WBGene00001	dpy-23	0.3173328664	0.0079796211	1.7483295446	0.00806352271954898

WBGene00001	dyn-1	0.7946768754	4.3435777240	1.1917978854	0.0280659064190795
WBGene00001	eef-1A.2	0.8471211998	1.2596234793	1.0234278863	0.0365902084867971
WBGene00001	emb-9	1.2093383378	1.2776827267	1.4730159083	0.000587457909556777
WBGene00001	fat-3	0.3923349060	0.0193264740	1.2589506364	0.0332656119558407
WBGene00001	fis-2	0.9406447966	1.0407023163	1.1953368697	0.0408014524631908
WBGene00001	fmo-4	1.5134110708	6.8744037111	1.2741311587	0.0235191322117101
WBGene00001	fog-1	0.4528502320	7.3857760379	0.8766318808	0.0135007178184262
WBGene00001	frm-1	0.6197274998	1.8594565846	0.8928104767	0.0156574305595428
WBGene00001	frm-7	0.2069901301	0.0112645075	1.1999455233	0.041945720655523
WBGene00001	gei-3	0.5729573051	0.0030175465	2.2094863555	0.00952187994619803
WBGene00001	meg-3	0.5047173490	7.3589237397	1.0474402171	0.00675876427329768
WBGene00001	gex-2	0.2370651289	0.0005885743	0.9415144250	0.0236748756689071
WBGene00001	gfi-2	0.1139333087	0.0387001779	0.9494083428	0.0205556531925389
WBGene00001	gst-4	1.7491597214	4.5530832215	2.1620422880	0.000587457909556777
WBGene00001	gst-24	0.9610852768	0.0312778821	4.0980694573	2.16364064048971e-13
WBGene00001	his-6	0.2369145399	0.0499369819	-3.5765918309	5.16268683725816e-10
WBGene00001	his-32	0.8524415767	0.0001078234	-2.8387689854	2.32860711994388e-08
WBGene00001	his-38	0.9668533783	5.4122867797	-2.7398611333	0.00942429983180476
WBGene00001	his-40	0.8531248123	8.0007743116	-2.7487319646	1.91616686475813e-06
WBGene00001	his-68	0.4334701702	7.1660634183	-1.9317819510	2.3345764972507e-07
WBGene00002	iff-2	0.4262601333	0.0022119600	0.9671727964	0.0346144563133377
WBGene00002	ina-1	0.5485535817	7.9386470797	1.3337286933	0.0215500955508471
WBGene00002	klp-4	0.9749674725	9.4821792151	1.7914495605	0.0454862984367192
WBGene00002	ksr-2	0.1643737165	0.0220234202	1.1011870901	0.00912555288157131
WBGene00002	lbp-1	0.4766272516	0.0387644302	1.3208429888	0.0129154452124318
WBGene00002	lbp-6	0.7660815735	5.1561536973	2.2302903144	7.51483618292984e-05
WBGene00002	lec-4	0.6294373339	9.4102901997	1.5000879812	0.0126937340895077
WBGene00002	lec-5	1.6310457707	2.0052454575	1.7036697539	0.00332096721720804
WBGene00002	let-2	1.1078401582	3.2147533148	1.5192123128	0.000142700630375082
WBGene00002	let-19	0.3001239561	0.0121407077	0.9173581014	0.0417295549414075
WBGene00002	let-413	0.3961836633	0.0008876045	1.5422284911	0.0387527791729912
WBGene00002	lim-7	1.2670508533	1.1198750434	1.8120165782	0.0373746614319323
WBGene00003	lys-7	1.0781872375	0.0149976420	5.4893042006	0.00035042184114175
WBGene00003	mes-1	0.3907052066	0.0024582393	1.3333098507	0.0351358120738652
WBGene00003	mex-3	0.1216477797	0.0147642849	0.8251514042	0.0381958853095823
WBGene00003	mig-15	0.5400429648	6.3814593635	1.4827463641	0.0373057477802643
WBGene00003	mlp-1	1.2230446537	4.8380444796	2.2501269948	0.00423697759441933
WBGene00003	mom-4	0.2407131092	0.0027333514	1.0842086041	0.00738368517951859

WBGene00003	msi-1	0.4153494187	0.0131650980	1.9024940238	0.0382061898732465
WBGene00003	dcap-2	0.3339309069	1.4231022422	0.8421081021	0.0403033346544568
WBGene00003	nfm-1	0.4488069335	0.0031128661	2.0435178213	0.0236922101583485
WBGene00003	nhr-84	1.3282030475	2.5515479479	2.1787788327	0.0461749028997023
WBGene00003	nmy-1	0.7925745031	1.6961405178	2.1869338375	2.01021136054315e-07
WBGene00003	nrf-5	1.2799694833	0.0009027124	2.7353800804	0.0021394879293794
WBGene00003	ost-1	1.0019045250	3.4466669398	1.4275097852	0.000361350013647058
WBGene00003	oxi-1	0.4159118594	2.0031981499	0.7450173178	0.0380826555033644
WBGene00004	parp-1	0.2091303938	0.0001292103	0.7840821778	0.0409304072927436
WBGene00004	tank-1	0.5993196355	2.6302174597	0.9990958363	0.0115327950954228
WBGene00004	pqn-21	1.2889561465	3.7766943790	1.7096740971	1.13012248214922e-06
WBGene00004	rbc-1	0.4795812995	8.7178881144	1.1851551629	0.0278609393263951
WBGene00004	rig-4	0.0791522264	0.0440569854	0.9656275374	0.0142933257088891
WBGene00004	rpl-25.1	1.0775420603	1.3737582916	1.4106870852	0.0011759418423118
WBGene00004	sdc-1	0.3816557010	0.0012860292	1.4204719485	0.00360746772975649
WBGene00004	sek-1	0.2667761238	0.0409804530	1.7809654540	0.0161518182402066
WBGene00004	sel-12	0.3681359068	0.0084995592	1.7240654712	0.0162911066951935
WBGene00004	sem-5	0.3064468854	0.0016679820	1.3554399906	0.0236774564002575
WBGene00004	sex-1	0.4891986842	0.0079109773	1.4100049199	0.00654898433652986
WBGene00004	skn-1	0.5214204275	2.2824070998	0.8661441212	0.02598056971727
WBGene00004	sli-1	0.5991511127	7.9630116664	1.2181060187	0.0169233036117202
WBGene00004	sop-2	0.3158238540	0.0235066792	1.3967132607	0.0269718755027512
WBGene00005	sqv-5	0.3242427981	2.6414720545	0.8824171479	0.0235551549873585
WBGene00006	sto-1	1.0204654622	4.6199150169	1.6172428994	0.00884188169677257
WBGene00006	sur-5	0.3671542929	0.0018364661	1.2139509065	0.0243138899128504
WBGene00006	taf-3	0.3051112326	0.0084362023	1.6678763919	0.00230390817754383
WBGene00006	lim-9	0.6152247776	0.0003650217	2.2689809460	0.0321132663638764
WBGene00006	kcc-1	0.3435803516	5.8444184639	1.3585557318	0.00293491880207218
WBGene00006	madd-3	0.3049574257	0.0021131258	1.4756061626	0.00924849189475974
WBGene00006	tap-1	0.6949040940	0.0006142091	1.5933529432	0.0325987156046246
WBGene00006	tba-4	0.5584689229	0.0090356193	1.5789510592	0.0146508527910821
WBGene00006	tbh-1	0.7251336081	0.0006364944	1.1708372198	0.0170106070434896
WBGene00006	tbx-33	0.6575210046	0.0008952139	1.7837740676	0.0039835275127462
WBGene00006	tol-1	0.1444669127	0.0266683322	0.9599028768	0.0176109583884111
WBGene00006	tpi-1	0.5276973764	6.3993603286	0.8781067163	0.02598056971727
WBGene00006	tps-1	1.1259097391	2.6997696875	1.6156719637	0.0152204464533136
WBGene00006	tra-3	0.2702735429	0.0134497469	1.1494122775	0.0483415143198372
WBGene00006	unc-26	0.3793229631	1.0528215683	1.0691617507	0.0103974794594557

WBGene00006	unc-32	0.1121139803	0.0120072060	0.8949553809	0.0199340180016796
WBGene00006	unc-33	0.9109148154	3.5923258856	1.2486295083	0.0133347993206383
WBGene00006	unc-40	0.1297922115	8.1161359133	0.8995140255	0.0273190189871856
WBGene00006	unc-53	0.8633214681	1.4464204574	2.4562105035	0.00329286963378462
WBGene00006	unc-112	0.3095816488	0.0026502287	1.5810699310	0.0140686438598502
WBGene00006	ver-3	0.8570502655	2.1338770379	1.7032544860	0.0176395758101266
WBGene00007	chd-7	0.3363363038	0.0187059812	1.1874800952	0.00714776898588186
WBGene00007	eri-12	0.4192792853	1.2379237232	1.2821320708	0.0273190189871856
WBGene00007	lron-3	1.2900750657	4.7689848235	1.8437274704	0.0173303157041122
WBGene00007	C04F12.1	1.1584337048	1.0790784888	1.6261412287	1.0420981813283e-06
WBGene00007	C05C9.3	1.9484588482	3.8182158113	2.9549318403	0.000386142291953241
WBGene00007	C07E3.9	1.4640896666	5.1617181525	1.8769537337	0.0337614792690729
WBGene00007	C18D4.6	1.5636699640	1.6269486134	2.7252933719	6.54708260381763e-07
WBGene00007	C27C12.1	0.5716901341	1.0778387487	1.5250410832	0.00138194782651652
WBGene00007	rsu-1	0.5102634587	6.3570560354	1.4318451088	0.000386626463845555
WBGene00008	C38D9.2	1.8033320585	2.8265765194	2.8930501871	0.00367463331249773
WBGene00008	din-1	0.4437217376	4.1012488928	0.9671483442	0.0173374876563467
WBGene00008	F09C8.2	0.5389750637	0.0010598161	1.9733798400	0.000320737008007391
WBGene00008	git-1	0.3945079038	0.0006054479	2.0132948372	0.0189327497567198
WBGene00008	F15D4.5	0.6700864052	9.8547651615	2.6313872651	0.0010297446474987
WBGene00008	F19C6.2	0.4554045069	0.0012039714	1.7794634835	0.0175693620017325
WBGene00009	aptf-4	1.4227287385	0.0015409089	4.0137447110	0.00100375272686938
WBGene00009	F28H6.4	0.6703458781	2.0807953530	1.3989312271	0.0006373069915679
WBGene00009	rict-1	0.2953738629	8.1739458901	1.5658813285	1.91616686475813e-06
WBGene00009	F31B9.3	1.3258710799	4.7343226144	1.0325071514	0.0490785725796147
WBGene00009	F31F6.2	0.7202802402	4.7111905268	1.3768204148	0.0382061898732465
WBGene00009	fasn-1	1.1335667482	5.6232297988	1.0608733914	0.0148101023668697
WBGene00009	F34D10.3	1.8420298928	6.1824464657	1.5733457243	0.0136686664329052
WBGene00009	F35E12.10	1.0701460995	1.5367281055	1.3640512559	0.0122456032813657
WBGene00009	cyld-1	0.1258898799	0.0095581195	1.1207093028	0.00169046382872165
WBGene00009	F45G2.10	0.5489376735	9.3178470525	1.1046589778	0.00294785822294085
WBGene00009	ipla-2	0.5679574341	5.2658786400	1.3038727090	0.0253967667973545
WBGene00009	gpdh-1	1.9926279060	0.0002617228	2.5902428540	0.0367410153257638
WBGene00009	F49E2.2	0.8084672018	0.0004822015	2.0816482482	0.0011759418423118
WBGene00009	F49E2.5	1.0197166399	8.4233344210	1.8081715942	0.00279156019689652
WBGene00009	swan-2	0.3527391712	0.0077700109	1.3507052536	0.0166892020772943
WBGene00009	swan-1	0.6467840640	1.3867627826	1.3527721812	0.0146508527910821
WBGene00010	F58G1.2	0.7446103090	9.5283866061	1.0400792769	0.0125197162631088

WBGene00010	copz-1	0.7030665425	2.0665374525	1.1065634327	0.00485831041281645
WBGene00010	ttr-51	1.8941169128	1.4424661359	2.0449857713	0.00179868565857806
WBGene00010	K02B7.3	2.2260291459	7.9177102235	3.6387033294	3.25218146319758e-05
WBGene00010	meg-1	0.5581154591	3.3779691129	0.8460536894	0.0235191322117101
WBGene00010	meg-2	0.5392610601	2.9394382846	1.5205864735	0.00646272191772102
WBGene00010	mak-1	0.5296657986	1.1405256615	1.0402995301	0.0108630392395372
WBGene00010	cysl-2	1.0345566534	2.0732601501	1.5178435847	0.00318451241078498
WBGene00010	M117.1	1.6168835566	1.1232064252	2.3794269668	0.00715469312478028
WBGene00010	ndfl-4	1.9793922155	1.7064288053	1.7714395348	0.00339211007142601
WBGene00010	nduo-1	1.1272126066	5.8827518202	1.5301346352	0.00652823330727302
WBGene00010	nduo-2	1.2242153476	4.1748508452	2.5082646321	2.7556999531596e-06
WBGene00010	nduo-5	1.1123203046	4.9696216367	2.6610059361	0.0261252586228313
WBGene00011	R10E4.1	0.4727863517	3.5745038903	1.1972783524	0.0227992157023324
WBGene00011	pck-2	0.3108604868	3.0800603988	1.0129988702	0.00558942081528504
WBGene00011	aakg-5	0.1765884863	0.0002570213	1.3351293242	0.000762435275597351
WBGene00011	T01E8.1	0.6970876174	0.0007859903	1.9438400207	0.0423296157548056
WBGene00011	T02G6.5	1.1045356943	1.2224364122	0.9298018175	0.0435121597973575
WBGene00011	aldo-1	0.4927791195	0.0283566324	1.4797618008	0.026111779600276
WBGene00011	nfya-1	0.3224216202	0.0286466940	1.1233915773	0.0296444447123829
WBGene00011	T12G3.2	1.0736758080	2.1116128651	1.6331953730	0.0242354245041834
WBGene00011	T18D3.1	0.5204952208	8.6327401871	1.3236515160	0.028088235706623
WBGene00011	prmt-9	0.3415480519	8.4126756905	0.8675256283	0.0199340180016796
WBGene00012	ucr-2.1	0.7536878906	1.9335572380	1.0847177282	0.0324317813872723
WBGene00012	W08E3.2	0.4975783970	4.4633626237	1.5860376397	0.024159501943747
WBGene00012	ztf-25	1.0192534118	1.0368359325	0.8005804702	0.0491753380503124
WBGene00012	mxt-1	1.2799349228	9.0236437439	1.9353505378	0.0178115489770295
WBGene00012	fbxb-7	1.4048855427	2.1928595690	1.7678162172	2.95814160843953e-06
WBGene00012	Y37D8A.4	0.8552954329	5.4476564688	1.0679244319	0.0261252586228313
WBGene00012	Y38E10A.14	0.4377869072	0.0426615189	1.8493285563	0.000156610483865346
WBGene00012	fbxa-150	0.6758612351	0.0006308651	3.3866287253	0.0180174722761054
WBGene00012	Y39B6A.10	0.8029848864	3.0568405928	1.3135339307	0.0332656119558407
WBGene00012	Y43F4B.7	0.3111728644	3.1478999746	0.9841003491	0.017768707167929
WBGene00012	cpt-1	0.5028828357	2.3067032215	0.9969658753	0.00798378887188276
WBGene00012	efhd-1	0.3741739415	0.0226013647	1.1246902281	0.0210972515941964
WBGene00013	cup-14	0.6604129580	3.1277853908	0.8921712652	0.00919825680043573
WBGene00013	Y67H2A.10	0.3278563699	4.6969351092	1.5961183244	3.07340127788268e-05
WBGene00013	fbxa-90	2.0507164494	5.7551740207	2.9272964700	0.0461766943311455
WBGene00013	Y105C5A.25	2.1644883231	1.0512845958	2.2977555301	0.0156574305595428

WBGene00013	fbxa-115	2.0545160461	9.5817824713	2.4641162925	0.0136093037324985
WBGene00013	cdk-11.2	0.4059267992	0.0009027645	1.1737998102	0.0238630248620487
WBGene00014	ZK637.14	0.5996520167	0.0009584524	1.1408823250	0.00803374610352617
WBGene00014	ZK930.2	0.8644844621	1.3023626859	1.2351205068	0.0212807746566505
WBGene00014	ZK1073.1	0.4155524252	0.0340224154	1.3607396105	0.0432109890811548
WBGene00014	C53C7.5	0.9784438661	6.6207727340	3.2767027055	0.000134374079802595
WBGene00014	F07H5.3	0.7537578641	1.1763356634	1.2370920401	0.000352530084109221
WBGene00014	F07H5.5	0.5063104977	0.0021022833	1.1415828903	0.00889060020941088
WBGene00015	B0041.8	0.3024315681	2.0131038616	-0.8881637670	0.0079488840503556
WBGene00015	B0212.3	0.8234954801	2.8946747264	1.2825375825	0.00336074959689006
WBGene00015	cpna-2	0.5620392579	0.0002928305	1.9745697262	0.0261252586228313
WBGene00015	B0281.5	1.0808803252	2.3584924808	1.6896086249	0.00230390817754383
WBGene00015	C03F11.4	1.9145820610	4.2396363891	2.7792824743	0.00530316637230017
WBGene00015	sor-3	0.5618736140	0.0010468180	1.5509455536	0.0136093037324985
WBGene00015	hyls-1	0.2896519729	3.5025753360	0.9166352248	0.0116603908719766
WBGene00015	C14F11.4	1.5573679684	5.2206147749	1.4179561873	0.00685635971153677
WBGene00015	kynu-1	1.4015246397	5.1495106167	2.8010962882	0.00180557581903888
WBGene00016	**hpo-15**	**1.6351775913**	**8.5568999822**	**2.6239548208**	**0.0145584411311045**
WBGene00016	cht-3	1.2804520491	6.2361699858	1.9380297248	2.00441266324475e-05
WBGene00016	eri-9	0.3938061711	5.3892439287	1.2080674141	0.000121099974662245
WBGene00016	sec-15	0.5403839422	1.3485508447	1.3558384208	0.0169233036117202
WBGene00016	lntl-1	0.9276228811	2.7638269972	1.6717889112	0.012934290340192
WBGene00016	C41A3.2	2.0914493918	5.0337900127	1.9373206059	0.00700749018329233
WBGene00016	C50A2.3	1.3598406989	6.0798567894	2.4824724765	0.00895635473259128
WBGene00016	C52A10.1	1.3135614864	2.1029461996	3.1357909313	0.00027638248706594
WBGene00016	fbxb-97	2.5561436961	1.2337751817	3.3029607351	7.81915863353169e-09
WBGene00016	pgph-3	0.9036737474	0.0052401598	3.5063134129	0.000294564619108989
WBGene00016	C53D5.1	0.5997740538	5.7275657295	1.3885259125	0.0210972515941964
WBGene00016	ztf-3	0.6019206436	1.9384068470	1.2502917755	0.0231050428490513
WBGene00017	utx-1	0.3574561832	0.0050208384	1.1303059110	0.0427430240124337
WBGene00017	D2092.4	1.5030120600	2.8277288436	1.8538478470	0.0409432326310322
WBGene00017	DC2.5	1.0165742999	0.0011937167	2.2166145158	0.043156163420299
WBGene00017	F08F3.6	0.4517034169	1.5808031407	0.8528662468	0.0486610012200231
WBGene00017	F10D7.5	0.5247011521	8.3556257475	1.3107213476	0.0147603758236877
WBGene00017	F10E9.3	0.4078067396	1.7195026412	1.3049738142	0.0102085934165896
WBGene00017	F13B9.1	0.4307572560	0.0219568710	0.9695644307	0.0331096221507528
WBGene00017	F13C5.2	0.6082839509	9.1577072274	1.7146066582	0.00378143298932292
WBGene00017	F21F3.7	0.3774112640	0.0030830686	1.2228232221	0.0120983277433306

WBGene00017	pals-34	0.7805840029	0.0361944361	1.6790448410	0.0200550783827705
WBGene00017	F31A3.5	0.5045535032	0.0005006892	1.3154228487	0.0437482643927757
WBGene00018	F35A5.1	1.2439540213	1.9515916629	1.2943279496	0.0341266246156233
WBGene00018	F37C4.5	0.6563427027	1.1465693083	1.3325123229	0.00219544124564106
WBGene00018	F44A2.5	0.8290884941	3.6215948515	2.6980777555	0.00236951555240148
WBGene00018	acs-1	0.9191818786	2.2812111557	1.2894551882	0.00873390708500994
WBGene00018	F46H5.7	1.0669302986	2.6691753500	1.8991408397	1.65613772220892e-05
WBGene00018	F55A3.2	0.4205818707	1.4192102637	0.9443436871	0.02598056971727
WBGene00018	glit-1	0.5669433884	0.0375093539	1.6877189260	0.0188912239323777
WBGene00018	F56C9.10	0.2945001941	4.9809896909	1.0131658022	0.0116616553137507
WBGene00018	F56F10.2	1.3491055956	0.0044984893	2.3146783044	0.0261252586228313
WBGene00019	spg-20	1.1178046173	6.8577737097	1.5857171403	3.02424394986255e-05
WBGene00019	ttr-47	1.2322912443	2.1568360237	2.0255358466	0.0463960888159386
WBGene00019	K10B3.5	0.5436248665	1.9090274909	1.7396351965	0.014976618573615
WBGene00019	K11H12.8	0.6597983185	3.6784005144	0.9583047392	0.0110737583840972
WBGene00019	sago-1	0.8940616817	4.4078655734	2.1244961038	1.60096930108931e-05
WBGene00019	ipla-1	0.3149637233	2.8831160736	1.1232218126	0.0029769490410596
WBGene00019	aass-1	0.9811200050	6.1885960338	1.1490908569	0.0328572059873037
WBGene00020	eppl-1	1.5628300609	1.0012690280	1.2423211592	0.0456233515442048
WBGene00020	aak-2	0.3260659054	0.0085479218	1.3117435793	0.020583124723461
WBGene00020	T05A12.4	2.4925234216	4.6075391976	1.1615911420	0.0378303338083639
WBGene00020	pho-14	1.3374497893	3.0851446357	1.4336333177	0.00836031682478536
WBGene00020	vha-15	0.4804442789	2.2045131269	1.0985605346	0.0175943731149859
WBGene00020	immt-1	0.5171500136	5.6255060500	1.1930149168	0.0192633305708344
WBGene00020	T19D12.6	1.0777058619	4.0972019846	1.2395130524	0.0418772570002025
WBGene00020	T20F5.6	0.1692285673	0.0001316756	0.7882935546	0.0320229663395672
WBGene00020	aakg-2	0.7588602058	6.5473592937	1.4140028116	0.0268879211098008
WBGene00020	T22B7.7	1.2659827739	0.0008273608	5.5910603232	1.11213158547634e-17
WBGene00020	T24A6.20	1.1111044771	6.5754832345	1.4127283623	0.0442907004844807
WBGene00021	W06A11.4	1.3959527756	2.3576110642	2.8133093480	0.00230390817754383
WBGene00021	W09C3.7	0.4340536318	0.0020717344	1.2248622182	0.00199066835822691
WBGene00021	Y18H1A.9	0.9541297430	0.0410039269	2.3262135856	0.0147603758236877
WBGene00021	Y34B4A.2	0.4314043037	0.0094753183	1.8909940080	0.00893643434105514
WBGene00021	Y37E11AM.2	0.4911930111	1.6220485069	1.1273616874	0.0437482643927757
WBGene00021	ppgn-1	0.4437222688	3.7371878296	0.9999571255	0.0236176868995733
WBGene00021	Y47G6A.3	2.4219423250	1.8016558058	2.5298054965	0.0112012834910723
WBGene00021	mis-12	0.5330174500	1.2159326745	1.1767577979	0.00545930197412032
WBGene00021	Y53G8AM.8	0.4674208152	4.2969694600	1.4942395288	0.0093802098399202

WBGene00021	Y54F10AM.5	0.5858435865	5.3450491412	0.7810131584	0.0422344819764757
WBGene00021	samt-1	1.4341532532	1.4999216206	2.0142582435	0.00529282784196875
WBGene00022	mppa-1	0.5233125723	4.5320462977	1.0709011854	0.0238630248620487
WBGene00022	Y71H10B.1	1.2879474132	9.2296455096	1.2228214204	0.0101966804763955
WBGene00022	Y119D3B.21	0.7024982667	0.0118598779	2.0061517491	0.0178187746756022
WBGene00022	ZC53.1	0.6595953258	4.2689908257	1.2365163268	0.0175693620017325
WBGene00022	cyy-1	0.2281439237	0.0005376745	1.0718996148	0.00372524059373357
WBGene00022	ZK484.3	0.2138889641	0.0006357930	0.9352481082	0.0349915165568052
WBGene00022	cth-2	1.1930409937	6.6404962606	1.3265609231	0.00809816817866127
WBGene00022	ZK1290.5	1.7536303306	2.8571278876	2.1279274045	0.000840298870140819
WBGene00023	rpl-41.1	1.6686331075	1.0893332230	1.1573868592	0.0292474849082205
WBGene00023	ZC513.7	0.7076759598	0.0001140982	2.4702572507	0.0017573618466768
WBGene00023	swm-1	2.9970504299	6.6580069013	2.1479412014	0.00675876427329768
WBGene00023	lin-15B	0.9864788391	8.2720704762	1.6854945005	2.3795541151114e-06
WBGene00023	lin-15A	0.8904026246	2.1294043479	1.1810564733	0.0166389848337867
WBGene00044	Y32F6A.6	1.0985036429	2.3199462952	1.2469283938	0.0286155137890765
WBGene00044	R04A9.7	1.9095012819	1.8953821229	4.7275986302	0.00027638248706594
WBGene00045	aho-3	0.2484141481	6.7996630977	1.0230096029	0.00754173239372364
WBGene00045	C08A9.11	1.2509948395	0.0019532173	3.1131382995	4.4302094283508e-06
WBGene00077	Y71A12B.19	0.6667988606	0.0214109088	2.5518021116	0.00244032702664022
WBGene00219	F56D6.16	0.9320631926	0.0195802990	3.6846211491	4.14751167725426e-05

Table S2. List of gene commonly misregulated in *sin-3(tm 1276)* and *sin-3(syb2172)* mutants with SIN3 binding at promoter region

id_gene	gene_name
WBGene00022159	mppa-1
WBGene00021350	Y37E3.8
WBGene00020625	mrrf-1
WBGene00009161	cox-7C
WBGene00007712	mrpl-34
WBGene00010419	atp-1
WBGene00009305	metl-17
WBGene00018961	mrps-16
WBGene00011759	mrps-18B
WBGene00007686	tomm-40
WBGene00011273	R53.4
WBGene00011527	cchl-1
WBGene00012992	mrpl-20
WBGene00021849	Y54F10AM.5
WBGene00003967	pdr-1
WBGene00017121	cyc-2.1
WBGene00016844	sucg-1
WBGene00010317	idh-1
WBGene00013462	micu-1
WBGene00020275	atp-4
WBGene00009139	F25H9.7
WBGene00020511	immt-1
WBGene00012158	ucr-2.1

Table S3

Positive Mode Gradient

Time (mir	%A	%B
0	2	98
3	2	98
11	30	70
12	40	60
16	95	5
18	95	5
19	2	98
25	2	98

Negative Mode Gradient

Time (min	%A	%B
0	4	96
2	4	96
5,5	12	88
8,5	12	88
9	14	86
14	14	86
17	18	82
23	35	65
24	35	65
24,5	4	96
30	4	96

	A	B	C	D	E	F	G	H	I	J	K	L	M	N	O	P	Q	R	S	T	U	V	W	X	Y
1	Table S4																								
2																									
3	Metabolite Information				QC			N2								*sin-3*							Statistics		
4																									
5	Name	formula	m/z, [M-H]-	RT	QC_001	QC_002	QC_003	N2_001	N2_002	N2_003	N2_004	N2_005	N2_006	N2_007	N2_008	sin-3_002	sin-3_003	sin-3_004	sin-3_005	sin-3_006	sin-3_007	sin-3_008	QC RSD %	log2 foldchange	p-value
6	alpha-keto-glutaric acid	C5H6O5	145,014	12,871	7047,11005	7560,5554	7519,6389	3084,28846	7530,61319	5775,513	8262,96591	6918,91004	7504,16663	4856,5724	5765,72243	5067,46432	12608,0186	5460,01317	5125,58683	6964,1791	9969,3826	2617,85566	3,9	0,14	0,6729
7	succinic acid	C4H6O4	117,019	13,37	269573,54	193724,328	161026,78	232149,156	277230,574	275819,95	228816,228	266235,584	238396,713	179963,28	187676,311	159264,774	230636,059	229056,145	204421,768	127923,28	202819,14	248383,134	26,8	-0,23	0,1154
8	fumaric acid	C4H4O4	115,004	15,11	179158,036	173282,506	163298,79	139838,877	160023,717	183851,01	186557,559	157707,463	158577,951	109190,43	126795,747	169524,358	177257,015	102748,105	130980,291	108711,87	139163,9	126508,535	4,7	-0,16	0,2710
9	malic acid	C4H6O5	133,014	14,958	479555,382	431896,85	409168,68	362976,625	393252,498	518809,83	451428,902	425031,838	421302,944	278386,1	348688,852	419447,994	479178,495	265413,976	375062,023	296952,22	376239,47	352853,455	8,2	-0,13	0,3852
10	glucose-6-P	C6H13O9P	259,022	19,756	54813,0516	60590,0108	71238,804	95148,2945	104832,748	144148,53	81081,0886	100731,901	100927,349	89459,131	55927,3117	49395,1641	95582,9309	88091,7371	89739,458	87138,503	170503,58	66461,501	13,4	-0,06	0,8119
11	glucose-1-P	C6H13O9P	259,022	18,569	127191,493	131939,79	134144,3	106545,367	161334,981	220544,1	218989,766	164283,449	185612,186	158587,44	130122,591	82913,1706	119363,751	122131,423	117066,402	86429,6	150610,63	110516,078	2,7	-0,58	0,0060
12	Fructose-1,6-bis-P	C6H14O12P2	338,989	24,137	41918,1122	41004,6937	45264,501	30144,4863	50440,9609	65050,489	63504,8439	54278,1203	53881,4079	48226,792	41656,4202	25250,9967	41336,1502	45445,6276	41230,4289	33087,675	49101,522	39644,0813	5,2	-0,37	0,0384
13	trehalose	C12H22O11	341,109	8,312	607284,506	645171,169	732235,27	620674,097	802741,805	936072,95	1089218,75	755652,826	853015,225	851981,44	633826,178	484448,88	636988,219	1083398,92	678338,94	606937,89	901777,72	1067882,43	9,7	-0,07	0,7254
14	trehalose-6-phosphate	C12H23O14P	421,075	21,441	87843,2286	97306,135	101212,5	83434,0841	84759,4153	140985,24	138356,825	100222,587	114432,527	95783,124	69462,2969	85281,7256	106007,881	95078,5202	99726,236	90702,633	145301,67	84636,4286	7,2	-0,03	0,8421
15	UDP-Glucose	C15H24N2O17P2	565,048	13,653	391237,591	448666,907	467662,22	291033,391	406465,598	488308,67	536713,693	410260,082	456003,729	398038,45	315754,394	352045,11	527458,834	544418,27	513138,354	436395,11	578133,84	487671,255	9,1	0,25	0,0770
16																									

Table S5

	Metabolite Information				QC			N2								*sin-3*							Statistics		
Name	Formula	m/z, [M+H]+	RT		QC_001	QC_002	QC_003	N2_001	N2_002	N2_003	N2_004	N2_005	N2_006	N2_007	N2_008	sin-3_002	sin-3_003	sin-3_004	sin-3_005	sin-3_006	sin-3_007	sin-3_008	QC RSD %	log2 foldchan	p-value
Alanine	C3H7NO2	90,055	10,466		18215,327	18382,5563	17832,0267	33196,1628	28760,9483	17401,0161	19480,1886	20498,0311	16053,2709	18000,0473	31542,9659	22682,5149	19618,8601	30379,6161	35988,3898	31985,5644	42146,0045	42520,3941	1,6	0,48	0,0505
Arginine	C6H14N4O2	175,119	13,226		2661428,7	2700931,07	2733846,84	4590222,17	4918271,85	3446331,2	3307446,54	3653622,99	2979197,93	2977768,13	4088952,3	3799374,8	2956089,89	3947242,42	4219531,01	4137696,97	4600589,63	5257123,8	1,3	0,14	0,3173
Asparagine	C4H8N2O3	133,061	11,063		5687,0887	6534,12577	6127,44896	11103,1789	11942,8727	6101,53018	7926,74142	8918,7258	6371,91071	6885,62543	12482,1531	7384,86078	6231,55771	12523,7409	12403,7401	11201,4306	14504,5378	17770,9525	6,9	0,39	0,1479
Aspartic acid	C4H7NO4	134,045	12,106		4931,25129	5182,16197	4868,41125	6383,75063	10945,5183	6312,23599	7952,90832	6819,25934	8110,3417	7013,39668	8502,17505	5434,92044	4943,12697	4153,33683	4781,20929	4817,89291	5310,1037	5791,0606	3,3	-0,62	0,0011
Glutamine	C5H10N2O3	147,076	10,997		86861,8525	91770,6196	92816,1998	164162,9	176186,136	102315,183	121186,652	119597,205	91153,6278	101026,331	173798,174	125940,522	100371,385	172848,797	178932,726	175305,276	205743,833	231209,976	3,5	0,37	0,0887
Glutamic acid	C5H9NO4	148,060	11,498		200987,716	210580,013	218247,262	376237,43	442531,41	240005,839	285650,921	318553,875	245064,619	241929,059	453781,267	303345,956	215180,491	400589,758	430968,173	385595,245	454525,494	554175,362	4,1	0,27	0,2229
Histidine	C6H9N3O2	156,077	12,909		508906,068	521410,824	512659,604	707646,326	766268,272	639874,319	644119,207	614850,625	585593,209	549302,669	709335,213	606308,142	511964,727	567332,781	644665,795	623933,759	705151,97	734290,151	1,2	-0,06	0,5364
Isoleucine	C6H13NO2	132,102	8,324		61468,3089	62792,862	59150,46	102754,217	113173,723	79967,2527	64141,413	75505,1033	58322,0448	65472,2442	88783,0659	66109,3907	61854,4837	76584,4115	84072,1084	73971,2658	98975,7579	107970,466	3,0	0,01	0,9710
Leucine	C6H13NO2	132,102	7,978		97706,7043	93881,3965	93089,6849	140626,725	164000,169	119112,248	96167,651	116177,791	93441,819	102475,422	142354,009	102429,721	103507,707	127498,281	138948,61	115821,036	175341,717	159593,802	2,6	0,11	0,4782
Lysine	C6H14N2O2	147,113	13,488		170922,004	176531,806	180605,536	304628,845	321659,544	178699,167	183588,025	222019,173	158212,357	169570,874	305370,338	285611,706	206884,542	335422,269	386522,932	358911,428	442186,78	452991,499	2,8	0,61	0,0119
Methionine	C5H11NO2S	150,058	8,639		23988,6926	23624,5	24993,0287	38246,3225	41965,7144	34088,3409	27847,3298	28663,0428	27502,1143	26643,4083	35255,6668	20996,4108	24860,5219	30270,6912	29341,8533	22159,6871	41021,3349	29045,2108	2,9	-0,20	0,2112
Proline	C5H9NO2	116,071	9,285		266764,008	265874,102	272575,841	433345,01	488349,203	264362,703	228342,915	340564,104	200580,63	285018,337	396966,386	344884,696	322017,561	409418,999	495632,684	464265,916	583903,377	611632,159	1,4	0,49	0,0345
Serine	C3H7NO3	106,050	11,066		4484,54364	4785,15546	5119,85135	7998,66681	7574,74326	4515,54207	5599,75922	5331,63532	4173,63853	4986,76272	9129,24465	7426,89881	5848,7913	12449,8247	12588,2573	11910,5573	12646,942	18990,7199	6,6	0,92	0,0128
Threonine	C4H9NO3	120,066	10,561		5619,70737	6236,16641	6652,52568	9002,02358	11103,8532	5863,24646	7001,8818	7386,52561	5830,39644	6381,81572	10972,5478	8324,27443	6488,82826	11384,7599	13693,1245	11194,7789	15471,0269	18316,0419	8,4	0,61	0,0382
Tryptophan	C11H12N2O2	205,097	8,055		95259,5576	102486,634	107182,599	98774,4556	117149,528	119855,95	138448,17	113048,181	112841,155	124011,215	129365,683	101509,338	97032,3489	113078,6	120060,282	127795,868	157329,022	148139,097	5,9	0,05	0,6575
Tyrosine	C9H11NO3	182,081	8,972		171594,586	175684,058	141391,982	196164,598	206437,293	200590,146	179113,205	189374,514	156301,85	170352,925	176335,087	171238,894	161319,784	146379,262	178972,775	132264,1	173400,628	188684,118	11,5	-0,16	0,0600
Valine	C5H11NO2	118,086	8,548		6044491,87	5880055,62	5736347,3	8899125,29	9042259,87	7358026,51	5193066,55	7608835,78	5025599,88	5952129,11	7289489,48	9110593,06	7319331,21	6273516,06	7743425,12	8316083,34	8246326,33	10106200,3	2,6	0,21	0,1448
GSH	C10H17N3O6	308,091	13,187		28891,1022	27940,8811	28539,4191	57536,8015	65428,8287	49803,6488	51017,5382	54138,8324	23554,6534	18358,0878	52802,6805	53306,4681	36896,1553	48680,0123	73487,3308	62001,2465	35067,7207	58595,5283	1,7	0,17	0,4576
GSSG	C20H32N6O1	613,159	14,173		287152,651	308663,846	313130,145	775143,471	911324,723	371343,968	491976,406	623566,764	392134,267	441680,485	999426,364	406963,218	327090,308	620591,246	629619,239	749774,462	903651,445	842115,8	4,6	0,03	0,9065
Ornithine	C5H12N2O2	133,097	13,562		8737,51998	8241,59094	9003,45149	17182,9169	17840,79	9935,54456	10152,7226	13270,1689	9129,47979	10163,533	17172,6025	13230,1526	9322,2725	13714,9557	15451,5794	15107,1895	16811,6075	17949,5858	4,5	0,15	0,4238
Citrulline	C6H13N3O3	176,103	11,555		59772,4554	70200,6881	78408,1143	65917,8345	60346,611	40928,5709	36857,8755	46184,5767	36159,9539	47852,6159	55460,8195	123308,924	90618,5332	139717,046	168449,892	159424,418	171871,274	208254,05	13,4	1,64	0,0002
Dimethyl argin	C8H18N4O2	203,150	12,232		18351,174	18703,6731	18112,2555	23022,403	22919,7242	16006,939	17942,0533	17509,1992	13576,1674	18045,3652	21727,7131	24110,9661	19432,9137	26781,2278	29492,7004	28394,2934	37904,2723	40038,9337	1,6	0,64	0,0075
Sarcosine	C3H7NO2	90,055	10,683		1211,32239	1831,30296	1786,96192	2418,01284	2071,01829	955,2936	1552,29044	2125,38046	1479,39139	1476,31138	3810,13267	2087,22927	1652,87636	4105,86965	4772,89011	3253,02839	5295,27052	5579,17748	21,5	0,94	0,0209
CoA	C21H36N7O1	768,123	8,815		1758,16349	3431,86225	3230,23985	4265,26097	4040,89264	2552,42763	3525,53537	3400,04645	1813,66968	1775,80351	2546,88584	6964,37063	4910,85486	5739,38934	3364,02936	3757,36494	2465,79068	4915,81149	32,6	0,62	0,0379
CoA 2:0	C23H38N7O1	810,133	12,767		14467,046	15122,2542	13806,4296	20657,1414	38327,1664	17450,6532	21250,7368	29579,3591	24374,1396	20983,1928	44951,7662	18968,894	12908,3767	29740,714	36703,3386	25892,0262	33789,2623	45216,9341	4,5	0,09	0,7387
CoA 3:0	C24H40N7O1	824,149	12,196		3192,40523	3249,68535	2947,38622	4729,98483	7930,07228	3198,42805	4112,95283	4388,9957	3815,94251	4113,26396	8299,56568	3822,54273	2456,33275	4434,84425	5089,17352	5886,13965	5713,03539	6311,03044	5,1	-0,08	0,7676
CoA 4:0	C25H42N7O1	838,164	11,721		3710,4865	3651,89347	3543,84042	6960,3289	9627,76809	3622,56429	4584,80164	6668,52256	5046,92107	4006,271	10313,7262	4631,14124	4035,37031	9180,7322	9269,73446	8045,23958	9793,34137	13023,0212	2,3	0,38	0,2165
CoA 5:0	C26H44N7O1	852,180	11,332		15900,649	14990,7667	14019,31	28458,5933	32009,8764	15349,2411	16645,621	21397,1188	15342,2819	13596,0895	29289,2877	27402,1	19450,9774	39304,6017	37788,2121	37315,5355	37222,0996	49734,7998	6,3	0,72	0,0095
Tiglyl-CoA	C26H42N7O1	850,164	11,534		9230,68191	8612,17641	8740,30476	14738,3246	21256,1648	11153,6472	12214,3118	13056,6976	12471,883	10846,1343	19282,2262	16349,5867	11860,8042	21630,4733	20366,5157	20930,2962	17222,4922	29091,0835	3,7	0,45	0,0550
SAM	C15H22N6O5	399,145	13,361		760954,986	778463,181	767318,08	1282426,96	1469450,14	971330,083	1135167,74	1161346,5	906641,333	947169,145	1223209,35	863078,78	617048,233	750555,96	858239,846	864189,876	930022,265	1008629,2	1,2	-0,43	0,0038
SAH	C14H20N6O5	385,129	10,681		9517,48064	10450,9558	9991,53995	21748,8045	24697,4934	13949,6462	15693,7056	16532,2089	11621,9297	12666,3671	22500,5775	11470,9652	9658,02581	15309,0661	17877,8261	14458,4729	20102,2078	22231,4224	4,7	-0,13	0,5352
Cystathionine	C7H14N2O4S	223,075	13,255		704570,4	715318,857	725363,285	1480454,2	1776751,75	849329,427	1026500,8	1185490,45	857766,417	875989,895	1686992,03	1083511,67	773232,37	1472286,82	1574723,65	1423594,92	1680265,6	1923054,99	1,5	0,22	0,3281
S-Adenosylme	C14H23N6O3	355,155	14,168		5480,78994	5474,69932	5207,0464	10151,8161	10826,7069	6763,58757	7328,95001	11379,5457	10067,6082	11662,6729	10502,0011	2884,71215	2170,63904	2307,28836	2385,76041	3275,04723	2349,07248	3075,02128	2,9	-1,90	0,0000
5'-Methylthio	C11H15N5O3	298,097	13,359		40606,3406	40907,1755	40645,6548	69239,1106	79782,3152	51935,2017	58465,5326	64511,8583	48198,6555	49972,1335	66801,5261	47737,3636	34220,1647	43389,3716	49348,39	48971,5898	50690,0013	55571,8884	0,4	-0,37	0,0110
Succinyl-coa	C25H40N7O1	868,139	13,861		1528,59377	1769,7061	1470,12612	2403,55066	7915,64501	2261,90898	3371,55828	3274,32712	2902,26641	3848,47842	5350,64266	2818,36257	2788,22592	5108,82945	4575,81369	5580,77781	3692,32985	7864,90132	10,0	0,24	0,4634
Folic acid	C19H19N7O6	442,147	11,001		2120,63183	3199,21995	2809,28986	4768,79866	4406,60481	3120,9102	3263,37194	2635,62295	1896,87311	2142,11755	3304,86673	3578,1291	2778,53543	2760,08681	3593,01543	3470,86703	3388,35186	4076,95996	20,2	0,08	0,6502
5-methyl tetra	C20H25N7O6	460,194	11,071		2148,99577	2961,31492	2407,88103	5559,30151	6496,10956	2943,67112	1934,18766	3548,72066	2274,94435	2872,5004	5643,1422	3637,90655	2447,47738	4680,00495	4442,42271	4755,7894	5445,02428	7346,9857	16,6	0,26	0,3762
Dihydrofolic a	C19H21N7O6	444,163	12,911		12879,1477	9679,51134	8296,37975	8948,04492	11272,5145	8854,0216	10144,445	9488,98353	10477,1499	7472,68722	9408,01282	9995,17336	10086,807	7103,83494	8015,9789	7556,18995	7865,07968	9215,2777	22,9	-0,15	0,1417
Carn 2:0	C9H17NO4	204,123	8,301		805367,307	826284,95	787852,792	948193,139	1320194,42	948559,603	863967,836	1116101,11	861126,218	1046198,86	1452350,16	1179098,82	967034,781	1134951,62	1348211,16	1456032,2	1031494,63	1910938,31	2,4	0,27	0,1562
Carn 3:0	C10H19NO4	218,139	6,615		413049,665	411022,625	411507,117	607302,85	762442,332	434615,921	429424,189	524004,045	384426,798	514064,688	675027,164	537722,581	479689,322	605595,59	663186,393	591811,226	552155,691	1076975,99	0,3	0,25	0,2737
Carn 4:0	C11H21NO4	232,154	5,121		341525,343	339732,624	335636,414	496724,005	552651,796	319657,177	324144,514	414898,521	290341,504	359078,797	548640,88	351640,425	322963,509	597865,197	641685,178	520791,504	670092,456	931349,799	0,9	0,48	0,0939
Carn 5:0	C12H23NO4	246,170	4,149		628906,055	635604,505	638117,445	954763,051	1019029,03	637725,086	648994,118	768624,605	541485,98	648508,682	932102,028	769616,98	701244,142	957199,082	1000352,36	1008485,4	1068913,7	1385308,45	0,8	0,36	0,0632
Tiglyl-Carnitin	C12H21NO4	244,154	4,525		47611,8769	47435,1297	47903,9502	65421,0842	84625,6107	54583,0994	50643,1521	59337,176	45971,3777	50844,9931	74318,7673	39566,3726	52967,3638	68443,6305	72734,1667	34067,5692	85577,264	91290,7472	0,5	0,07	0,7758
Riboflavine	C17H20N4O6	377,146	4,133		193243,842	200878,167	190971,746	203210,45	239804,571	209496,861	264989,094	214639,309	209910,768	184449,945	243535,334	130152,609	153631,1	188353,965	191202,951	155198,679	209962,719	176951,948	2,7	-0,36	0,0038
Pantothenic a	C9H17NO5	220,118	3,17		407315,721	402670,904	399152,07	439885,919	505295,888	312939,979	369444,277	438263,672	308371,518	354670,852	599646,678	515729,828	382360,096	507395,797	673240,102	606344,984	656146,777	925465,653	1,0	0,55	0,0271
N-Acetyl sperm	C9H21N3O	188,176	13,749		1328246,04	1300711,18	1258667,76	1995949,76	2049425,21	1193640,77	1237151,84	1925244,21	1127578,13	1417278,85	2010105,83	1937582,88	1379200,59	1778273,25	2051165,36	2245003,4	2559793,33	2713575,93	2,7	0,37	0,0569
Agmatine	C5H14N4	131,129	13,608		12351,2498	12166,4502	11179,8977	9122,32002	10319,8289	8916,08924	8277,31597	10089,6811	7691,2395	9089,48231	10359,88	16766,1111	14121,4487	15364,2098	18393,4596	15683,0247	25399,5071	18623,1036	5,3	0,94	0,0007
Cadaverin	C5H14N2	103,123	13,837		3427,66539	3234,80975	3134,82611	3574,85772	3385,97443	3774,42736	2695,55025	3971,69413	3008,44104	2832,3371	3089,75233	6092,74413	3929,94574	3533,63996	4999,80567	4513,02667	5414,64261	5734,85792	4,6	0,57	0,0032
Putrescine	C4H12N2	89,107	14,123		16355,945	15778,6703	15739,9191	23152,4004	22006,8216	21200,5933	15159,8501	18063,1725	16959,6567	16480,0716	15305,4898	24547,9069	18910,0242	15074,7835	17647,0415	19196,1128	18317,2014	20825,336	2,2	0,05	0,6738
N-Acetyl putre	C6H14N2O	131,118	8,911		57465,8973	56251,3295	54163,9012	120457,422	129844,647	74167,01	60949,7036	83481,9714	58919,4467	75909,6684	103255,265	68649,7709	56128,3428	71441,7713	84135,3278	77371,4227	89802,0141	118865,13	3,0	-0,13	0,5476
N-Acetyl sperm	C12H28N4O	245,234	15,227		6836,0567	6945,0949	7109,31012	1869,29785	1907,31569	1478,98019	1439,80773	3068,55053	1747,18961	3703,2866	4602,12381	14734,6829	3819,3599	10553,4855	15817,0963	11362,5373	16996,6245	22530,5546	2,0	2,47	0,0021
Serotonin	C10H12N2O	177,102	11,562		5104,50717	6054,79398	6932,29965	5575,19555	4671,11261	3139,05937	3384,49376	3750,93893	2675,99142	4283,95344	4647,08883	9987,68696	7411,98972	11294,3662	13059,4665	13278,1858	13773,5174	17103,8691	15,2	1,61	0,0003
Saccharopine	C11H20N2O6	277,139	13,358		41324,0667	41702,3704	44943,1797	73485,7029	76408,5898	39360,1835	48789,5768	58961,68	44231,394	44715,7945	80870,2986	78629,9104	51627,2411	102977,177	121170,797	94484,2296	129126,658	140493,861	4,7	0,81	0,0081
L-2-Aminoadi	C6H11NO4	162,076	11,022		106777,629	113189,451	108486,115	189149,151	216287,564	108258,825	133824,646	154086,233	109323,941	116848,524	250678,216	164963,924	115692,509	232717,323	254264,869	230533,866	286372,651	348025,359	3,0	0,55	0,0577
Spermidine	C7H19N3	146,165	15,408		339471,282	344154,901	344695,016	75176,974	98926,8377	59816,9739	50831,3831	151308,521	82388,873	167849,151	206096,104	761536,673	149504,72	428390,93	526334,479	410079,547	452880,577	836559,015	0,8	2,19	0,0034